# CRC Report No. AVFL-28

# Gasoline Direct Injection (GDI) Engine Wear Test Development

## Final Report

**January 2018**

**COORDINATING RESEARCH COUNCIL, INC.**
**5755 NORTH POINT PARKWAY • SUITE 265 • ALPHARETTA, GA 30022**

**The Coordinating Research Council, Inc. (CRC) is a non-profit corporation supported by the petroleum and automotive equipment industries. CRC operates through the committees made up of technical experts from industry and government who voluntarily participate. The four main areas of research within CRC are: air pollution (atmospheric and engineering studies); aviation fuels, lubricants, and equipment performance, heavy-duty vehicle fuels, lubricants, and equipment performance (e.g., diesel trucks); and light-duty vehicle fuels, lubricants, and equipment performance (e.g., passenger cars). CRC's function is to provide the mechanism for joint research conducted by the two industries that will help in determining the optimum combination of petroleum products and automotive equipment. CRC's work is limited to research that is mutually beneficial to the two industries involved. The final results of the research conducted by, or under the auspices of, CRC are available to the public.**

**SOUTHWEST RESEARCH INSTITUTE®**
**San Antonio, Texas**
**Fuels and Lubricants Research Division**

# GASOLINE DIRECT INJECTION (GDI) ENGINE WEAR TEST DEVELOPMENT

## Final Report

**CRC Project No. AVFL-28**
**SwRI Project No. 08-22469 Revision 1**

**Conducted for:**

**Coordinating Research Council**
**5755 North Point Parkway, Suite 265**
**Alpharetta, GA 30022**
**Attention: Brent Bailey**

**October 9, 2017**

**Prepared by:**

**Dr. Peter Lee, Staff Engineer**
**Tribology Research and Evaluations**
**Engine Lubricants Research Department**

**Reviewed by:**

**Michael Lochte, Director**
**Engine Lubricants Research Department**
**Fuels and Lubricants Research Division**

## TABLE OF CONTENTS

**Page**



**APPENDICES** **No. of Pages**

As per the contract, this report is presented as a scientific paper ready for Journal submission. This will give an excellent project overview. Additional supporting data and project specifics are given in the appendices.

## LIST OF TABLES

**Table** **Page**

## LIST OF FIGURES

**Figure** **Page**

## 1.0 ABSTRACT

Existing engine lubrication wear tests based on ILSAC and ACEA specifications were developed for engines and operating conditions representative of port fuel injection (PFI) engine technology. The automotive industry is trending away from the PFI engine towards gasoline direct injection (GDI) technology with approximately 40 percent of passenger cars sold in 2014 having GDI engines, many of which are turbo-charged. These turbo-charged GDI engines often produce more severe operating conditions than PFI engines due to their higher operating temperatures, cylinder pressures, and specific torques. In addition, most turbo GDI engines are downsized, therefore operating at higher loads for a greater portion of their operating cycle. Some vehicles use alternative combustion cycles or stop-start technology which further subjects the engine and lubricants to higher levels of stress compared to conventional PFI engines.

In an effort to guide the development of engine lubrication wear tests in the next ILSAC and ACEA categories, the rings, liner and rod bearings of a modern turbo charged GDI engine, a Ford 2.0L Ecoboost engine, were irradiated and the engine assembled and placed on a test stand. The irradiation of these engine components resulted in the formation of different isotopes, depending on the component material. A series of in-field operating conditions were selected and the engine operated at these conditions using both a SAE 5W-30 oil and a SAE 0W-16 oil with the same additive package. Using the SwRI® Radioactive Tracer Technology (RATT®) the level of radioactive particles in the oil, present due to wear of the irradiated engine components, can be detected and the strength of the signal for each isotope can be correlated with the mass of wear material in the oil.

Results showed no measureable wear in the connecting rod bearings, higher wear response from transient than steady state engine operating conditions, noticeably higher wear during stop-start and roughly only two thirds of the operating conditions resulted in higher wear in the measured engine components using SAE 0W-16 oil over SAE 5W-30 oil.

## 2.0 INTRODUCTION

Tests designed by ASTM for inclusion in the current API/ILSAC oil specifications dictate modern oil formulations, with many oils available to consumers only meeting the minimum standard of quality specified. Additionally, these tests serve as a readily available, standardized, and well administrated method to test engine lubricant performance in situations other than API/ILSAC certification, often providing a test-bed for research in this area or formulating lubricants to exceed the current requirements. The current low-temperature valve-train wear test procedure (Sequence IVA, ASTM D6891), as part of the ILSAC GF-5 oil specification, requires use of a naturally-aspirated, port fuel injected, 3 valve per 4-cylinder, low-compression 2.4L Nissan engine first in service in 1988. Significant advances in mechanical engine design, combustion strategies, materials, and coatings have been made since 1988 resulting in lubricants for modern engines operating in conditions which this dated test cannot emulate.

The replacement test, currently under development for ILSAC GF6, also requires use of a naturally aspirated, port fuel injected engine using a 4 valve per 4-cylinder 1.5L Toyota Engine. While this is certainly an improvement over the previous version of the test with respect to

modern engine architecture, it does not provide a method of testing lubricants in the unique environment encountered in gasoline direct injected turbocharged engines. GDI engines are found in a significant portion of new passenger cars being sold today, and are expected to continue to expand across model lines as consumer demand for higher power and regulatory demand for lower emissions and higher fuel economy continues. GDI engines produce significantly higher abrasive soot content in the oil and higher levels of sump fuel dilution, along with unique pre-ignition phenomenon, higher pressures, power densities, and lubricant temperatures, all which present new challenges for oil formulations.

In any engine there are numerous components that exhibit wear, and different engine conditions result in different wear rates of these components in various ways. In addition, the wear of each engine component is influenced through various means, for example mechanical design, metallurgy, surface finish, coatings, and/or lubrication strategies. The Sequence IVA is currently the only approved test specifically designed for engine wear, and only measures valve-train wear. The IVB, again valve-train wear only, is still in development for GF6 and the Chain Wear test is pending inclusion in GF6. With modern engine production schedules of 5-6 years, it is clear that 30 year old engine technology is inappropriate for guiding modern lubricant formulations.

In an effort to guide the development of engine lubrication wear tests in the next API/ILSAC and ACEA categories, the rings, liner, and rod bearings of a modern turbo charged GDI engine, a Ford 2.0L Ecoboost engine, were irradiated and the engine was assembled on a test stand. The irradiation of these engine components results in different isotopes being formed, depending on the material from which the components are manufactured. Using the SwRI® Radioactive Tracer Technology (RATT®) the level of radioactive particles in the oil, present due to wear of the irradiated engine components, can be detected, and the strength of the signal for each isotope can be correlated with the mass of wear material in the oil. A test matrix was developed to operate the engine through a series of in-field operating conditions expected to create wear of the engine components. The aim of the project was to discover which engine conditions created wear in which engine components, thereby guiding future wear test development. The engine was operated at these conditions using both the recommended lubricant grade for the engine – SAE 5W-30, and a low viscosity lubricant - SAE 0W-16, to investigate effects of reduced viscosity. The same additive package was used in both oils to ensure observed differences were an artifact of viscosity grade only.

## 3.0 SCOPE OF WORK

### 3.1 Test Engine and Test Cell

The engine selected for this work was the Ford 2.0L EcoBoost engine used in the 2012 Ford Explorer. This engine was selected for a number of reasons, including being representative of current and future engine technology (downsizing, turbo, high BMEP), being early in its product life cycle, and guaranteed support from the manufacturer. The engine was installed in a test cell with engine control and absorbing dynamometer. The cell was chosen for its location away from high foot traffic and space for the radiation detector and peripheral equipment. This engine is the same as currently used for the Chain Wear and low speed pre-ignition (LSPI) tests being developed for the ILSAC GF6 oil specification, therefore the project team had a high level of

familiarity with the engine and its control systems. This engine, like many turbo charged down-sized engines, has a tendency for LSPI. In order to reduce the chance of engine damage, aftermarket pistons were chosen as they have more material below the second ring and thought to be more robust.

A slave engine was used to develop the test cycles to be run and LSPI events were avoided by working closely with Ford in order to program the ECU appropriately. All target operating points of interest were achieved with knock-avoidance and operating temperatures maintained below critical levels, in part achieved through the use of a cooling fan directed at the turbo.

### 3.2 Power Cylinder Metallurgical Analysis

The power cylinder components were the focus for the wear study and detailed metallurgical information for the power cylinder components listed in Table 1 were obtained using Energy-Dispersive X-ray Spectroscopy (EDS) on a Scanning Electron Microscope (SEM). Cross section images of the power cylinder components at various magnifications illustrate the orientations and concentrations of the alloying elements within the parent materials.

**Table 1. Candidate parts for wear analysis**

| | | |
|---|---|---|
| Top ring | Second ring | Engine liner |
| Main bearing | Rod bearing | Turbocharger thrust washer |
| Camshaft lobe | Timing chain | Valve guide |

Due to material type overlap between components, only the top ring face and side, second ring, liners and the connecting rod crankshaft bearings were irradiated. Therefore only these are reported in this paper. A second phase of this work will be undertaken which will include valvetrain and turbocharger component wear.

<u>Top Ring</u>

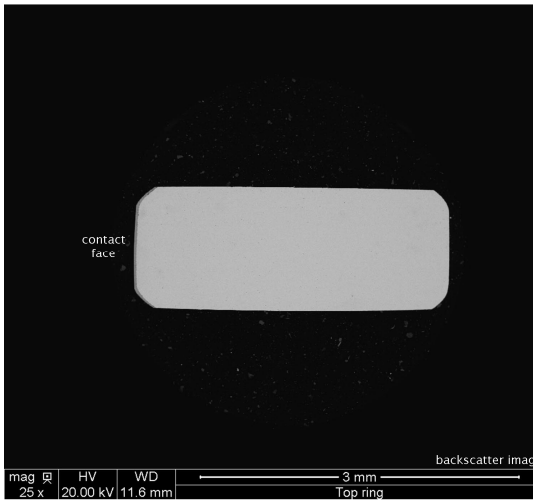


**Figure 1. Top ring cross section**

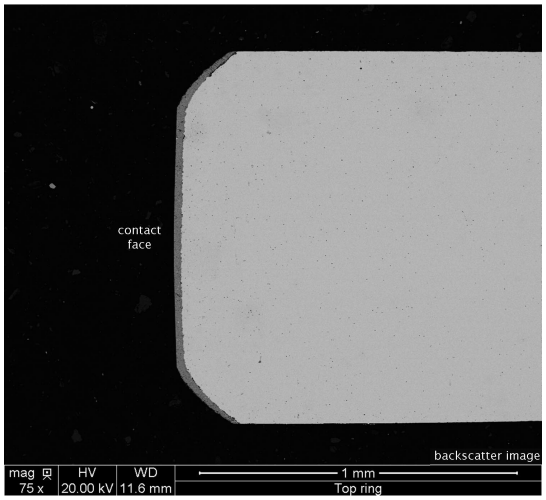


**Figure 2. Top ring contact face**

The top piston ring shown in Figure 1 is a rectangular cross section with rounded corners and a slight barrel on the contact face. The ring bulk material is iron and the contact face of the ring comprises a chromium based coating that extends from the top, across the face, to the bottom, as shown in Figure 2. Figure 2 also shows pockets of black material within the coating on the top ring face. These pockets are elemental molybdenum and are largely concentrated where the peripheral coating connects with the parent ring substrate. The molybdenum is likely present to improve durability and/or flexibility of the adhesion between the hard chromium coating and the base iron material. Full elemental analysis is given in Table 2.

**Table 2. Elemental analysis of wear components**

| | Percent Mass Concentration by Element % | | | | | | | | | | |
|---|---|---|---|---|---|---|---|---|---|---|---|
| | **Mg** | **Al** | **Si** | **V** | **Ti** | **Cr** | **Mn** | **Fe** | **Cu** | **Sn** | **Zn** |
| Top ring running surface | | 0.57 | 0.42 | | | 98.35 | | 0.66 | | | |
| Top ring base material | | | 2.17 | | | 0.61 | 0.65 | 96.57 | | | |
| Second ring material | | | 0.55 | | | 0.07 | 0.74 | 98.64 | | | |
| Cylinder Block | 0.51 | 81.45 | 14.45 | | 0.15 | | 0.31 | 0.46 | 2.2 | | 0.46 |
| Cylinder liners | | 0.19 | 3.43 | | | 0.12 | 0.72 | 94.22 | 2.9 | | |
| Rod bearing babbit running surface | | 89.11 | 5.2 | 0.21 | | | | | 1.1 | 4.38 | |
| Rod bearing base material | | 0.62 | 0.66 | | | | 0.34 | 98.37 | | | |

Second Ring

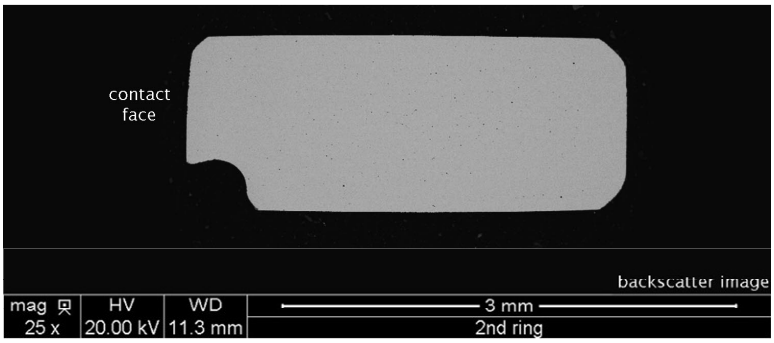


**Figure 3. Second ring profile**

The profile SEM image in Figure 3 depicts the tapered napier profile of the second ring and the homogenous material comprising the ring. The second ring has no coating, but is shown by the EDS results to be an alloyed iron material, as shown in Table 2.

Liner

The liner on this engine is an integral iron sleeve cast into the block and elemental analysis showed the liner to be primarily iron in the aluminum silica alloy engine block, as shown in Table 2.

Connecting Rod Crankshaft Bearing

The connecting rod bearings in this engine are bimetallic with primarily iron base material and aluminum top coat, as shown in Table 2.

### 3.3 Engine Component Activation

There was substantial overlap in the power cylinder component metallurgy, as shown in Table 2. This influenced the decision on how to activate the components in order to obtain distinct isotopes for detection of wear particles in the oil. Some components were bulk activated and others were surface layer activated (SLA) using different activation beams, as summarized in Table 3 and discussed below.

**Table 3. Summary of test part, activation technique and resulting isotopes**

| Test Part | Activation Technique | Isotopes Generated |
|---|---|---|
| Top ring running surface | Bulk activation | Cr-51 (Chromium-51) |
| Top ring base material | Bulk activation | Fe-59 (Iron-59) |
| Second ring material | Surface layer activation, deuteron beam | Co-57 (Cobalt-57) |
| Cylinder liners | Surface layer activation, proton beam | Co-56 (Cobalt-56) |
| Rod bearing inner diameter | Bulk activation | Sn-113 (Tin-113) |

Top Ring

The top ring was bulk activated, giving two isotopes, Cr-51 for the ring face coating and Fe-59 for the ring sides, being the base material of the ring. The rings were activated for 50 hours to yield a wear rate resolution of 35µg/hr. Details for this are given in Table 4. A total of eight top rings were activated to ensure that sufficient spares were available should rings be broken during installation or the ring faces finish became compromised during activation. Four of the activated top rings were used in the engine build.

**Table 4. Total activity for bulk activation parts**

| Bulk Activation Products | | | | | | | |
|---|---|---|---|---|---|---|---|
| Reactor neutron flux = 6.811e12 per $cm^2s$ | | | | | | | |
| Irradiation time = 50hrs | | | Delay for short life decays = 7 days | | | | |
| **Material** | **Mass (g)** | **Original Nuclide** | **Mass (g)** | **Process** | **Product Nuclide** | **Activity** | **Half Life** |
| Iron | 143.6 | Fe-54 | 8.048 | (n,G)-> | Fe-55 | 54.15 mCi | 2.7 years |
| | | Fe-58 | 0.4471 | (n,G)-> | Fe-59 | 31.80 mCi | 44.53 days |
| Chromium | 0.74 | Cr-50 | 0.03092 | (n,G)-> | Cr-51 | 46.48 mCi | 27.7 days |
| Tin | 0.01 | Sn-112 | 9.43e-05 | (n,G)-> | Sn-113 | 0.9598 µCi | 115.1 days |

Second Ring

The base material for both the top and second piston ring are very similar and would produce overlapping iron isotopes if both were bulk activated. Therefore, the second ring activation was achieved through a SLA technique using a deuteron beam to produce a Co-57 isotope within the second ring face. The total activity generated by the SLA was 278 µCi of Co-57 giving a 60µg/hr wear resolution. To achieve this, the second rings were mounted on a rotating drum fixture fabricated to provide a tension fit on the inner diameter of the rings. The fixture allowed for eight second rings to be activated in one process by simultaneously rotating the drum and transposing the beam across all eight rings. The resulting activity-depth profile is shown in Figure 4 and activation details given in Table 5. All four second ring faces were activated.

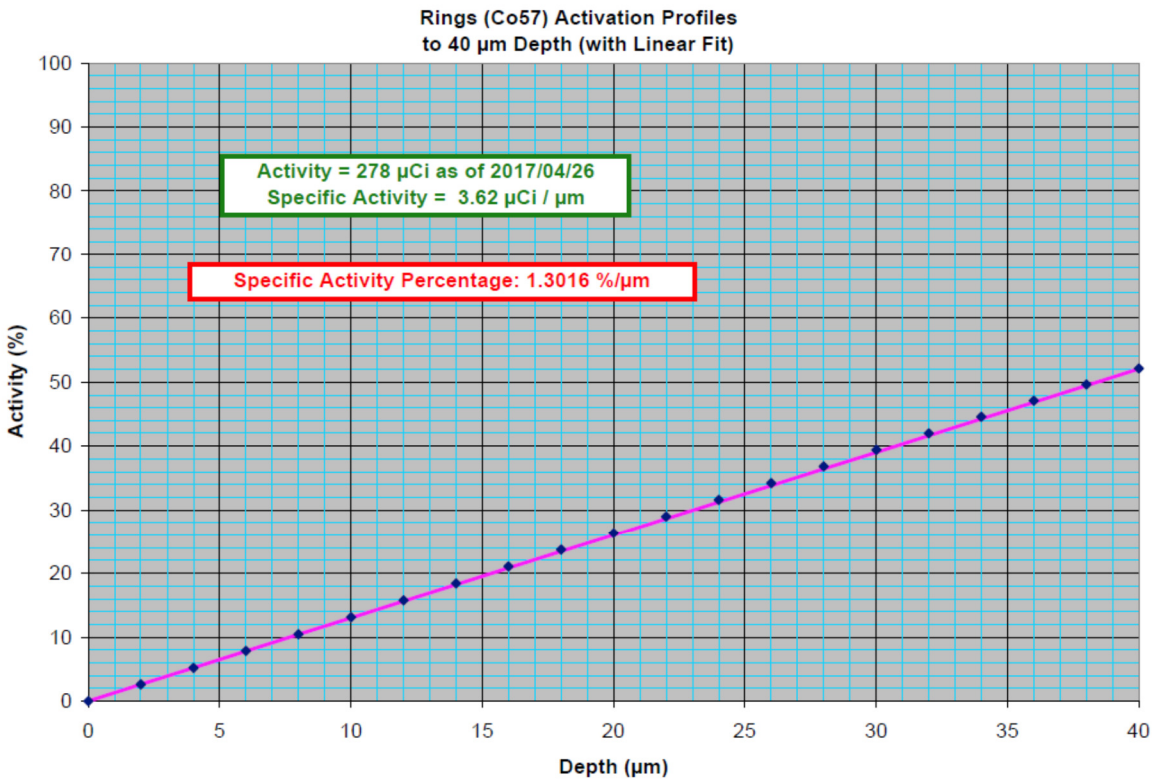


**Figure 4: Second rings activation profile**

**Table 5. Surface Layer Activated (SLA) parts**

| Surface Layer Activated Products | | | | | | | | |
|---|---|---|---|---|---|---|---|---|
| **Material** | **Activation Area** | **Depth of Activity (µm)** | **Original Nuclide** | **Mass (g)** | **Process** | **Product Nuclide** | **Activity** | **Half Life** |
| Iron (Cylinder Liner) | 20mm x 10mm | 100 | Fe-56 | 94.22 | (p,n) | Co-56 | 282 µCi | 77.2 days |
| Iron (Second Ring) | Full circumference of face | 100 | Fe-56 | 98.64 | (d,n) | Co-57 | 278 µCi | 272 days |

<u>Liner</u>

As the liners were integral to the block, it was not feasible to bulk activate the entire block as it would result in too large a mass of irradiated material. For this reason the cylinder liners had a targeted surface layer activation at the top ring turnaround area of the thrust side of the cylinder liner. The masked window activation created a 20mm wide (around the circumference of the liner) x 10mm tall (axially down the liner) area of radioactive material starting 5mm below the top of the liner, being the highest wear area of the piston stroke. This provided the greatest

sensitivity to lubricant and operating conditions at the piston ring and liner interface. The total activity generated by the SLA on the cylinder liner was 282µCi of Co-56 giving a 1nm/hr wear resolution. This was produced on the thrust side of all four of the cylinder liners. Figure 5 shows the cylinder liner activity-depth profile and activation details are given in Table 5.

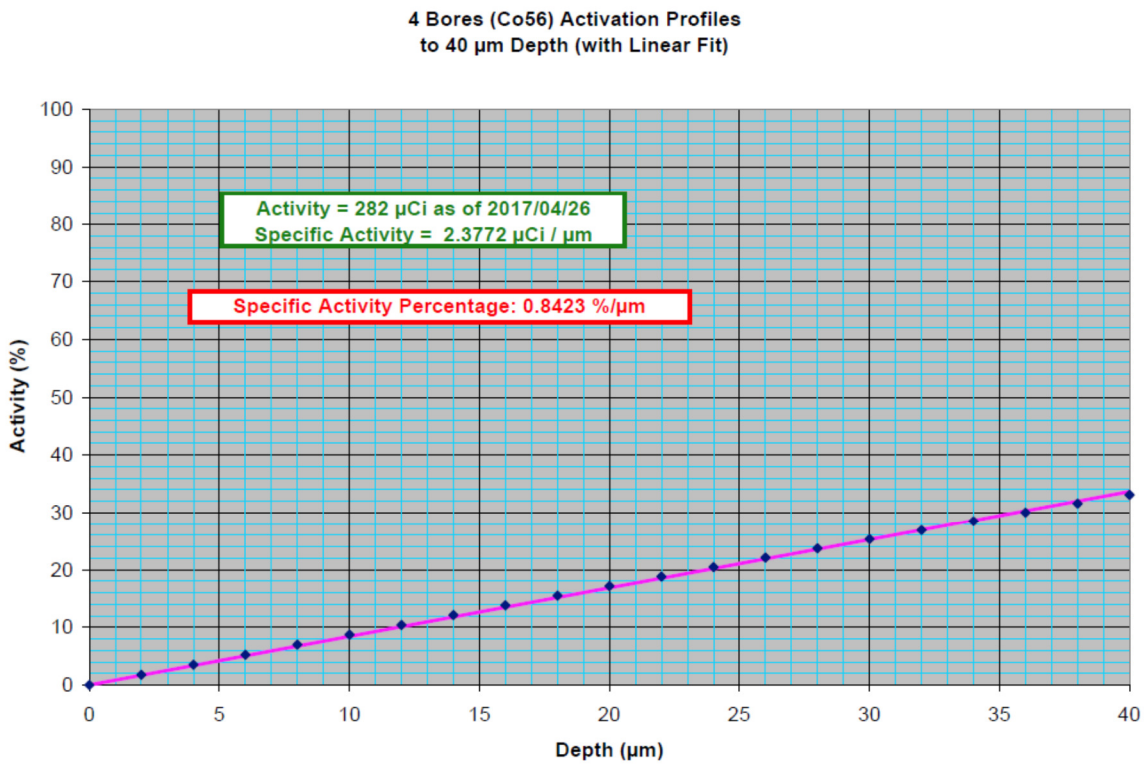


**Figure 5: Cylinder liner activation profile**

Connecting Rod Crankshaft Bearing

There was no unique elemental difference between the rod and main bearings, so a single selection was necessary. The authors' previous experience was that the rod bearings are much more sensitive to combustion pressures, which will be higher in a turbocharged GDI engine than a port injected naturally aspirated engine. In addition, due to their physical dimensions and overall weight, the rod bearings were the best candidates for bulk activation. The bulk activated rod bearings produced a Sn-113 isotope from the elemental tin in the bearing's inner diameter contact layer. The 50 hour activation yielded a 35µg/hr wear rate resolution. Further details are available in Table 4. All four sets of upper and lower connecting rod bearings were irradiated.

## 3.4 Test Fuels and Lubricants

### *3.4.1 Test Fuels*

Two fuels were chosen for this work. Pump grade Premium Unleaded Gasoline with 10% Ethanol was used for the engine run-in. This was chosen to control overall project costs. For the engine test portion of the work, Lube Certified EEE fuel from Halterman was used, thereby increasing repeatability as this fuel is certified for industry engine testing.

### *3.4.2 Test Lubricants*

Testing was conducted using two oils containing the same additive package - a SAE 5W-30 and a SAE 0W-16. The oils were low LSPI dexos1™ Gen2 oils. The SAE 5W-30 was selected as this is the manufacturer-recommended lubricant for the Ford 2.0L Ecoboost engine. The SAE 0W-16 was selected as this represents the current lubricant trend of reducing viscosity. Using the same additive package ensured that difference in wear rates were attributable to the change in viscosity only. Viscometrics for the lubricant blends are given in Table 6.

**Table 6. Test lubricant viscometrics**

| Lubricant | Temperature (°C) | ASTM D7042 | | |
|---|---|---|---|---|
| | | Dynamic (cP) | Kinematic (cSt) | Density (kg/m$^3$) |
| SAE 5W-30 | 40 | 56.621 | 69.013 | 0.820 |
| | 100 | 9.488 | 12.122 | 0.783 |
| SAE 0W-16 | 40 | 28.584 | 34.981 | 0.817 |
| | 100 | 5.493 | 7.067 | 0.777 |

## 3.5 Engine Run-in

Prior to running the engine through the designed test matrix of operating conditions, the engine was run-in using the SAE 5W-30 oil for 76 hours following a Ford recommended eight hour break-in procedure. The break-in consists of several low to moderate load steady state conditions in increments between 1500 rpm and 5,000 rpm. The eight hour break-in procedure was repeated until the wear rates detected by RATT® approached steady conditions. Initially 100 hours was allocated for running in, but the engine displayed steady wear rates from 45 hours onwards. No oil filter was fitted during the break-in or the engine testing phase of this project. This was to ensure all wear particles collected in the lubricating oil was available to pass through the radiation detector.

## 3.6 Engine Testing

Following the run-in, the engine oil was drained and the engine flushed before being re-filled with SAE 5W-30 oil. Fresh oil was used at the start of each day in order to maintain repeatability across the test matrix and ensure the effect of oil aging was negated from the results. Initially three baseline steady state conditions were run – low load at low, medium and high speed. The medium speed baseline steady state condition was run every time the SAE 5W-30 oil was run in the engine, as a baseline point of reference.

Testing conditions were developed to subject the engine and oil to severe conditions and/or subject the engine to anticipated high wear events. They were chosen to be representative of the anticipated most severe wear conditions for the engine when operated in the field. Operating conditions are shown in Table 7, with the set points shown in Table 8. The turbo was replaced half way through the testing as a preventative measure against failure.

Each of the operating conditions were tested using both the SAE 5W-30 and the SAE 0W-16 oils. After each set of conditions were run using SAE 5W-30 oil, the engine was drained, flushed with SAE 0W-16 and then filled with SAE 0W-16 oil before the same engine conditions were repeated. Once completed, the next set of conditions were run using SAE 5W-30 after flushing with SAE 5W-30 oil. This allowed direct comparison at the same stage of overall engine wear. The only exception to this was that the cold start condition was run every morning when the engine had been lying idle overnight. In addition, after the initial baseline steady state conditions were run on the first day, the "Baseline Steady State Mid Speed" was repeated each time the SAE 5W-30 oil was in the engine. This was used as a baseline point of reference. In total 97.5 hours of engine testing were performed in this program.

**Table 7. Engine operating conditions**

| Operation Condition | Description |
|---|---|
| Baseline: Steady State, Low Speed | Hold engine at low speed and low load for extended period at warm engine temperatures. |
| Baseline: Steady State, Moderate Speed | Hold engine at moderate speed and low load for extended period at warm engine temperatures. |
| Baseline: Steady State, High Speed | Hold engine at high speed and low load for extended period at warm engine temperatures. |
| Cold Start | Once an engine has cooled and settled overnight, start engine and immediately accelerate to max torque for 30 seconds, ramp to low speed/moderate load for one minute, repeat three times. |
| Turbo Transient | Start at low speed/low load and ramp to medium speed/high load at hot engine temperatures, repeat for extended time. |
| Transient Load: Low Speed, Low-High Load | Ramp torque from low to high at low speed and warm engine temperatures |
| Transient Load: High Speed, Low-High Load | Ramp torque from low to high at high speed and warm engine temperatures |
| Transient Load: High Speed, High-Low Load | Ramp torque from high to low at high speed and warm engine temperatures |
| Transient Speed: Low Load, Low-High Speed | Ramp engine speed from low to high at low engine torque and warm engine temperatures |
| Transient Speed: High Load, Low-High Speed | Ramp engine speed from low to high at high engine torque and warm engine temperatures |
| Transient Speed: High Load, Low to High Speed, 115°C Oil | Ramp engine speed from low to high at high engine torque and hot engine temperatures |
| Trailer Tow | Start at low speed/max load, decrease load incrementally below max load, increase speed at just below max load curve to high speed/high load, increase load incrementally above max load (causing engine lugging), allow engine to slow to low speed/high load, reduce load to just under max load (to prevent engine stall), repeat for extended time. Hot engine temperatures. |
| Trailer Tow, 115°C Oil | Start at low speed/max load, decrease load incrementally below max load, increase speed at just below max load curve to high speed/high load, increase load incrementally above max load (causing engine lugging), allow engine to slow to low speed/high load, reduce load to just under max load (to prevent engine stall), repeat for extended time. Oil temperatures elevated 5-10°C above standard trailer tow cycle. Air intake temperature also elevated 20°C. |
| Boundary Lubrication | Start at max load and moderate engine speed. Hold WOT while slowly ramping engine speed to idle. Warm engine temperatures. |
| Stop-Start, 4hr Hot Temp | Hot start, immediate hard acceleration at high load to moderate speed for 20 sec, drop to low load/ moderate speed for 10 sec, stop engine, hot soak 1 min, repeat for extended period of time. |

| | |
|---|---|
| Stop-Start | Hot start, immediate hard acceleration at high load to moderate speed for 20 sec, drop to low load/ moderate speed for 10 sec, stop engine, hot soak 1 min, repeat for extended period of time. Hot engine temperatures. |
| Stop-Start, Very Cold | Hot start, immediate hard acceleration at high load to moderate speed for 20 sec, drop to low load/ moderate speed for 10 sec, stop engine, hot soak 1 min, repeat for extended period of time. Very cold engine temperatures. |
| Wide Open Throttle (WOT) Transient Cold | Ramp engine speed from low to high speed at high engine torque and cold engine temperatures |
| WOT: Steady State, 2500rpm | Hold engine at low speed and high load for extended period at warm engine temperatures. |
| WOT: Steady State, 3500rpm | Hold engine at high speed and high load for extended period at warm engine temperatures. Normal boost. |
| WOT: Steady State, 5000rpm | Hold engine at high speed and high load for extended period at cold engine temperatures. Normal boost. |
| WOT: 3500rpm Max. Boost | Hold engine at high speed and high load for extended period at cold engine temperatures. Maximum boost. |
| WOT: 5000rpm Max. Boost | Hold engine at high speed and high load for extended period at cold engine temperatures. Maximum boost. |

**Table 8. Engine temperature and torque set points**

| **Temperature (°C) Set Points** | | | | | | **Engine Torque (N-m) Set Points** | | |
|---|---|---|---|---|---|---|---|---|
| Test Point | Very Cold | Cold | Warm | Hot | Very Hot | Engine Speed (rpm) | Low Load | High Load |
| Oil Gallery Temp | 25 | 60 | 70 | 95 | 120 | Low - 2000 | 50 | 280 |
| Coolant Temp | 35 | 57 | 70 | 90 | 100 | Medium - 3500 | 50 | 330 |
| Charge Air Temp | 15 | 67 | 30 | 35 | 40 | High - 5000 | 50 | 315 |

## 4.0 RESULTS AND DISCUSSION

Wear values for each irradiated engine part were compiled for all of the test conditions, comparing the SAE 5W-30 and SAE 0W-16 lubricants. Figures 6-9 depict the wear trend for the top ring face, top ring side, second ring face and liners for both lubricants over the full test matrix. For clarity, only those results giving measurable wear values with consideration to the measurement technique have been included in the graphs, these values are noted on the graph titles. No data is presented for connecting rod bearing wear as there was no measureable wear after initial running-in. Table 9 shows a matrix of irradiated engine component vs. engine test sequence giving a concise overview of noticeable wear. Wear values included in graphs 6-9 are shown as grey cells.

Baseline steady state conditions, as noted in lines 1-3 of Table 7, were run prior to the start of the test matrix. The moderate speed steady state condition was run each time the engine was filled with SAE 5W-30 oil. This was used to monitor the wear rates to ensure no significant change occurred throughout the test program. Steady state wear was achieved throughout the testing.

**Table 9. Matrix of wear of irradiated engine part vs. engine test sequence**

| | Top Ring Face | Top Ring Side | Second Ring Face | Liner | Connecting Rod bearing |
|---|---|---|---|---|---|
| Cold Start | | | | | |
| Turbo Transient | | ■ | | | |
| Transient Load: Low Speed, Low-High Load | | | | ■ | |
| Transient Load: High Speed, Low-High Load | | ■ | | | |
| Transient Load: High Speed, High-Low Load | | ■ | ■ | | |
| Transient Speed: Low Load, Low-High Speed | ■ | | ■ | | |
| Transient Speed: High Load, Low-High Speed | ■ | ■ | ■ | ■ | |
| Transient Speed: High Load, Low-High Speed, 115°C Oil | | ■ | ■ | | |
| Trailer Tow | | | | | |
| Trailer Tow, 115°C Oil | ■ | ■ | ■ | ■ | |
| Boundary Lubrication | | | | ■ | |
| Stop-Start, 4hr Hot Temp | | | ■ | | |
| Stop-Start | ■ | ■ | ■ | ■ | |
| Stop-Start, Very Cold | ■ | ■ | ■ | ■ | |
| Wide Open Throttle (WOT) Transient Cold | ■ | ■ | ■ | | |
| WOT: Steady State, 2500rpm | | | | ■ | |
| WOT: Steady State, 3500rpm | | | | | |
| WOT: Steady State, 5000rpm | | | | | |
| WOT: 3500rpm, Max. Boost | | ■ | | | |
| WOT: 5000rpm, Max. Boost | | | | | |

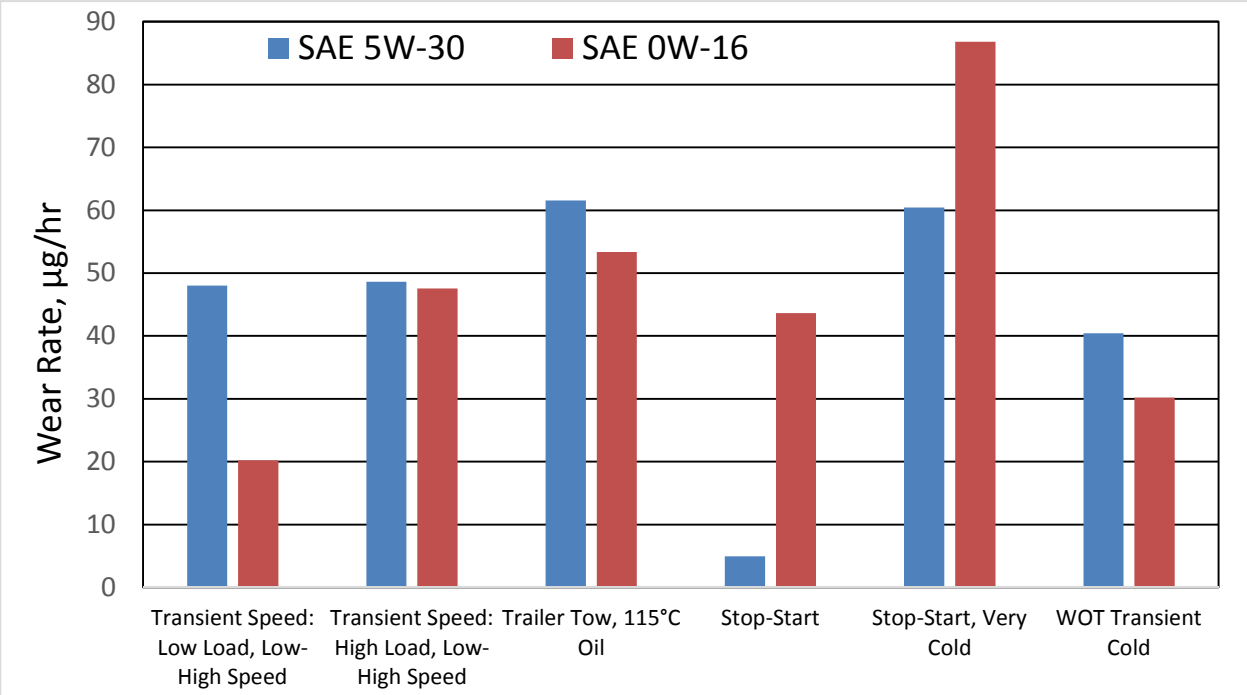


**Figure 6. Top ring face wear for test cycles showing greater than 40µg/hr on either oil**

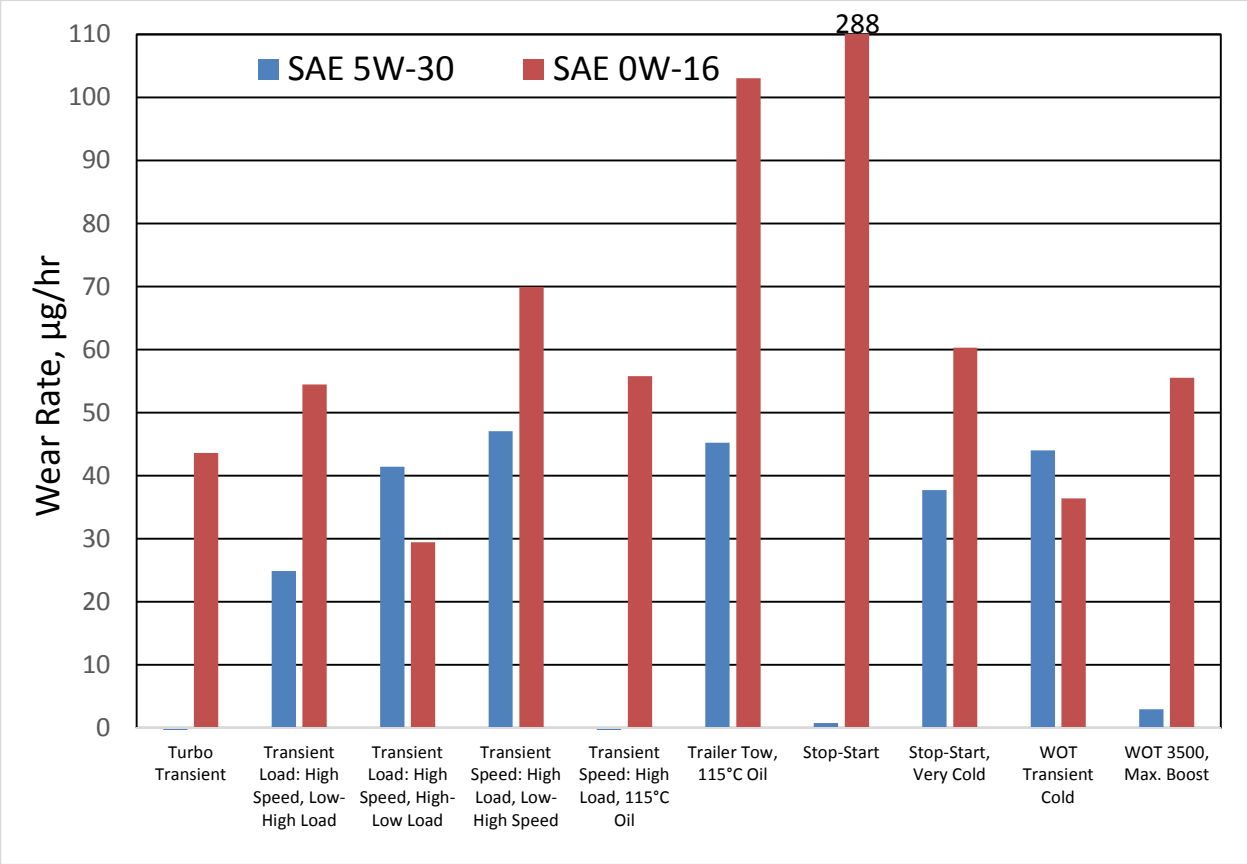


**Figure 7. Top ring side wear for test cycles showing greater than 30µg/hr on either oil**

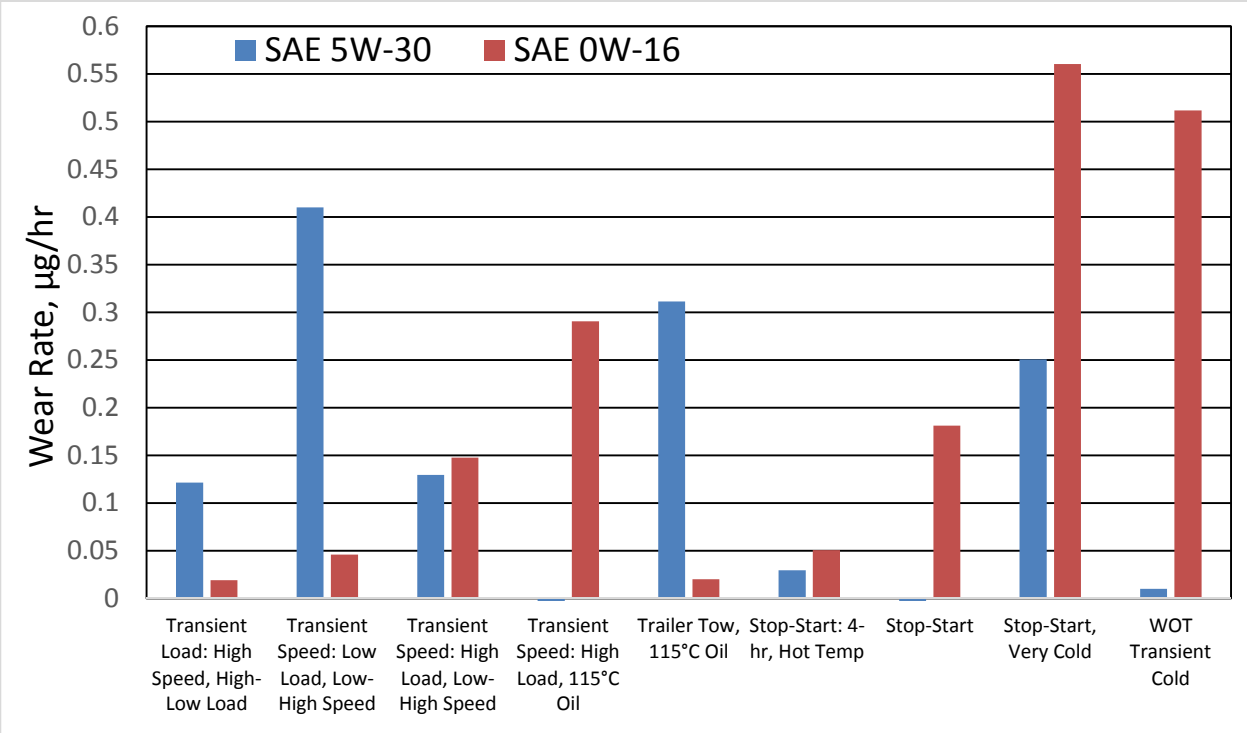


**Figure 8. Second Ring Face Wear for test cycles showing greater than 0.05µg/hr on either oil**

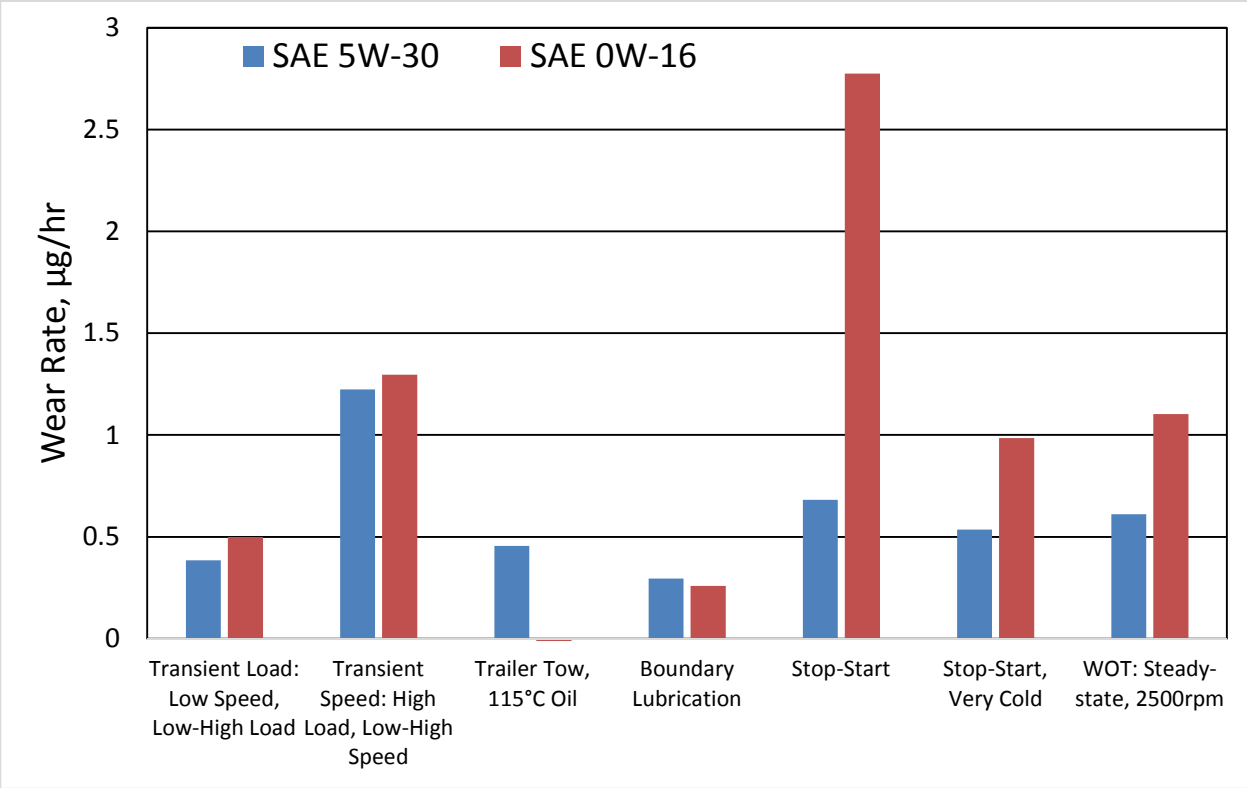


**Figure 9. Cylinder Liner Wear for test cycles showing greater than 0.3µg/hr on either oil**

Table 9 shows that there are a number of engine operating cycles that did not exhibit appreciable wear on any of the irradiated engine components. These include cold start, trailer tow at normal temperature, WOT 3500rpm and 5000rpm steady state, and WOT 5000rpm maximum boost. There are also some engine operating conditions that, if the rod bearings are ignored, exhibited wear across every component tested. These are the high load transient speed ramp from low to high speed, Trailer tow at 115°C and both the stop-start at normal and very cold temperature. In general, it can be seen from Table 9, that wear across engine components was more prevalent at transient conditions than at steady state conditions.

Although it may be expected that the SAE 0W-16 lubricant would give higher wear across all operating conditions and engine components tested, this did not prove to be the case, with a significant number of engine operating cycles giving higher component wear for the SAE 5W-30 oil.

The transient operating conditions gave higher top ring face wear for the SAE 5W-30 oil, whereas the top ring side wear was higher in almost all transient conditions for the SAE 0W-16 oil. No such clear distinction was evident for second ring face wear between viscosities during transient conditions with some favoring the lower and some the higher viscosity oil. The cylinder liner did not exhibit a significant difference in wear between lubricant viscosities under transient behavior.

There are very few steady state wear conditions with sufficient wear above the cut-off values used for the graphs, however the few available suggest that the SAE 0W-16 oil results in higher wear than the SAE 5W-30 oil. In all the engine components measured there is a large difference in wear between viscosities during stop-start operation, with SAE 0W-16 oil giving significantly higher wear values than SAE 5W-30 oil.

Seven engine operating conditions exhibited wear in one only engine component; three on the top ring side, one on the second ring face and three on the liner. These were:

- Transient Turbo, which showed wear for the top ring side using SAE 0W-16 oil only
- Transitioning from low to high load at high speed, which showed wear of the top ring side with more wear occurring for the SAE 0W-16 than the SAE 5W-30 oil
- Wide open throttle Maximum boost at 3500rpm, which showed higher wear for SAE 0W-16 oil than SAE 5W-30 oil.
- Stop-Start at high temperature , which showed wear for the second ring face
- Transitioning from low to high load at low speed, which showed wear of the liner with no differentiation between SAE 0W-16 and SAE 5W-30 oils.
- Boundary lubrication, which showed wear of the liner with no differentiation between SAE 0W-16 and SAE 5W-30 oils
- 2500rpm steady state with WOT, which showed wear of the liner showing higher wear with the SAE 0W-16 than the SAE 5W-30 oil.

Overall wear rates for the second ring face are two orders of magnitude lower when compared with those of the top ring face. This is a characteristic of the tapered napier profile on the second ring where a small contact exists between the liner and the second ring when compared with the contact between the liner and the top ring face.

From the results obtained, and considering a need to measure wear across lubricant viscosities, the following engine operating conditions could be used to obtain measureable wear in the engine components measured:

- Top ring face: Trailer tow at 115°C or very cold stop-start
- Top ring side: Trailer tow at 115°C or high load transition from low to high speed
- Second ring face: High load transition from low to high speed or very cold stop-start
- Liner wear: High load transition from low to high speed, very cold stop-start or WOT steady state at 2500rpm.

## 5.0 CONCLUSIONS

A project was undertaken to investigate the wear of rings, liner and connecting rod bearings in a Ford 2.0L Ecoboost engine using Radioactive Tracer Technology® to track real time wear of the components individually. The results clearly show the operating cycles that created significant wear in the irradiated engine components.

A significant amount of data was produced for the five irradiated engine components across the engine operating test matrix. The main findings are:

- After initial run-in, no measurable wear was recorded for the connecting rod bearings

- Comparing the wear rates using SAE 5W-30 and SAE 0W-16 oils, lower viscosity lubricant resulted in higher wear across roughly two thirds of the engine operating conditions

- In general, transient engine operating conditions created higher wear than steady state conditions

- The stop-start cycles produced some of the most significant difference in wear rates for the two lubricants and often the highest wear rates recorded

- The cold start cycles operated at the beginning of every day of testing did not exhibit appreciable wear rates on any of the irradiated components

- It is intuitive that higher load would result in higher wear between the ring face and liner. However, the results of this work show that not to be entirely accurate, with only transient speeds at high load giving significant top ting face, top ring side and liner wear. The WOT 3500 at maximum boost only produced significant wear on the top ring side when running with SAE 0W-16 oil.

# APPENDIX A

# Engine Specifications

| Item | Specification |
|---|---|
| **Engine** | |
| Displacement | 2.0L (122 Cubic Inch Displacement (CID)) |
| No. cylinders | 4 |
| Bore/stroke | 87.5 mm (3.4449 in) - 83.1 mm (3.2717 in) |
| Fire order | 1-3-4-2 |
| Oil pressure (hot @ 2,000 rpm) | 200 kPa (29.01 psi) - 268 kPa (38.87 psi) |
| Compression ratio | 9.3:1 |
| Spark plug | NGK T4025R |
| Spark plug gap | 0.8 mm (0.0315 in) |
| Engine weight (without accessory drive components) | 141 kg (311 lb) |
| **Cylinder Block** | |
| Cylinder bore diameter | 87.5 mm (3.4449 in) - 87.53 mm (3.4461 in) |
| Cylinder bore maximum out-of-round | 0.008 mm (0.0003 in) |
| Main bearing bore diameter | 57.018 mm (2.245 in) - 57.040 mm (2.246 in) |
| Head gasket surface flatness | 0.1 mm (0.0039 in) - 0.05 mm (0.002 in)/200 mm (7.874 in) x 200 mm (7.874 in) |
| **Piston and Connecting Rod** | |
| Piston diameter (grade 1) | 87.465 mm (3.4435 in) - 87.475 mm (3.4439 in) |
| Piston diameter (grade 2) | 87.4725 mm (3.4438 in) - 87.4875 mm (3.4444 in) |
| Piston diameter (grade 3) | 87.485 mm (3.4443 in) - 87.495 mm (3.4447 in) |
| Piston-to-cylinder bore clearance | 0.0225 mm (0.0009 in) - 0.0475 mm (0.0019 in) |
| Piston ring groove width - compression (top) | 1.23 mm (0.0484 in) - 1.25 mm (0.0492 in) |
| Piston ring groove width - compression (bottom) | 1.23 mm (0.0484 in) - 1.25 mm (0.0492 in) |
| Piston ring groove width - oil ring | 2.03 mm (0.0799 in) - 2.05 mm (0.0807 in) |
| Piston skirt coating thickness | 0.009 mm (0.0004 in) - 0.019 mm (0.0007 in) |
| Piston pin diameter | 22.497 mm (0.8857 in) - 22.5 mm (0.8858 in) |
| Piston pin length | 55.7 mm (2.1929 in) - 56 mm (2.2047 in) |
| Piston-to-pin clearance | 0.0035 mm (0.0001 in) - 0.045 mm (0.0018 in) |
| Piston pin-to-connecting rod clearance | 0.003 mm (0.0001 in) - 0.018 mm (0.0007 in) |
| Piston ring width ─ compression (top) | 1.2 mm (0.05 in) |

| Item | Specification |
|---|---|
| Piston ring width ─ compression (bottom) | 1.2 mm (0.05 in) |
| Piston ring width ─ oil | 2 mm (0.08 in) |
| Piston ring gap (in bore) ─ compression (top) | 0.17 mm (0.0067 in) - 0.27 mm (0.0106 in) |
| Piston ring gap (in bore) ─ compression (bottom) | 0.45 mm (0.0177 in) - 0.65 mm (0.0256 in) |
| Piston ring gap (in bore) ─ oil | 0.15 mm (0.0059 in) - 0.45 mm (0.0177 in) |
| Connecting rod bearing-to-crankshaft clearance | 0.027 mm (0.0011 in) - 0.052 mm (0.002 in) |
| Connecting rod bearing thickness | 1.495 mm (0.0589 in) - 1.519 mm (0.0598 in) |
| Connecting rod crankshaft bore diameter | 55.025 mm (2.1663 in) - 55.045 mm (2.1671 in) |
| Connecting rod pin bore diameter | 22.510 mm (0.8862 in) - 22.516 mm (0.8865 in) |
| Connecting rod length (center -to-center) | 155.869 mm (6.1366 in) |
| Connecting rod side clearance (assembled to crank) | 2.59 mm (0.1020 in) - 3.69 mm (0.1453 in) |
| Axial clearance | 0.014 mm (0.0006 in) - 0.36 mm (0.0142 in) |
| **Crankshaft** | |
| Main bearing journal diameter | 51.978 mm (2.0464 in) - 52.002 mm (2.0473 in) |
| Balance Shaft | |
| Main bearing clearance | 0.016 mm (0.0006 in) - 0.046 mm (0.0018 in) |
| Connecting rod journal diameter | 51.980 mm (2.0465 in) - 52 mm (2.0472 in) |
| End play | 0.22 mm (0.0087 in) - 0.45 mm (0.0177 in) |
| **Cylinder Head** | |
| Cylinder head gasket surface flatness | 0.08 mm (0.0031 in) maxim overall, a maximum of 0.05 mm (0.0020 in)<br>within 150 mm (5.9055 in) and a maximum of 0.025 mm (0.0010 in) within 25 mm (0.9843 in) |
| Maximum valve lift @ 0 lash ─ exhaust | 6.9 mm (0.2717 in) |
| Maximum valve lift @ 0 lash ─ intake | 7.9 mm (0.3110 in) |
| Valve guide diameter | 5.509 mm (0.2169 in) - 5.539 mm (0.2181 in) |
| Valve seat width - intake/exhaust | 1.40 mm (0.0551 in) - 1.50 mm (0.0591 in) |
| Valve seat angle | 45° |
| Valve eat runout | 0.075 mm (0.003 in) |
| Valve lash adjuster bore diameter | 31 mm (1.2205 in) - 31.03 mm (1.2217 in) |
| Cam bore diameter | 25.015 mm (0.9848 in) - 25.04 mm (0.9858 in) |
| **Valve** | |
| Valve head diameter - intake | 32.5 mm (1.2795 in) |

| Item | Specification |
|---|---|
| Valve head diameter - exhaust | 28 mm (1.1024 in) |
| Valve stem diameter - intake | 5.5 mm (0.2165 in) |
| Valve stem diameter - exhaust | 5.5 mm (0.2165 in) |
| Valve stem-to-guide clearance - intake | 0.03 mm (0.0012 in) - 0.07 mm (0.0028 in) |
| Valve stem-to-guide clearance - exhaust | 0.03 mm (0.0012 in) - 0.07 mm (0.0028 in) |
| Valve face runout | 0.05 mm (0.002 in) |
| Valve face angle | 45.25° - 45.75° |
| **Valve Spring ─ Compression Pressure** | |
| Intake and exhaust (installed) | 17 kg (37.478 lb) |
| Intake (valve open) 9.2 mm (0.3622 in) of lift | 39 kg (85.979 lb) |
| Exhaust (valve open) 9.2mm (0.3622 in) of lift | 42 kg (92.593 lb) |
| Free length | 47.91 mm (1.8862 in) |
| Assembled height | 37.9 mm (1.4921 in) |
| **Valve Tappet** | |
| Diameter | 30.98 mm (1.2197 in) - 30.964 mm (1.2191 in) |
| Tappet-to-valve clearance ─ intake | 0.19mm (0.0075 in) - 0.31 mm (0.0122 in) |
| Tappet-to-valve clearance ─ exhaust | 0.30 mm (0.0118 in) - 0.42 mm (0.0165 in) |
| Tappet-to-bore clearance | 0.02 mm (0.0008 in) - 0.06 mm (0.0024 in) |
| **Camshaft** | |
| Lobe lift ─ intake | - |
| Lobe lift ─ exhaust | - |
| Runout | 0.03 mm (0.0012 in) |
| Thrust clearance | 0.115 mm (0.0045 in) - 0.145 mm (0.0057 in) |
| Journal diameter | 24.96 mm (0.9827 in) - 24.98 mm (0.9835 in) |
| Journal-to-bore clearance | 0.035 mm (0.0014 in) - 0.08 mm (0.0031 in) |

# APPENDIX B

# Test Cycles

**Controlled Parameters**

| | |
|---|---|
| Engine Speed | rpm |
| Engine Load | Nm |
| Coolant Out Temp | deg C |
| Oil Gallery Temp | deg C |
| Air Charge Temp | deg C |
| Coolant Pressure | kPaG |

**Monitored Parameters**

| | |
|---|---|
| Inlet Air Temp | deg C |
| Inlet Air Press | kPaG |
| Exhaust Back Press | kPaA |
| Humidity | g/kg |
| Coolant Flow | L/m |
| Lambda | unitless |
| Barometric Pressure | kPaA |
| Oil Gallery Pressure | kPaG |
| Oil Head Pressure | kPaG |
| Oil Out Temp | deg C |
| Exhaust Temp | deg C |
| Crank Case Pressure | kPaG |
| Fuel Pressure | kPaG |
| Power | kW |
| Pre-Intercooler Air Pressure | kPaA |
| Ambient Temperature | degC |
| Coolant In Temperature | degC |
| Boost Pressure | kPaA |
| Fuel Temp | deg C |
| Fuel Flow | kg/hr |
| Manifold Absolute Pressure (MAP) | kPaA |

**PCM CAN Bus Parameters**

| | |
|---|---|
| Ignition Timing Advance for #1Cylinder | Deg |
| Absolute Throttle Position | % |
| Engine Coolant Temperature | Deg C |
| Intake Air Temperature | Deg C |
| Equivalence Ratio (Lambda) | unitless |
| Absolute Load Value | % |
| Intake Manifold Absolute Pressure | kPa |
| Fuel Rail Pressure | kPa |
| Accelerator Pedal Position | % |
| Boost Absolute Pressure - Raw Value | kPa |
| Turbocharger Wastegate Duty Cycle | % |
| Actual Intake (A) Camshaft Position | Deg |
| Actual Exhaust (B) Camshaft Position | Deg |
| Intake (A) Camshaft Position Actuator Duty Cycle | % |
| Exhaust (B) Camshaft Position Actuator Duty Cycle | % |
| Charge Air Cooler Temperature | Deg C |

# APPENDIX C

# Test Matrix and Engine Operating Conditions

| Test Condition | Oil |
|---|---|
| Note A = 5w30, B = 0w16. | |
| Cold Start | A |
| Baseline Steady State Low Speed | A |
| Baseline Steady State Mid Speed | A |
| Baseline Steady State High Speed | A |
| Stop-Start | A |
| *Oil Change to Oil B* | |
| Cold Start | B |
| Stop-Start | B |
| Transient Load, Low Speed, Low to High Load | B |
| *Oil Change to Oil A* | |
| Cold Start | A |
| Transient Load, Low Speed, Low to High Load | A |
| Transient Load, High Speed, Low to High Load | A |
| Baseline Steady State Mid Speed | A |
| *Oil Change to Oil B* | |
| Cold Start | B |
| Transient Load, High Speed, Low to High Load | B |
| Transient Load, High Speed, High to Low Load | B |
| *Oil Change to Oil A* | |
| Cold Start | A |
| Transient Load, High Speed, High to Low Load | A |
| Transient Speed, Low Load, Low to High Speed | A |
| Baseline Steady State Mid Speed | A |
| *Oil Change to Oil B* | |
| Cold Start | B |
| Transient Speed, Low Load, Low to High Speed | B |
| Transient Speed, High Load, Low to High Speed | B |
| *Oil Change to Oil A* | |
| Cold Start | A |
| Transient Speed, High Load, Low to High Speed | A |
| Baseline Steady State Mid Speed | A |
| | |
| Cold Start | A |
| Stop-Start | A |
| Baseline Steady State Mid Speed | A |
| *Oil Change to Oil B* | |
| Cold Start | B |
| Stop-Start | B |
| Transient Load, High Speed, Low to High Load | B |
| *Oil Change to Oil A* | |
| Cold Start | A |
| Transient Load, High Speed, Low to High Load | A |

| | |
|---|---|
| Transient Speed, High Load | A |
| Baseline Steady State Mid Speed | A |
| *Oil Change to Oil B* | |
| Cold Start | B |
| Transient Speed, High Load | B |
| ***Turbocharger Replacement*** | |
| Cold Start | A |
| WOT Transient | A |
| Baseline Steady State Mid Speed | A |
| *Oil Change to Oil B* | |
| WOT Transient | B |
| Cold Start | B |
| Trailer Tow | B |
| *Oil Change to Oil A* | |
| Cold Start | A |
| Trailer Tow | A |
| Turbo Transient | A |
| Baseline Steady State Mid Speed | A |
| *Oil Change to Oil B* | |
| Cold Start | B |
| Turbo Transient | B |
| WOT: steady-state, low speed | B |
| *Oil Change to Oil A* | |
| Cold Start | A |
| WOT: steady-state, low speed | A |
| Cold Start | A |
| WOT: steady state, moderate speed | A |
| Baseline Steady State Mid Speed | A |
| *Oil Change to Oil B* | |
| WOT: steady state, moderate speed | B |
| Cold Start | B |
| WOT: steady state, high speed | B |
| *Oil Change to Oil A* | |
| WOT: steady state, high speed | A |
| Cold Start | A |
| Boundary Lubrication | A |
| Baseline Steady State Mid Speed | A |
| *Oil Change to Oil B* | |
| Cold Start | B |
| Boundary Lubrication | B |

Once the original test matrix was completed, there were additional hours remaining. Therefore additional testing was undertaken to clarify some observations made during testing.

| **Test Description** | **Oil** |
|---|---|
| Stop-Start (4 hours) | Oil B |
| *Oil Change to Oil A* | |
| Stop-Start (4 hours) | Oil A |
| Trans Speed High Load (115 C Oil) | Oil A |
| Baseline Steady State Mid Speed | Oil A |
| *Oil Change to Oil B* | |
| Trans Speed High Load (115 C Oil) | Oil B |
| WOT 3500 | Oil B |
| *Oil Change to Oil A* | |
| WOT 3500 | Oil A |
| Trailer Tow (115 C oil) | Oil A |
| Baseline Steady State Mid Speed | Oil A |
| *Oil Change to Oil B* | |
| Trailer Tow (115 C oil) | Oil B |
| Stop-Start Very Cold | Oil B |
| *Oil Change to Oil A* | |
| Stop-Start Very Cold | Oil A |
| WOT 5000 cold | Oil A |
| Baseline Steady State Mid Speed | Oil A |
| *Oil Change to Oil B* | |
| WOT 5000 cold | Oil B |

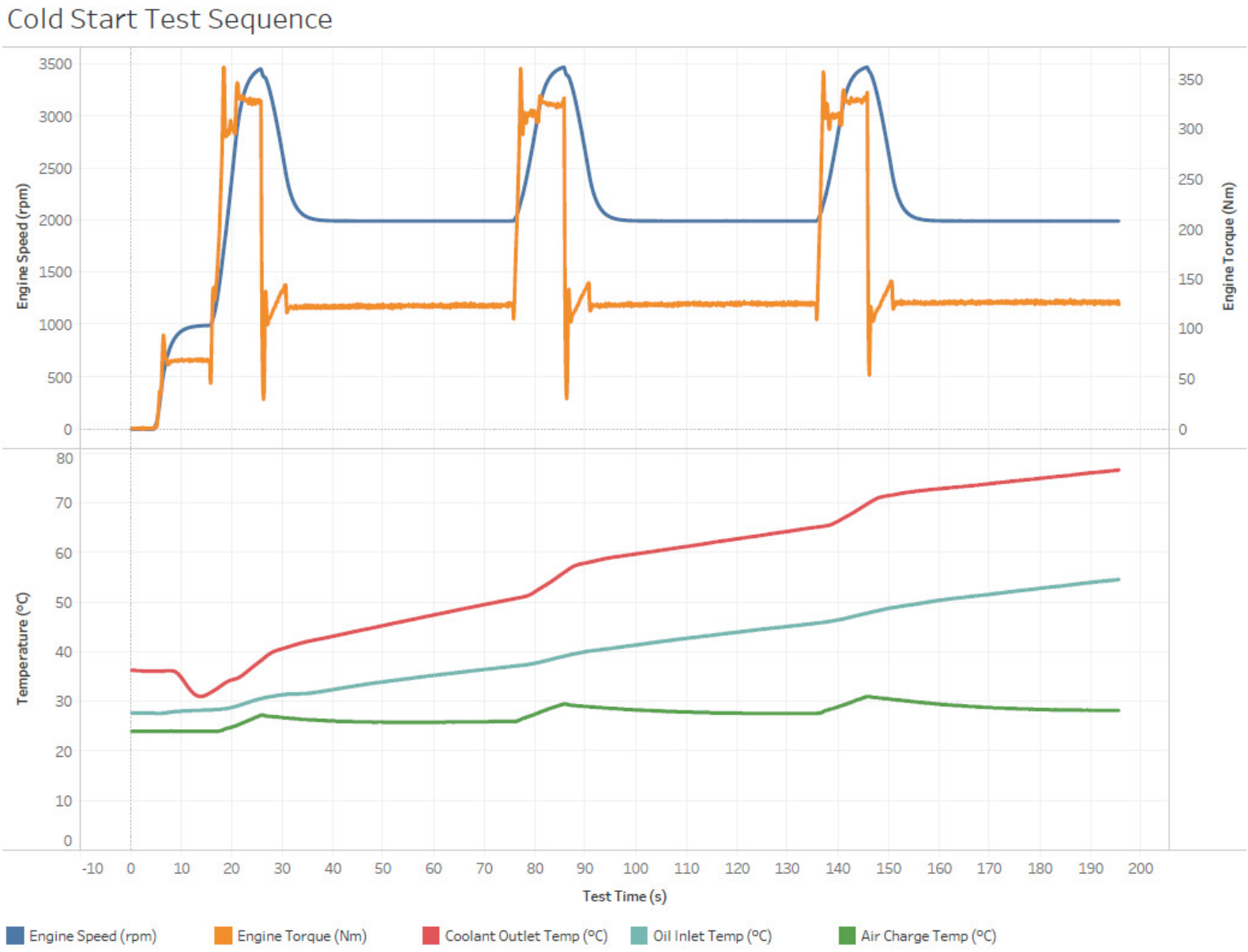
Cold Start Test Sequence
Engine Speed (rpm)
Engine Torque (Nm)
Temperature (°C)
Test Time (s)
Engine Speed (rpm)
Engine Torque (Nm)
Coolant Outlet Temp (°C)
Oil Inlet Temp (°C)
Air Charge Temp (°C)

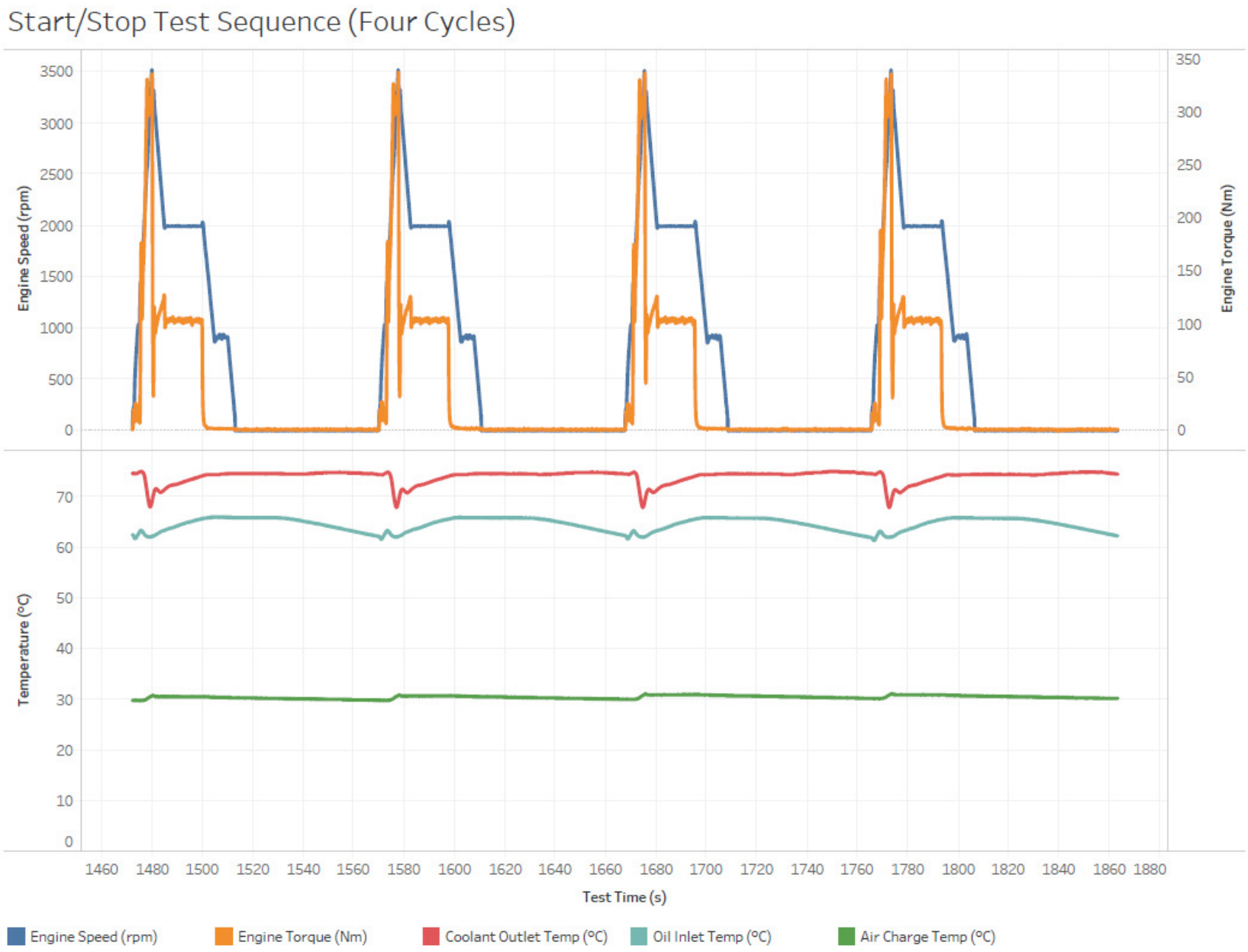
Start/Stop Test Sequence (Four Cycles)
Engine Speed (rpm)
Engine Torque (Nm)
Temperature (°C)
Test Time (s)
Engine Speed (rpm)
Engine Torque (Nm)
Coolant Outlet Temp (°C)
Oil Inlet Temp (°C)
Air Charge Temp (°C)

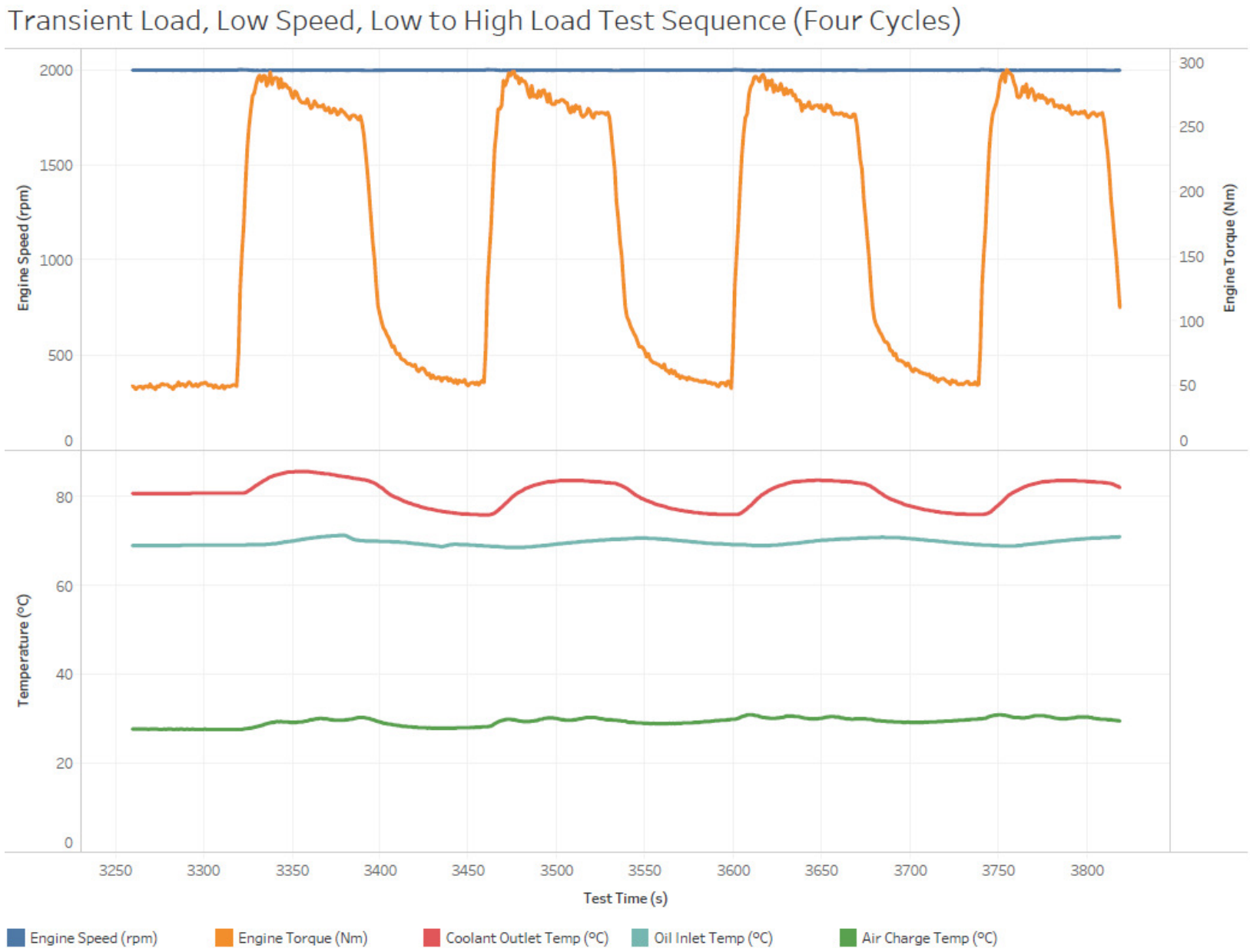
Transient Load, Low Speed, Low to High Load Test Sequence (Four Cycles)
Engine Speed (rpm)
2000
1500
1000
500
0
Engine Torque (Nm)
300
250
200
150
100
50
0
Temperature (°C)
80
60
40
20
0
3250
3300
3350
3400
3450
3500
3550
3600
3650
3700
3750
3800
Test Time (s)
Engine Speed (rpm)
Engine Torque (Nm)
Coolant Outlet Temp (°C)
Oil Inlet Temp (°C)
Air Charge Temp (°C)

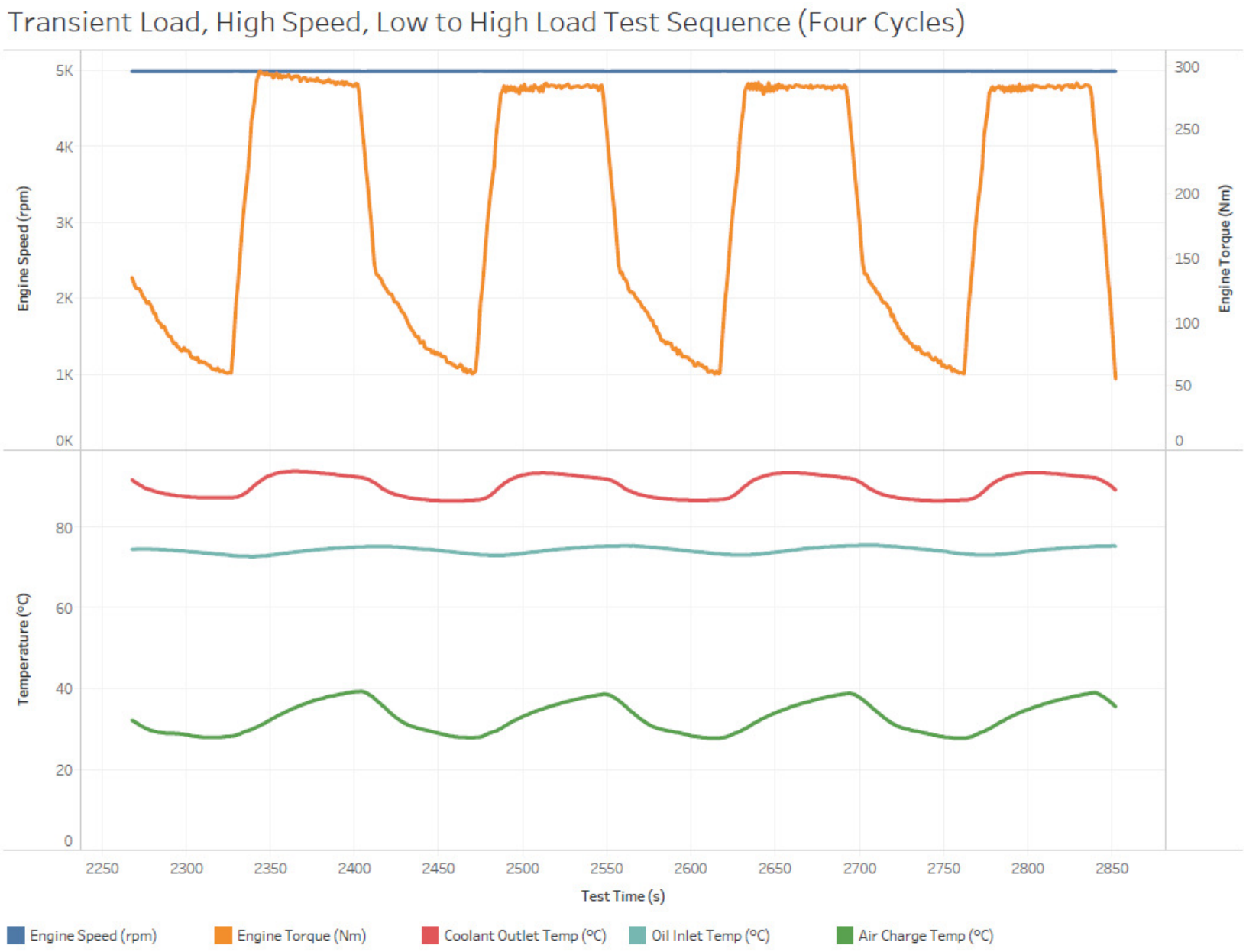
Transient Load, High Speed, Low to High Load Test Sequence (Four Cycles)
Engine Speed (rpm)
5K
4K
3K
2K
1K
0K
Engine Torque (Nm)
300
250
200
150
100
50
0
Temperature (°C)
80
60
40
20
0
2250
2300
2350
2400
2450
2500
2550
2600
2650
2700
2750
2800
2850
Test Time (s)
Engine Speed (rpm)
Engine Torque (Nm)
Coolant Outlet Temp (°C)
Oil Inlet Temp (°C)
Air Charge Temp (°C)

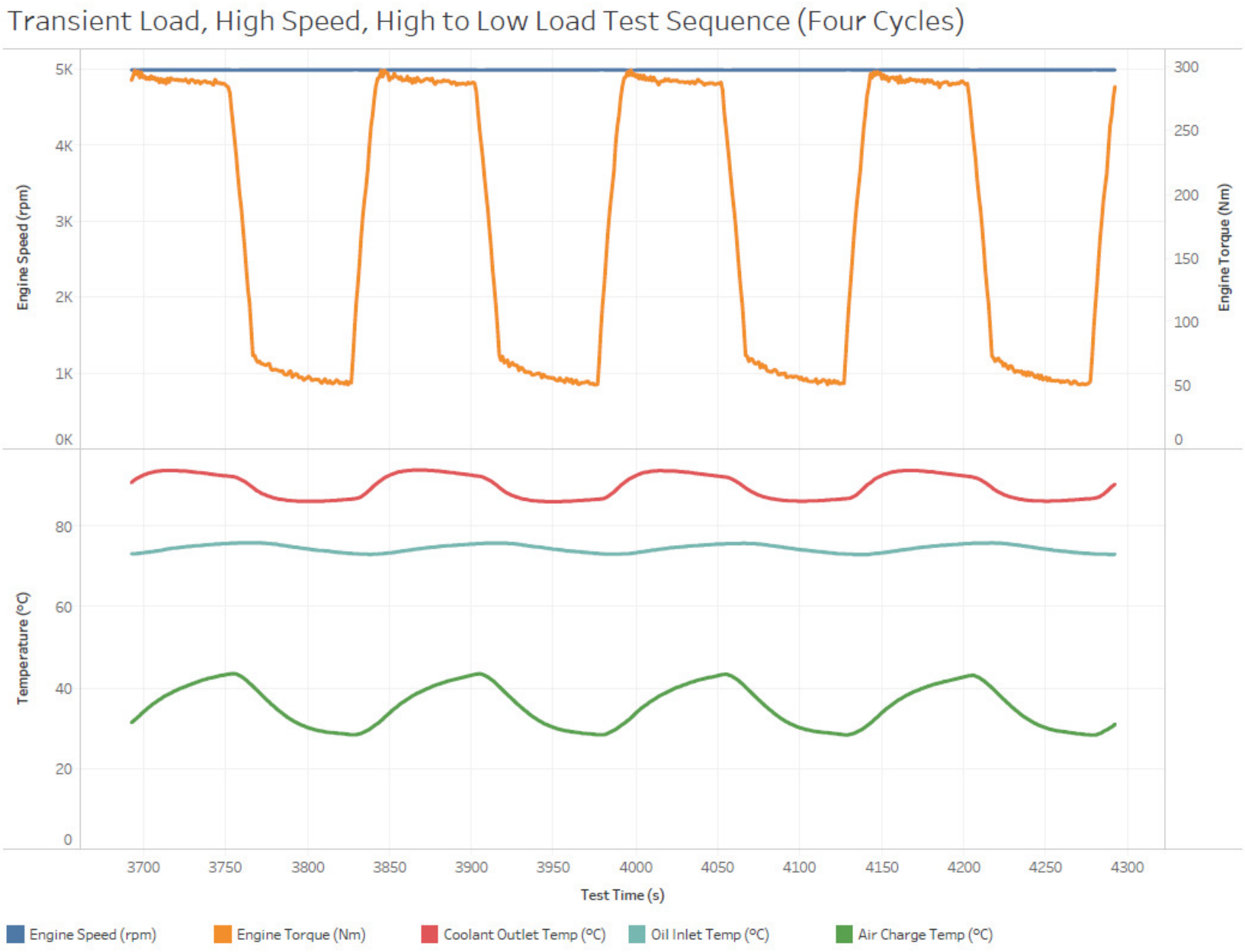
Transient Load, High Speed, High to Low Load Test Sequence (Four Cycles)
Engine Speed (rpm)
5K
4K
3K
2K
1K
0K
Engine Torque (Nm)
300
250
200
150
100
50
0
Temperature (°C)
80
60
40
20
0
3700
3750
3800
3850
3900
3950
4000
4050
4100
4150
4200
4250
4300
Test Time (s)
Engine Speed (rpm)
Engine Torque (Nm)
Coolant Outlet Temp (°C)
Oil Inlet Temp (°C)
Air Charge Temp (°C)

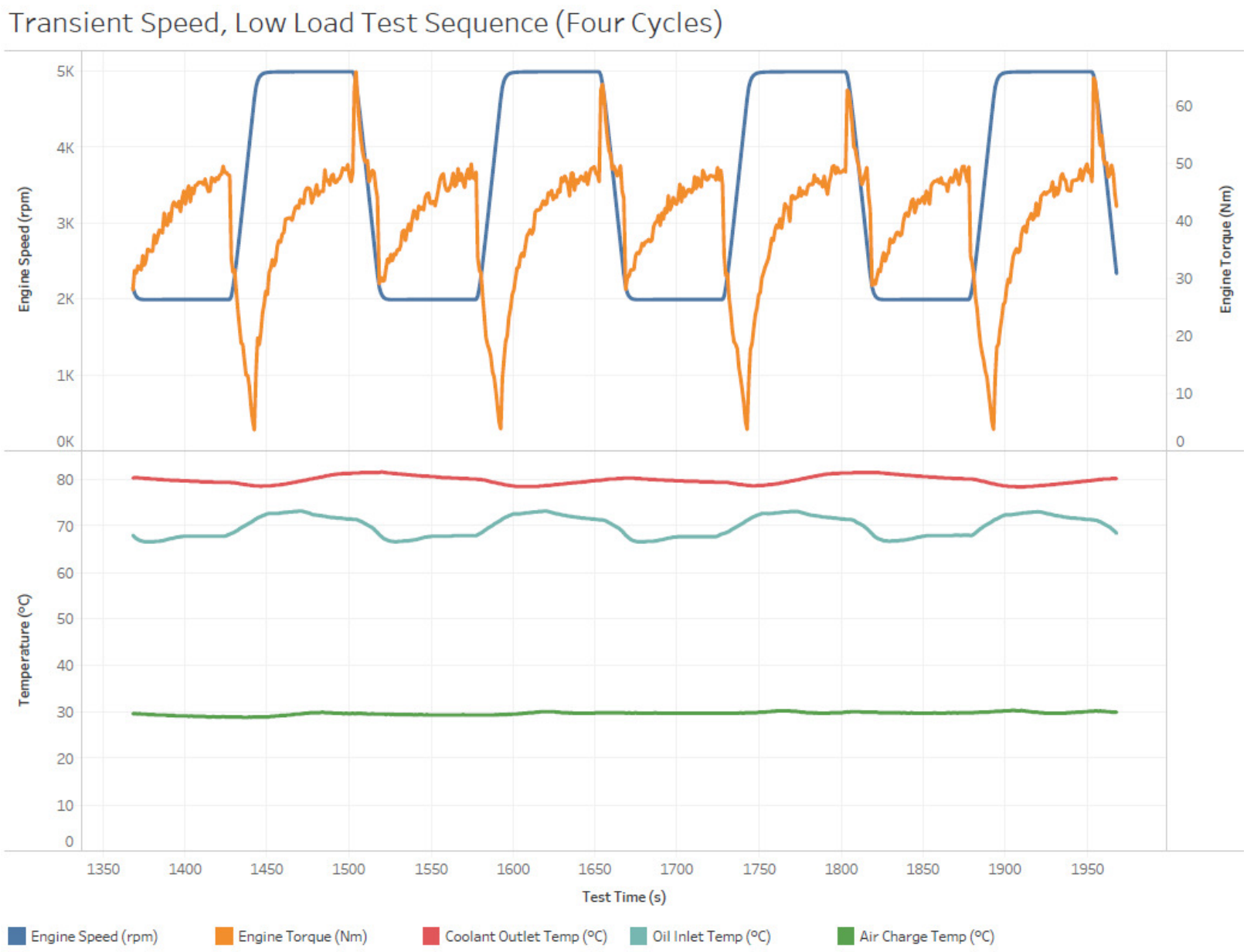
Transient Speed, Low Load Test Sequence (Four Cycles)
Engine Speed (rpm)
5K
4K
3K
2K
1K
0K
Engine Torque (Nm)
60
50
40
30
20
10
0
Temperature (°C)
80
70
60
50
40
30
20
10
0
1350
1400
1450
1500
1550
1600
1650
1700
1750
1800
1850
1900
1950
Test Time (s)
Engine Speed (rpm)
Engine Torque (Nm)
Coolant Outlet Temp (°C)
Oil Inlet Temp (°C)
Air Charge Temp (°C)

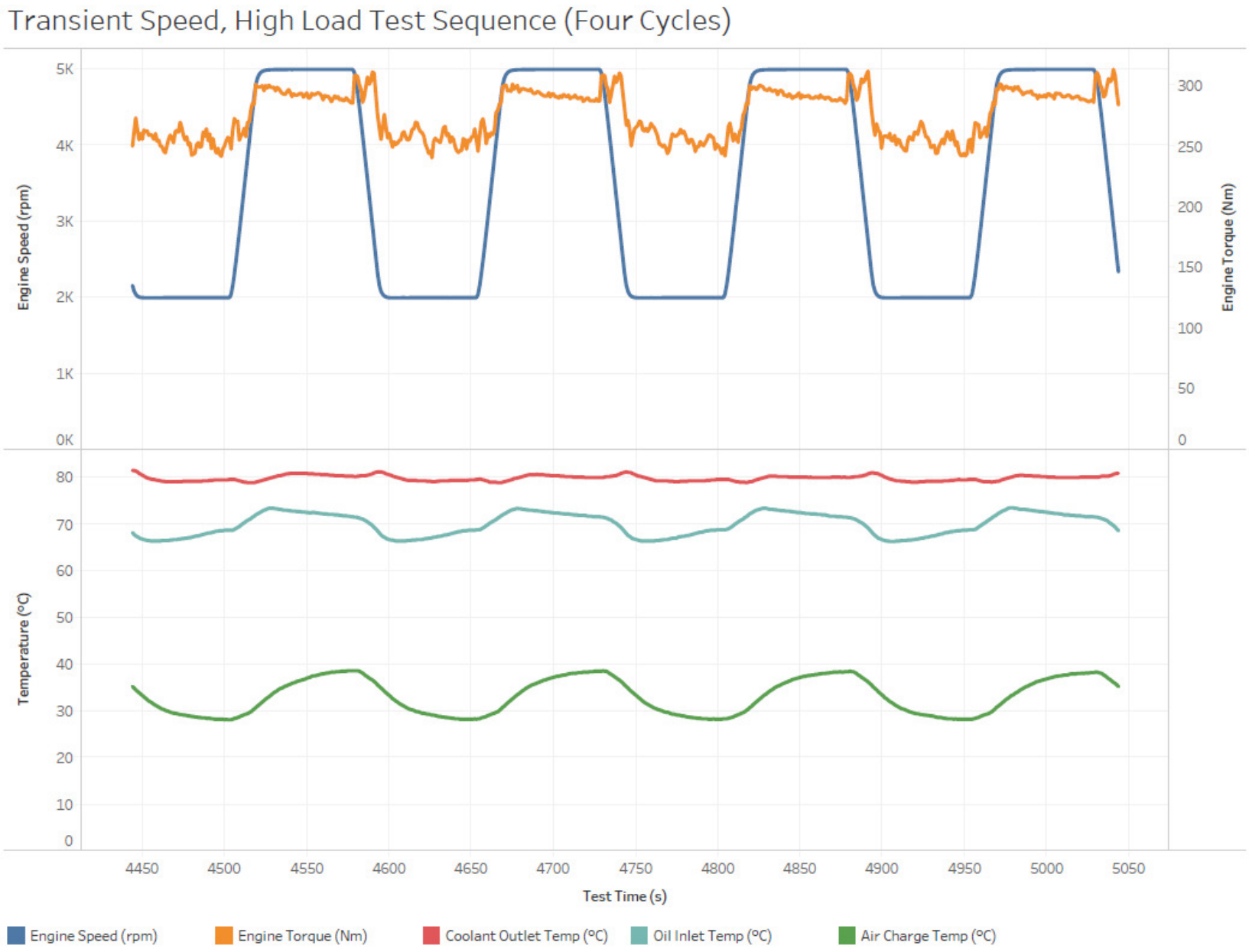
Transient Speed, High Load Test Sequence (Four Cycles)
Engine Speed (rpm)
5K
4K
3K
2K
1K
0K
Engine Torque (Nm)
300
250
200
150
100
50
0
Temperature (°C)
80
70
60
50
40
30
20
10
0
4450
4500
4550
4600
4650
4700
4750
4800
4850
4900
4950
5000
5050
Test Time (s)
Engine Speed (rpm)
Engine Torque (Nm)
Coolant Outlet Temp (°C)
Oil Inlet Temp (°C)
Air Charge Temp (°C)

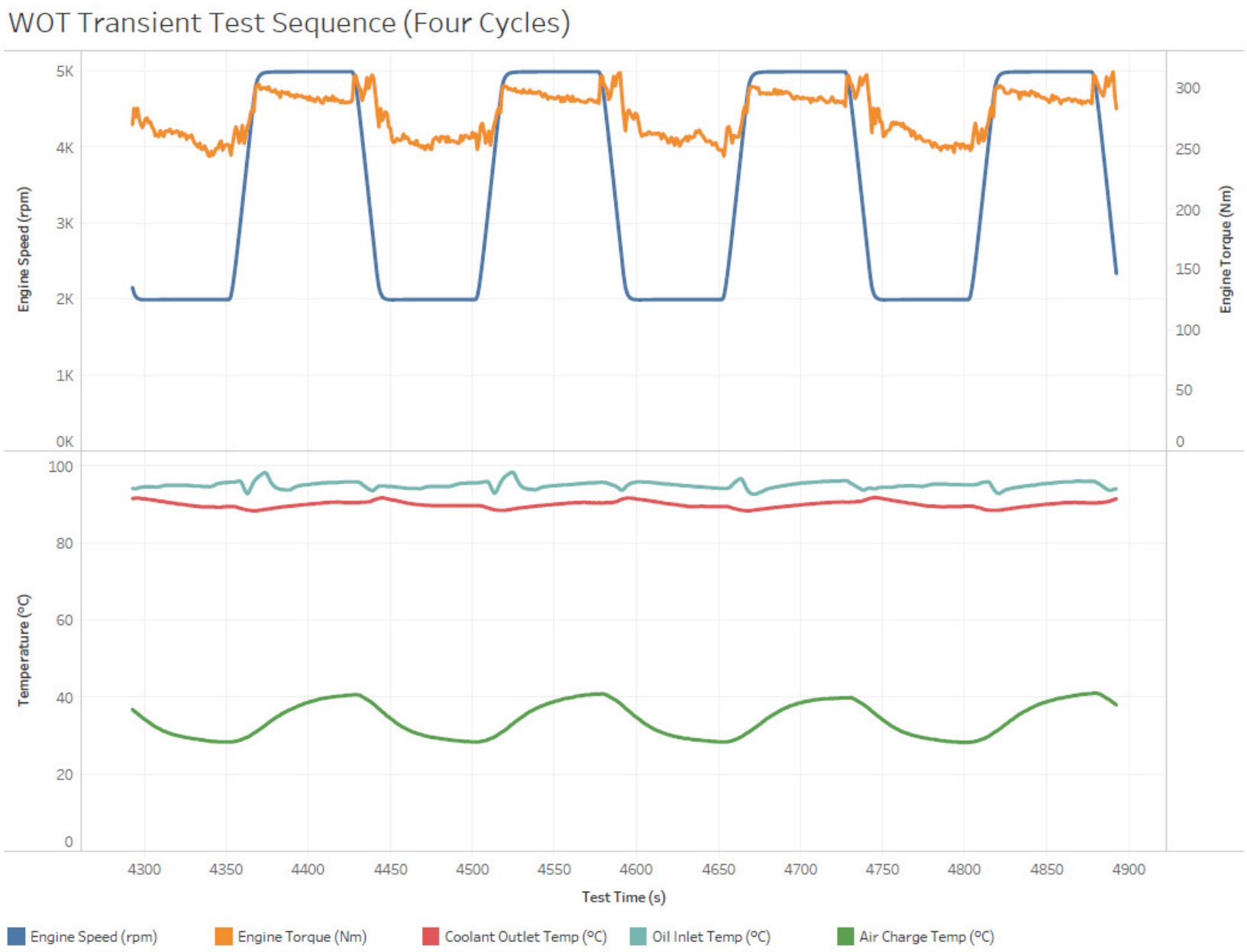
WOT Transient Test Sequence (Four Cycles)
Engine Speed (rpm)
5K
4K
3K
2K
1K
0K
Engine Torque (Nm)
300
250
200
150
100
50
0
Temperature (°C)
100
80
60
40
20
0
4300
4350
4400
4450
4500
4550
4600
4650
4700
4750
4800
4850
4900
Test Time (s)
Engine Speed (rpm)
Engine Torque (Nm)
Coolant Outlet Temp (°C)
Oil Inlet Temp (°C)
Air Charge Temp (°C)

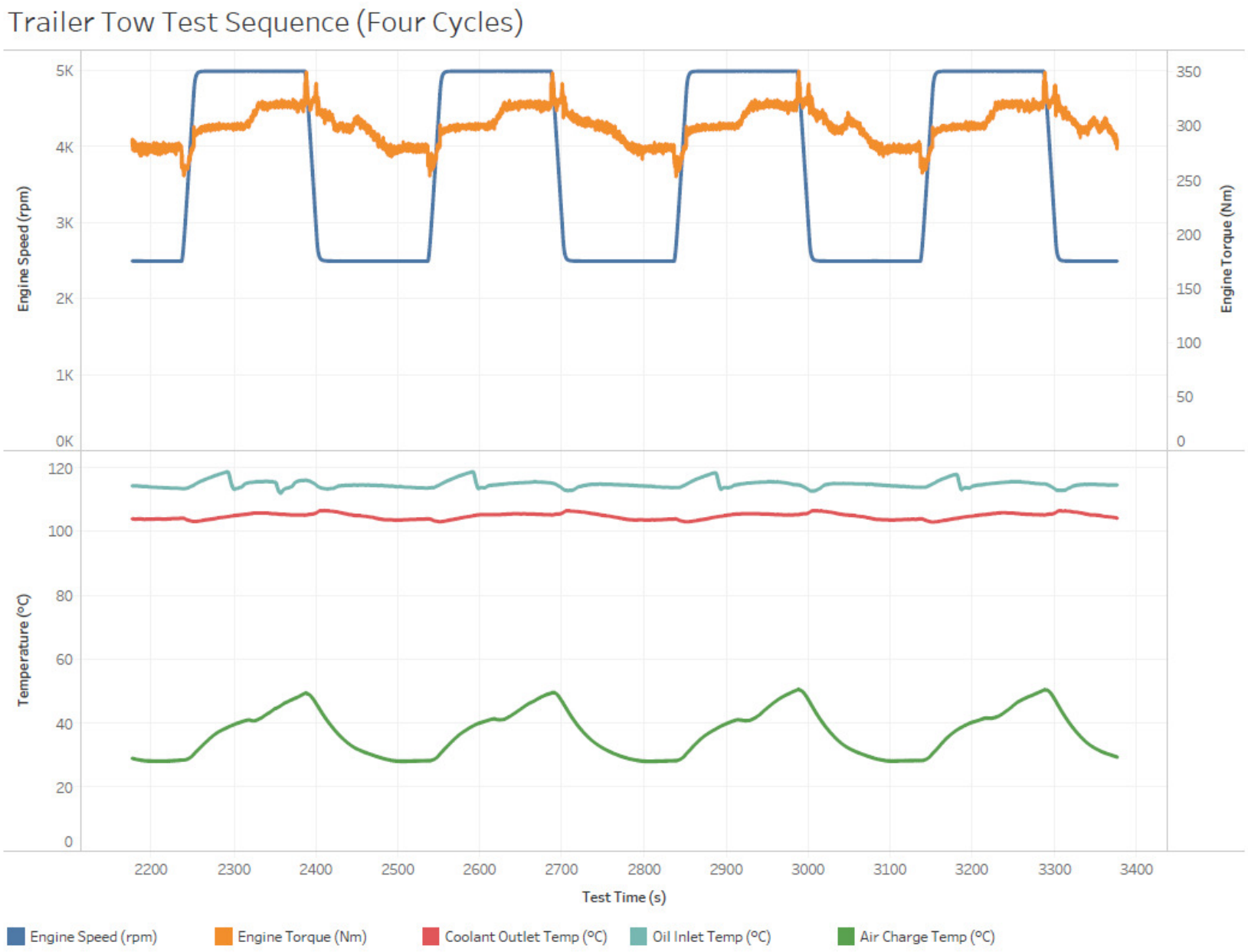
Trailer Tow Test Sequence (Four Cycles)
Engine Speed (rpm)
5K
4K
3K
2K
1K
0K
Engine Torque (Nm)
350
300
250
200
150
100
50
0
Temperature (°C)
120
100
80
60
40
20
0
2200
2300
2400
2500
2600
2700
2800
2900
3000
3100
3200
3300
3400
Test Time (s)
Engine Speed (rpm)
Engine Torque (Nm)
Coolant Outlet Temp (°C)
Oil Inlet Temp (°C)
Air Charge Temp (°C)

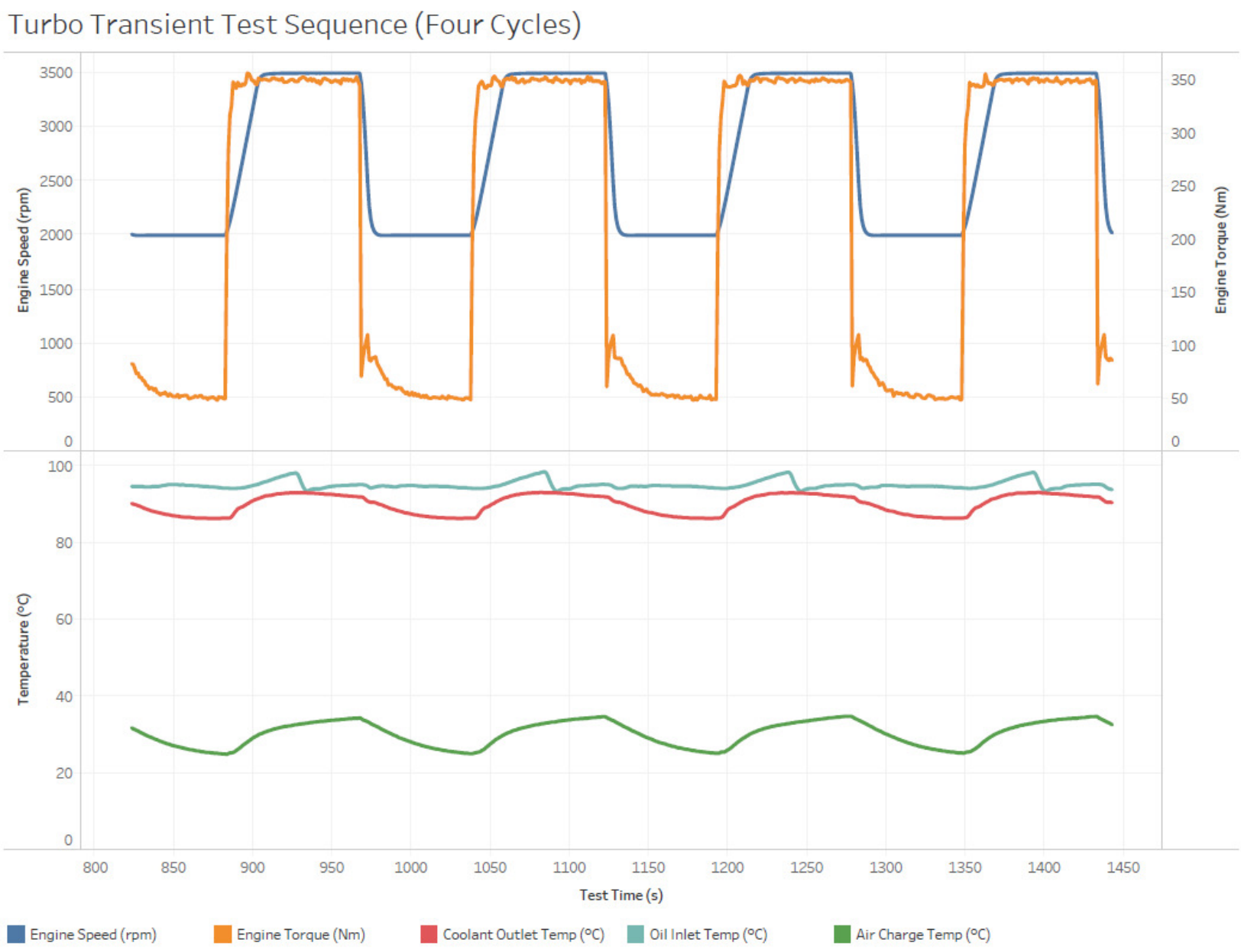
Turbo Transient Test Sequence (Four Cycles)
Engine Speed (rpm)
Engine Torque (Nm)
Temperature (°C)
Test Time (s)
Engine Speed (rpm)
Engine Torque (Nm)
Coolant Outlet Temp (°C)
Oil Inlet Temp (°C)
Air Charge Temp (°C)

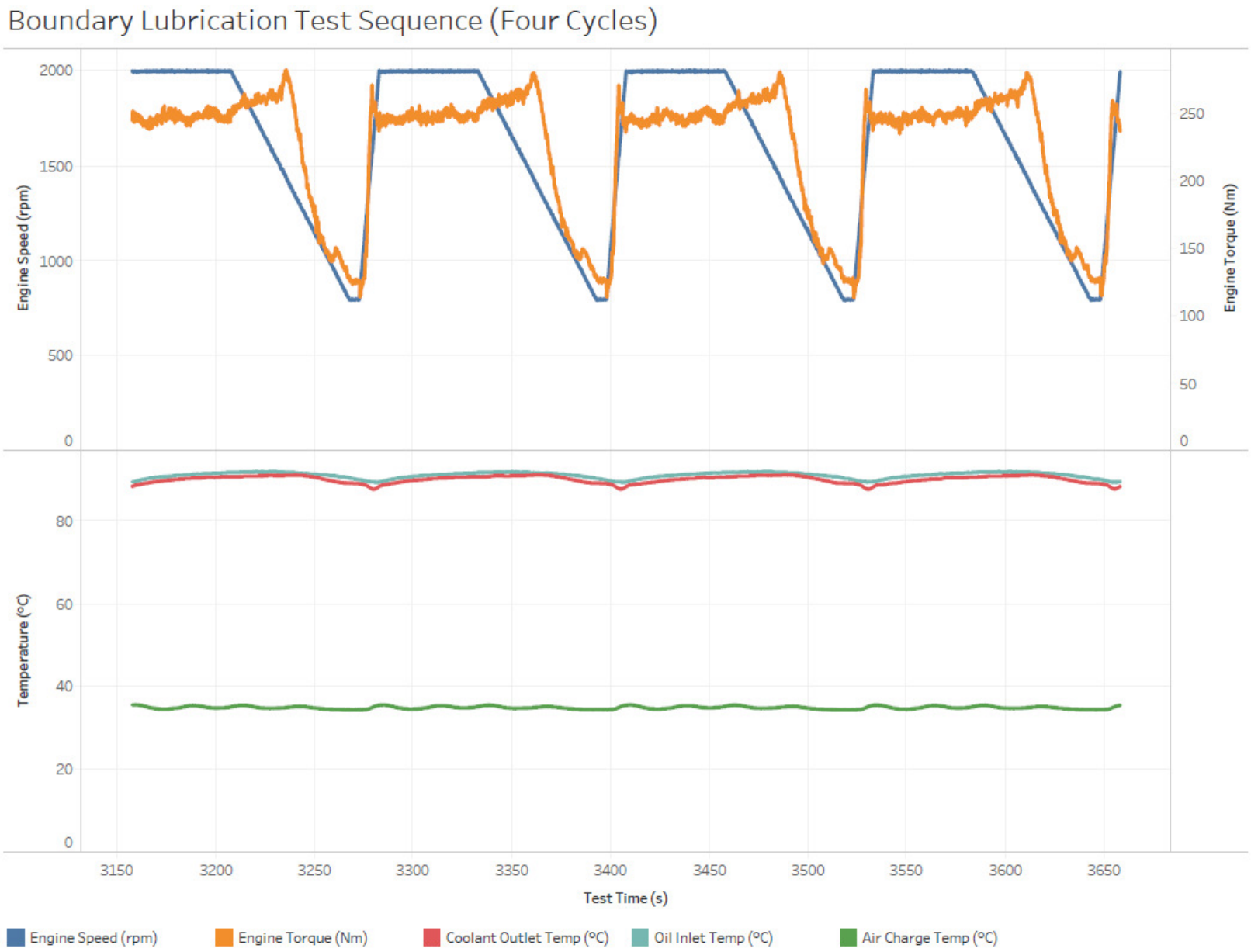
Boundary Lubrication Test Sequence (Four Cycles)
Engine Speed (rpm)
2000
1500
1000
500
0
Engine Torque (Nm)
250
200
150
100
50
0
Temperature (°C)
80
60
40
20
0
3150
3200
3250
3300
3350
3400
3450
3500
3550
3600
3650
Test Time (s)
Engine Speed (rpm)
Engine Torque (Nm)
Coolant Outlet Temp (°C)
Oil Inlet Temp (°C)
Air Charge Temp (°C)

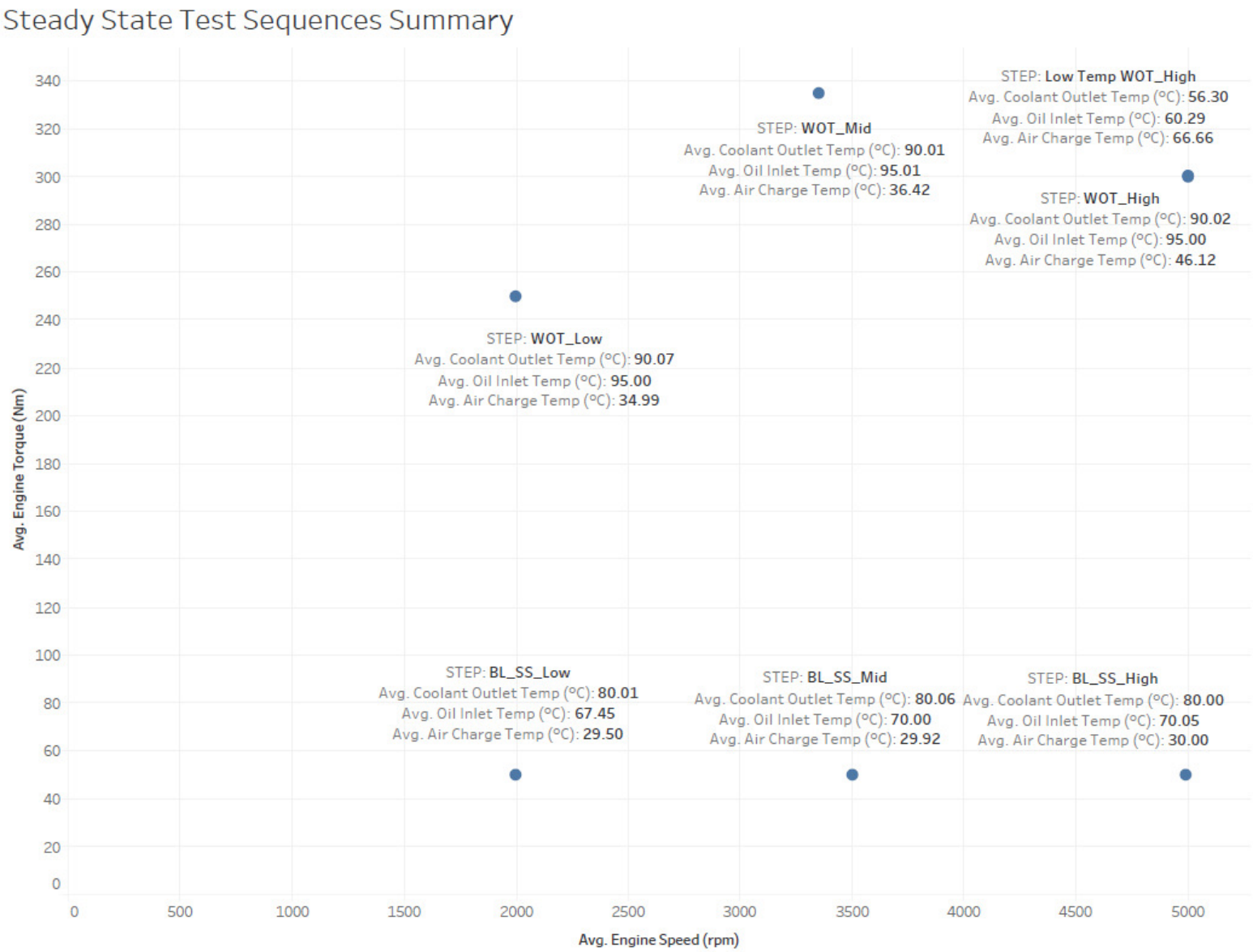


WOT = Wide Open Throttle. BL = Baseline

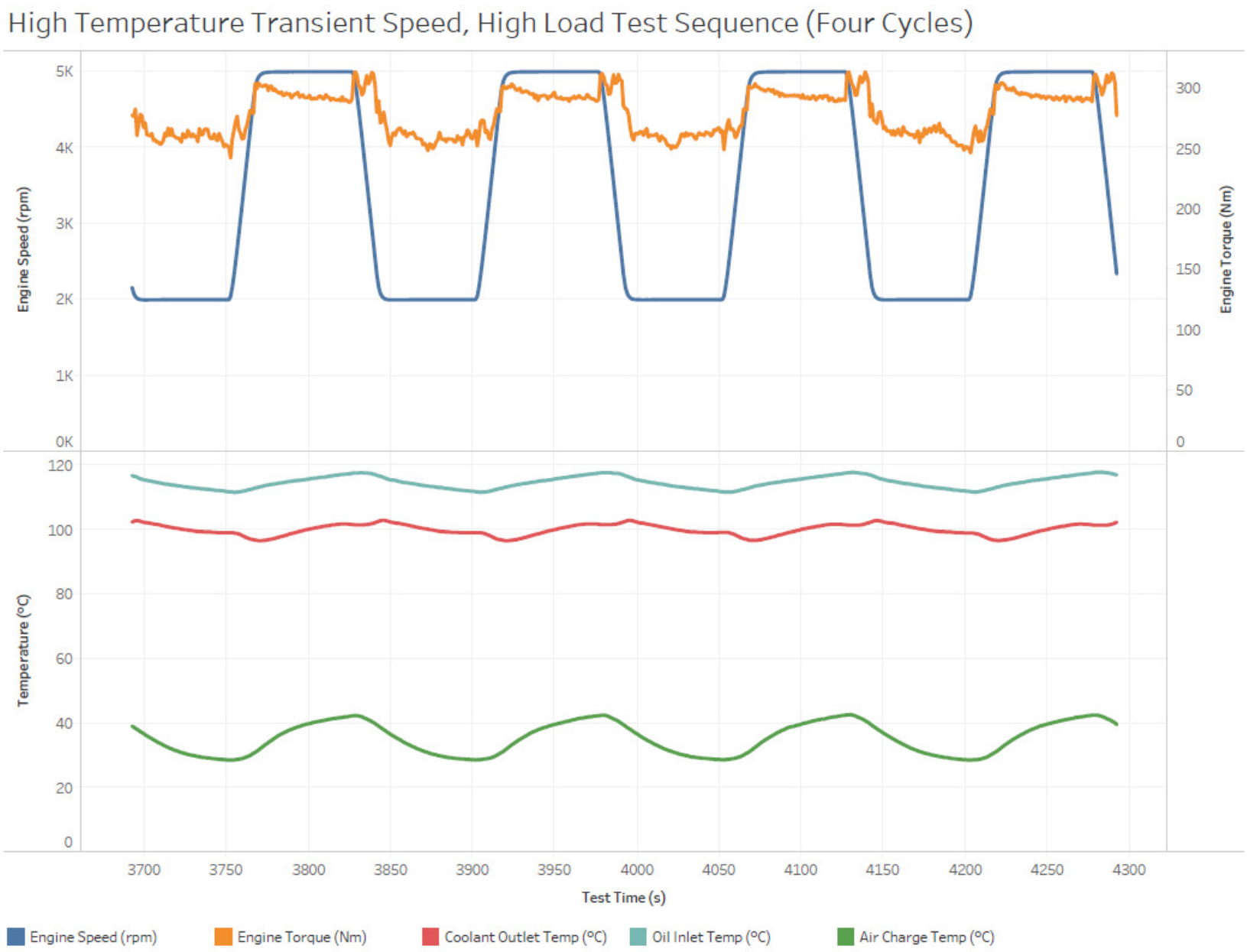
High Temperature Transient Speed, High Load Test Sequence (Four Cycles)
Engine Speed (rpm)
5K
4K
3K
2K
1K
0K
Engine Torque (Nm)
300
250
200
150
100
50
0
Temperature (°C)
120
100
80
60
40
20
0
3700
3750
3800
3850
3900
3950
4000
4050
4100
4150
4200
4250
4300
Test Time (s)
Engine Speed (rpm)
Engine Torque (Nm)
Coolant Outlet Temp (°C)
Oil Inlet Temp (°C)
Air Charge Temp (°C)

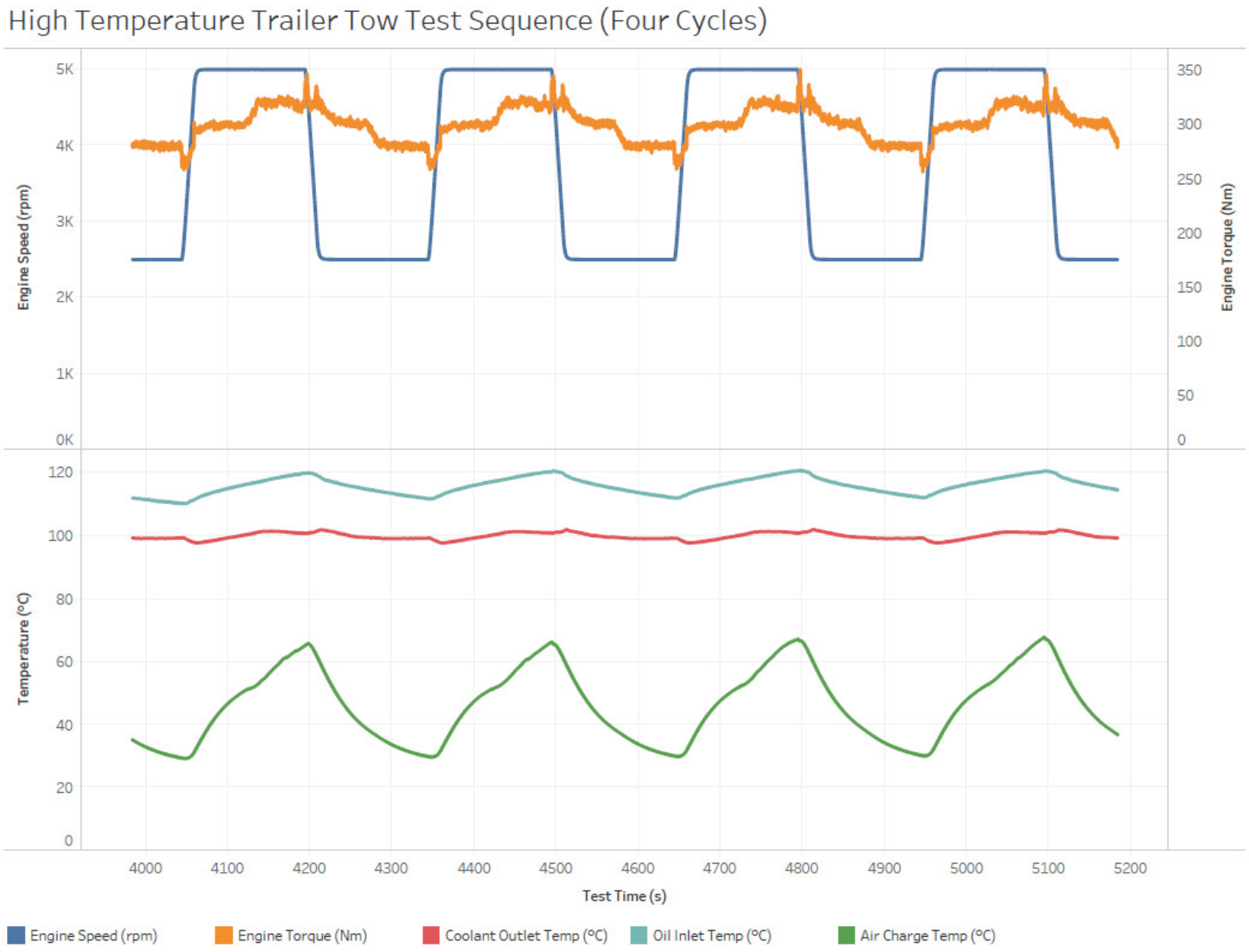
High Temperature Trailer Tow Test Sequence (Four Cycles)
Engine Speed (rpm)
5K
4K
3K
2K
1K
0K
Engine Torque (Nm)
350
300
250
200
150
100
50
0
Temperature (°C)
120
100
80
60
40
20
0
4000
4100
4200
4300
4400
4500
4600
4700
4800
4900
5000
5100
5200
Test Time (s)
Engine Speed (rpm)
Engine Torque (Nm)
Coolant Outlet Temp (°C)
Oil Inlet Temp (°C)
Air Charge Temp (°C)

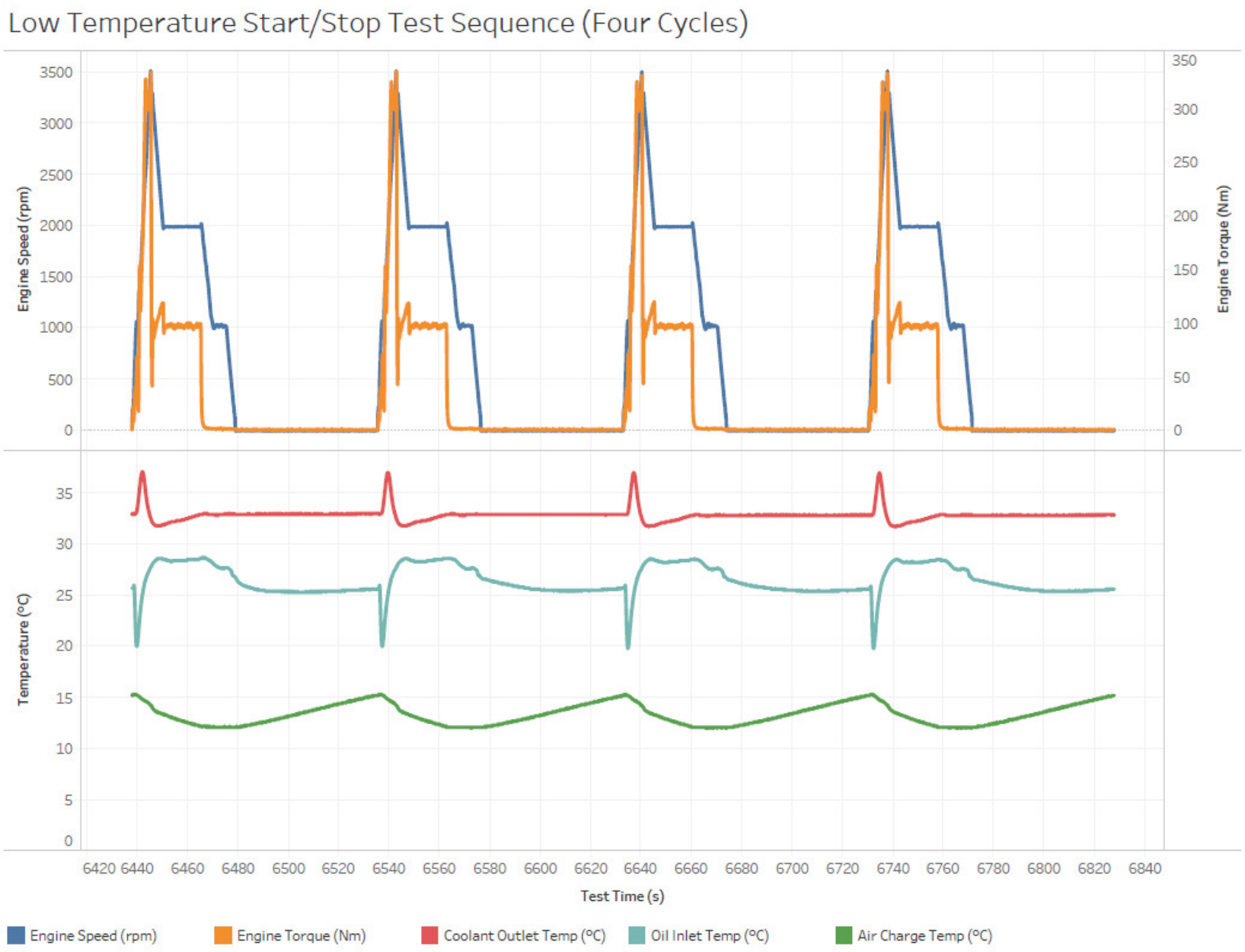
Low Temperature Start/Stop Test Sequence (Four Cycles)
Engine Speed (rpm)
Engine Torque (Nm)
Temperature (°C)
Test Time (s)
Engine Speed (rpm)
Engine Torque (Nm)
Coolant Outlet Temp (°C)
Oil Inlet Temp (°C)
Air Charge Temp (°C)

# APPENDIX D

# Run-in wear

This was a high-risk research project that required substantial support from Ford. Ford provided information and assistance regarding several questions that were critical to the success of the project including 1) verification that the ECU calibration provided sufficient knock mitigation to protect the engine from damage during the extensive high-load operation called for in the test matrix and 2) establishing safe operating limits to protect the turbocharger from overheating. Ford met their obligations to SwRI and the testing was successful. In addition there were a number of critical stage gates established so this project could be successful. Both CRC and SwRI met their obligations in meeting these stage gates.

Between 50 and 67 hours of the break-in cycle, the wear rates exhibited linear trends and the decision was made to move to the testing phase. Charts D1-D7 show the decay count data, and curve fits (with derivate).

Many of these graphs show cyclical variation with approximately an 8-hour period of oscillation. This is thought to result from the fact that the engine was operated 8 hours per 24 hour daily period. Wear particles likely settled from the oil overnight and took a while to become re-entrained in the oil during operation the next day, thus producing the daily signal oscillation.

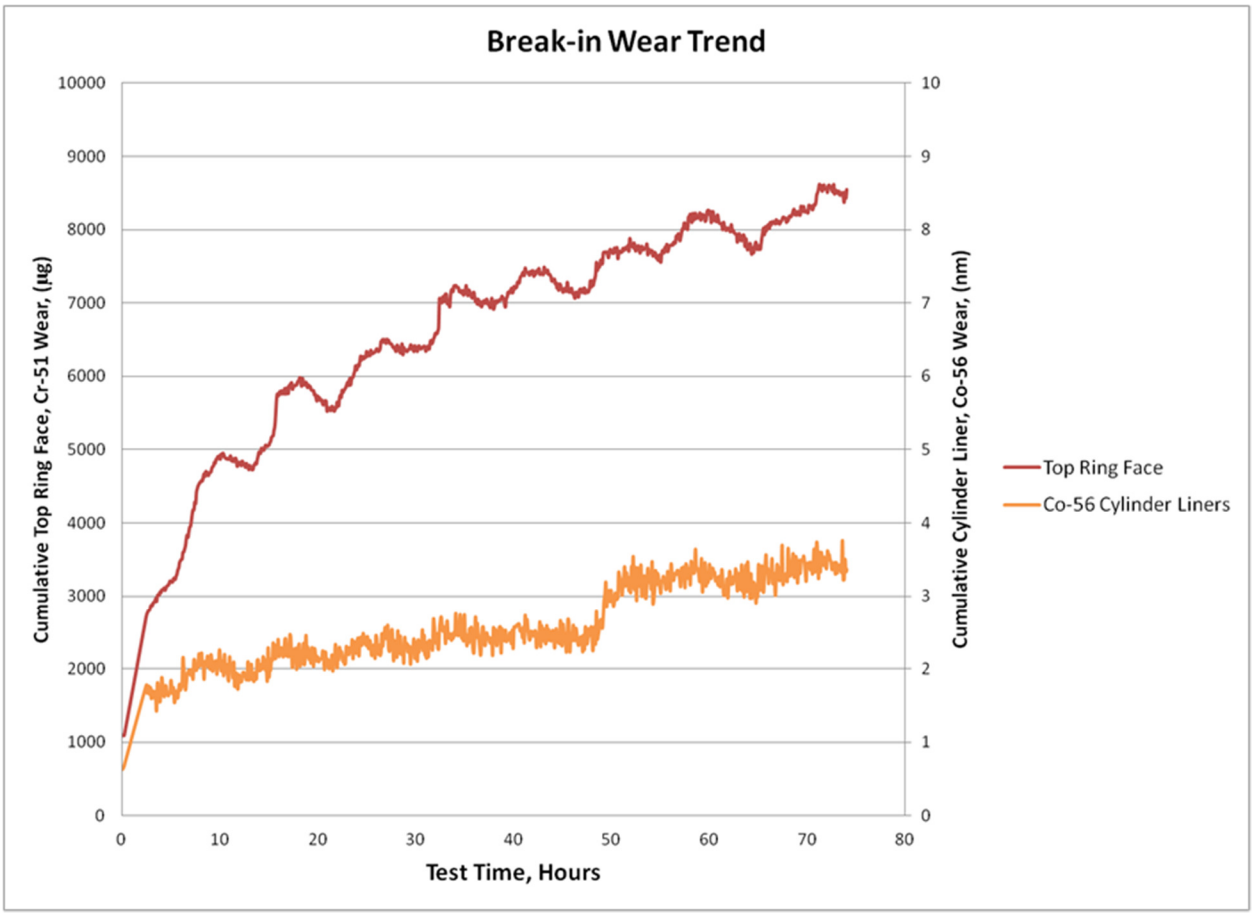


**Figure D1. Run-in Wear Trends for Cylinder Liners and Top Ring Face Isotopes**

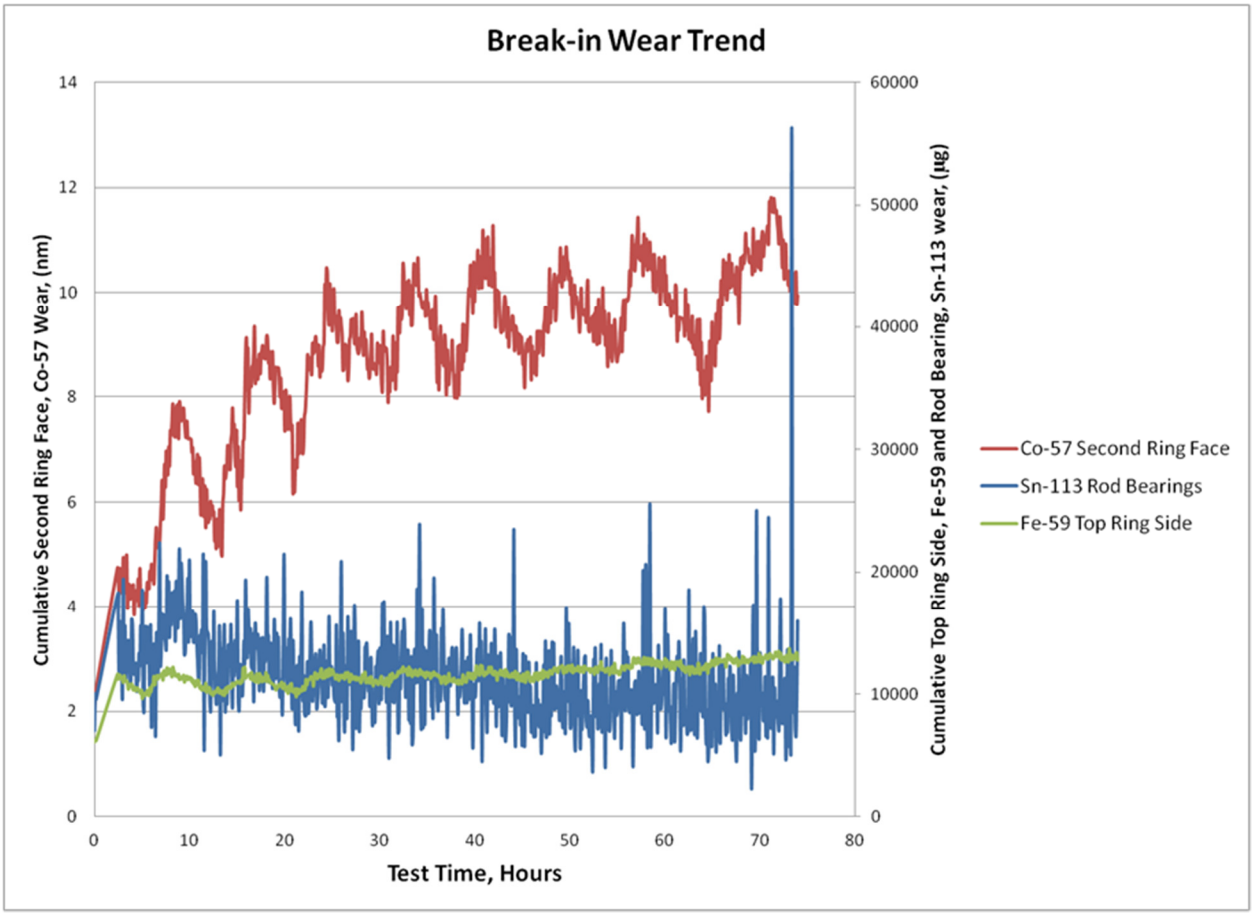


**Figure D2. Run-in wear trends for Top Ring Side, Rod Bearings, and Second Ring Face**

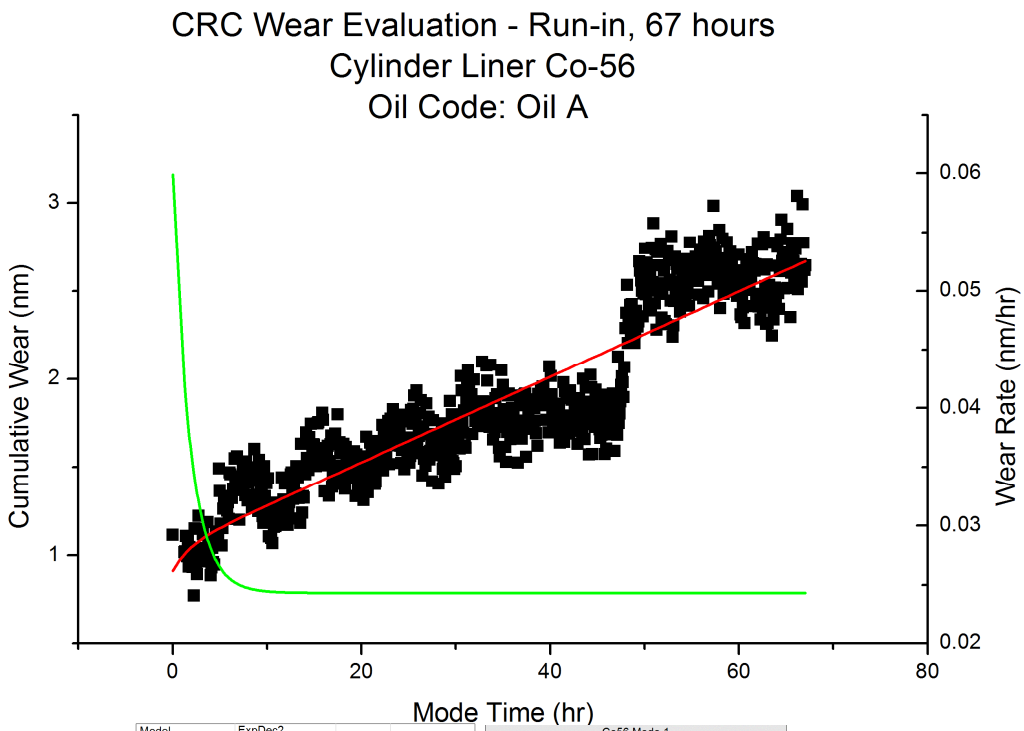


| Model | ExpDec2 | | |
|---|---|---|---|
| Equation | y = y0+A1*exp(-x/t1) + A2*x | | |
| Reduced Chi-Sqr | 0.03981 | | |
| Adj. R-Square | 0.84549 | | |
| | | Value | Standard Error |
| Second Ring Face Co56 | y0 | 1.03817 | 0.01806 |
| | A1 | -0.12519 | 0.16877 |
| | t1 | 1.7865 | 2.43893 |
| | A2 | 0.02434 | 4.41438E-4 |

| Co56 Mode 1 | | | | |
|---|---|---|---|---|
| | Wear Rate | SE | Units | RSE% |
| Initial | 0.09 | 0.13 | µg/hr | 142 |
| Steady State | 0.02 | 0.00 | µg/hr | 1.81 |
| Time Constan | 1.79 | 2.44 | hr | 137 |

**Figure D3: Cylinder Liner Wear Decay Counts and Curve Fits (Run-in)**

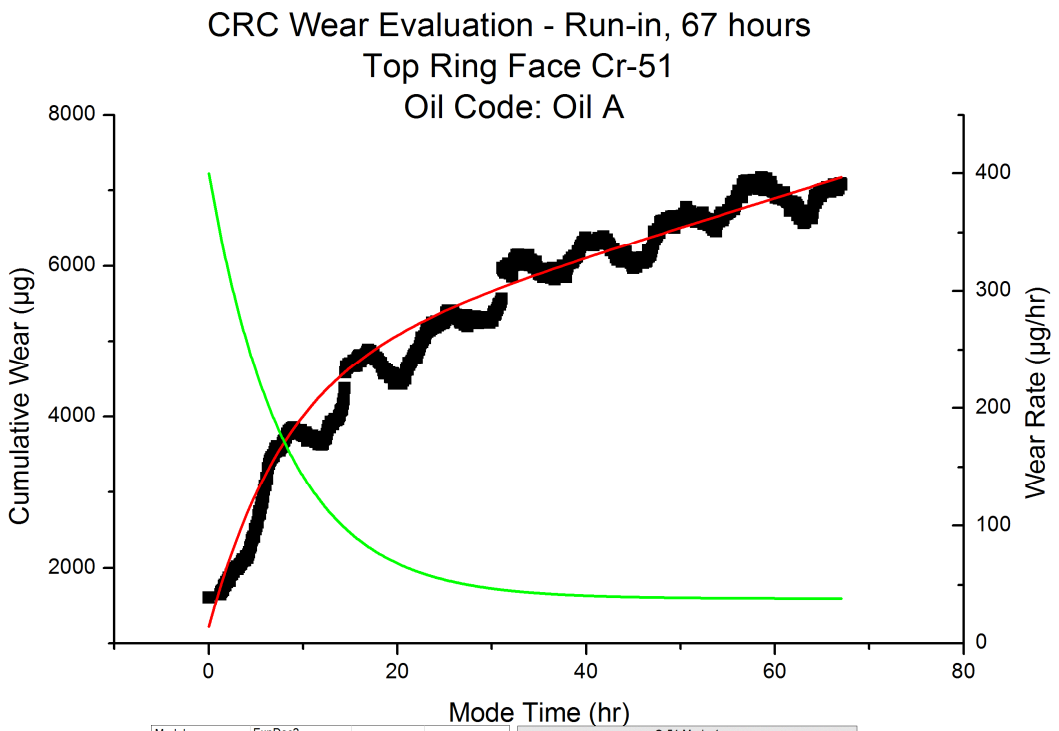


| | | | |
|---|---|---|---|
| Model | ExpDec2 | | |
| Equation | y = y0+A1*exp(-x/t1) + A2*x | | |
| Reduced Chi-Sqr | 70630.34107 | | |
| Adj. R-Square | 0.96346 | | |
| | | Value | Standard Error |
| Top Ring Face Cr51 | y0 | 4583.34999 | 64.5324 |
| | A1 | -3361.71399 | 77.45191 |
| | t1 | 8 | 0.42745 |
| | A2 | 38.62032 | 1.26128 |

| Cr51 Mode 1 | | | | |
|---|---|---|---|---|
| | Wear Rate | SE | Units | RSE% |
| Initial | 458.83 | 24.48 | µg/hr | 5.34 |
| Steady State | 38.62 | 1.26 | µg/hr | 3.27 |
| Time Constan | 8.00 | 0.43 | hr | 5.34 |

**Figure D4: Top Ring Face Wear Decay Counts and Curve Fits (Run-in)**

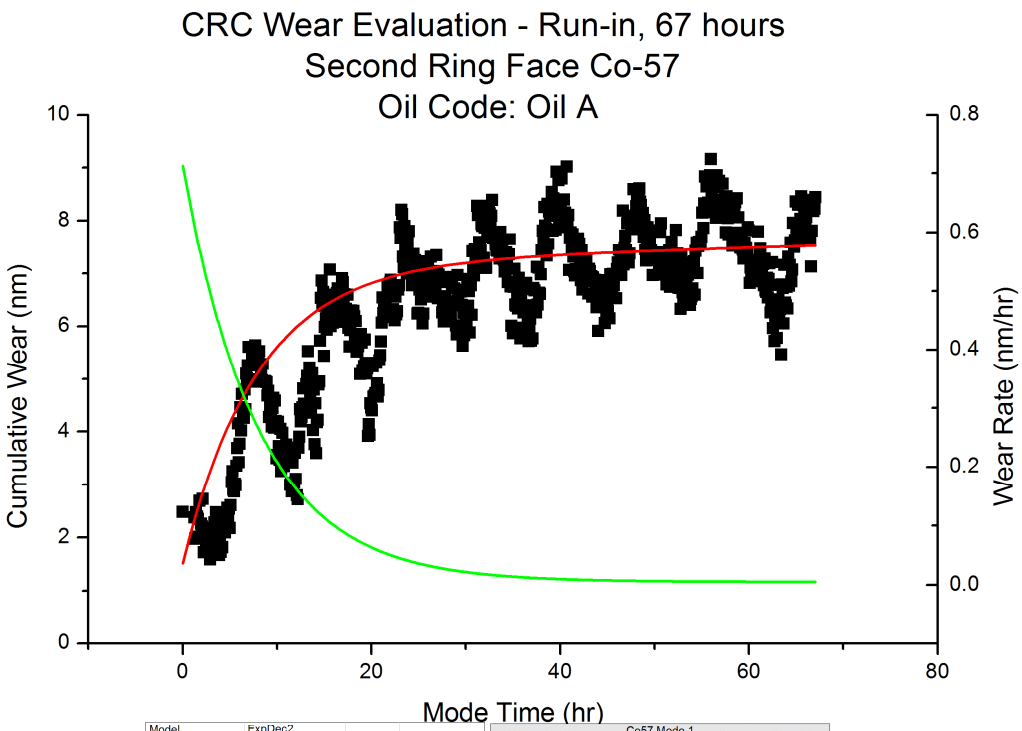


| | | | |
|---|---|---|---|
| Model | ExpDec2 | | |
| Equation | y = y0+A1*exp(-x/t1) + A2*x | | |
| Reduced Chi-Sqr | 0.96862 | | |
| Adj. R-Square | 0.65305 | | |
| | | Value | Standard Error |
| Cylinder Liner Co57 | y0 | 7.17537 | 0.23898 |
| | A1 | -5.65849 | 0.28682 |
| | t1 | 8 | 0.94043 |
| | A2 | 0.00529 | 0.00467 |

| Co57 Mode 1 | | | | |
|---|---|---|---|---|
| | Wear Rate | SE | Units | RSE% |
| Initial | 0.71 | 0.09 | nm/hr | 12.7 |
| Steady State | 0.01 | 0.00 | nm/hr | 88.3 |
| Time Constan | 8.00 | 0.94 | hr | 11.8 |

**Figure D5: Second Ring Face Wear Decay Counts and Curve Fits (Run-in)**

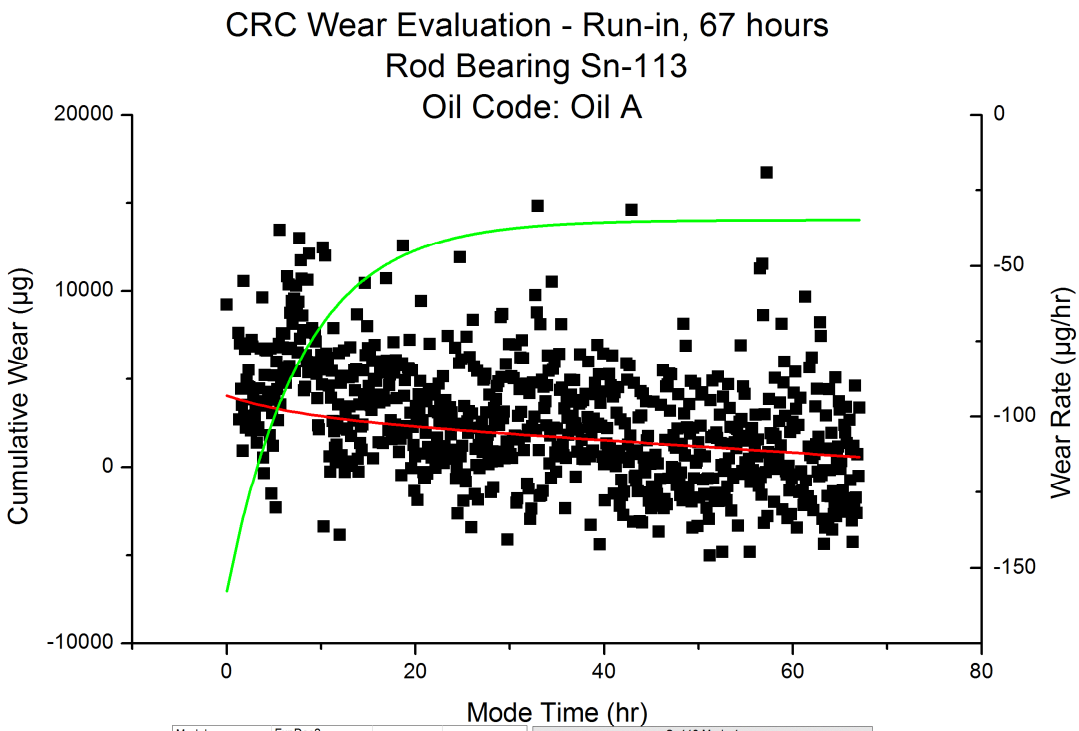


| | | | |
|---|---|---|---|
| Model | ExpDec2 | | |
| Equation | y = y0+A1*exp(-x/t1) + A2*x | | |
| Reduced Chi-Sqr | 1.0428E7 | | |
| Adj. R-Square | 0.10764 | | |
| | | Value | Standard Error |
| Bearing Sn113 | y0 | 2895.20857 | 784.11991 |
| | A1 | 1143.05774 | 941.10215 |
| | t1 | 8 | 15.27507 |
| | A2 | -34.71536 | 15.3256 |

| Sn113 Mode 1 | | | | |
|---|---|---|---|---|
| | Wear Rate | SE | Units | RSE% |
| Initial | -177.60 | 297.49 | µg/hr | 168 |
| Steady State | -34.72 | 15.33 | µg/hr | 44.1 |
| Time Constan | 8.00 | 15.28 | hr | 191 |

**Figure D6: Connecting Rod Wear Decay Counts and Curve Fits (Run-in)**

The apparent negative wear rate shown in Fig. D6 likely resulted from the deposition rate of wear particles exceeding the generation rate (the "true" wear rate) resulting in a net loss of wear material in the lube oil over time. This demonstrates that the "true" wear rate is very low, close to or within the noise level. We conclude that the wear rate is very low, essentially zero.

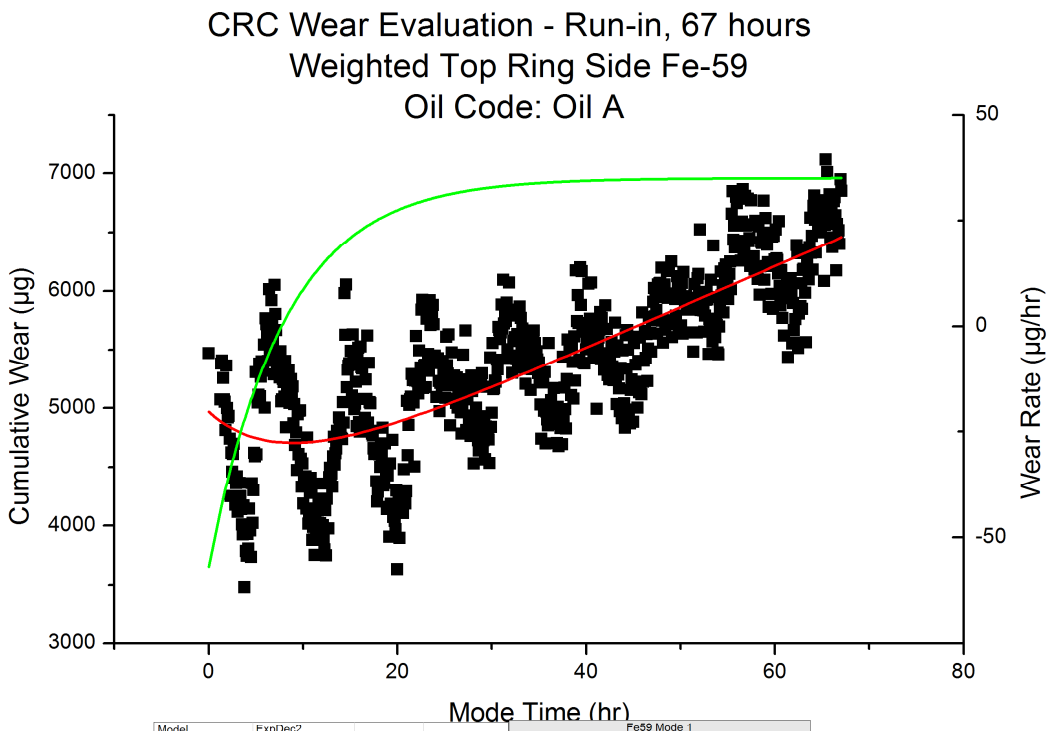


| | | | |
|---|---|---|---|
| Model | ExpDec2 | | |
| Equation | y = y0+A1*exp(-x/t1) + A2*x | | |
| Reduced Chi-Sqr | 195144.59632 | | |
| Adj. R-Square | 0.61451 | | |
| | | Value | Standard Error |
| Wgt Mean RingFe | y0 | 4111.50049 | 107.26559 |
| | A1 | 855.25379 | 128.74036 |
| | t1 | 8 | 2.79277 |
| | A2 | 35.01949 | 2.0965 |

| Fe59 Mode 1 | | | | |
|---|---|---|---|---|
| | Wear Rate | SE | Units | RSE% |
| Initial | -71.89 | 40.70 | µg/hr | 56.6 |
| Steady State | 35.02 | 2.10 | µg/hr | 5.99 |
| Time Constan | 8.00 | 2.79 | hr | 34.9 |

**Figure D7: Top Ring Side Wear Decay Counts and Curve Fits (Run-in)**

# APPENDIX E

# Engine Testing

Following the completion of the run-in, SwRI progressed through the test matrix with 5w-30 and 0w-16 oils. For consistent isotope counting acquisition times, the spectral captures were adjusted between 20-seconds and 5-minutes dependent upon the engine operating cycle. The cold start cycles conducted at the start of every test day used 20-second acquisitions to capture as many spectrums during this short and transient cycle as possible. Conditions where the team looked for Sn-113 rod bearing wear, 5 minute acquisitions were used. The 5-minute acquisitions allowed for a greater number of isotope decays to reach and be counted by the detector. Since the wear evaluations are based upon the peak area measured in a spectrum for the isotope's characteristic energy level, measured decays need to exceed a minimal level during a spectral capture in order to consistently count and report. At 30-second acquisitions, the Sn-113 isotope (rod bearings) did not incur sufficient counts to consistently identify and measure that peak for a number of cycles. Extending the acquisition time to 5 minutes provided additional time for the Sn-113 peak to accrue the necessary counts at the characteristic energy level to ensure the peak was identified and counted appropriately when it did occur. During testing, rod bearing wear was consistently measured as zero following the initial run-in.

The analyses of wear rates between operational conditions required additional work throughout the program due to the productive top ring face labeled with the chromium-51 isotope. Even at 30-second acquisition time a large chromium peak was present in each acquired spectrum. Depending on the shape and curvature of the large chromium peak, the real-time spectral analysis incorrectly fitted the chromium-51 peak with multiple peaks immediately adjacent to each other on many occasions. Figure E1 illustrates an instance where the chromium-51 peak was fit as a duplet, denoted by its aqua coloring (normal single peaks appear in red).

This introduced significant noise into the wear data of the top ring face. To correct this inconsistency a Gaussian curve fit program is used to post process each recorded spectrum for every test. Figure E2 shows a Gaussian curve fit image from a SwRI-authored, SciLab script used to correct spectral analysis inconsistencies.

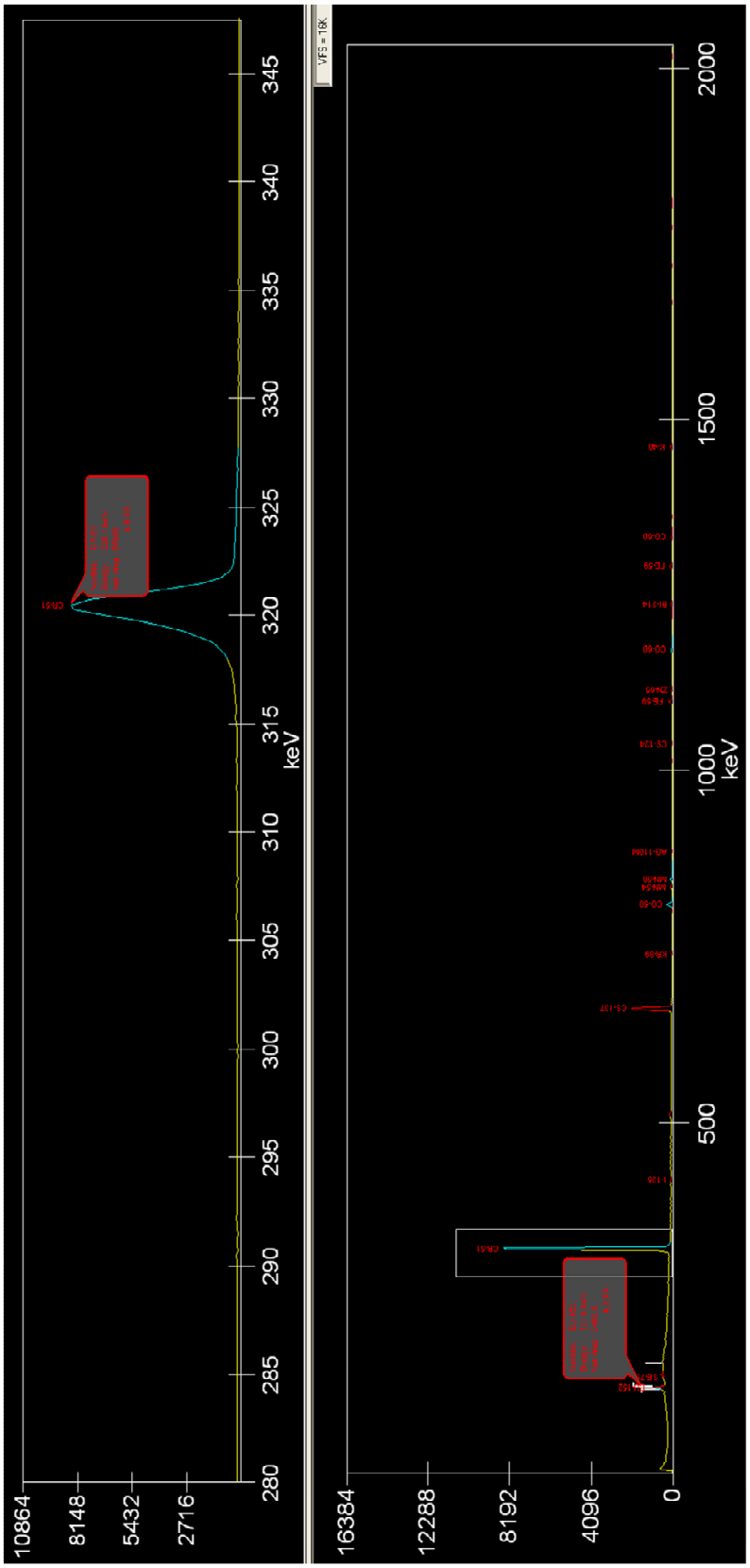


**Figure E1. Screenshot - Duplet Fitting of Chromium-51 (Peak Counts vs. keV)**

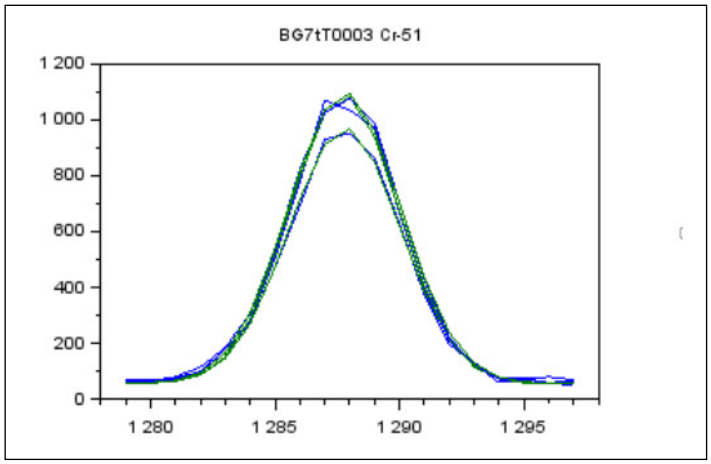


**Figure E2. Screenshot - Gaussian Curve Fit of Chromium-51 (Peak Counts vs. Backgrounds)**

The Gaussian post-processing was performed for each test cycle on every acquisition to ensure consistent fit criteria of the acquired spectrums. Multiple software applications are employed to reduce the capture spectrum to a 2-dimensional array of energy and counts, a second program performs the Gaussian curve fit and the background subtraction, and finally the cumulative spectral data is fit for a steady state wear rate using Origin plotting software.

The wear units for the second ring face were converted to mass loss from the surface activation data that is normally given in depth loss. The Co-57 isotope that labeled the second ring face was created using a particle accelerator. The surface layer activation technique generates a linear calibration factor of activity per depth which correlates the measured activity in the engine oil to a thickness of material removed from the contact surface. Using the cross section imaging from the electron microscope, a total contact area was determined for the second ring face. The contact area was used to convert the measured thickness loss into a volume removed from the contact surface. For the second rings a measured face of the second ring was found to be 0.725 millimeters in length on an installed bore of 87.5 millimeters. All four second rings constitute 797.18mm$^2$ of contact area. This area yields a conversion factor of 5.73969 micrograms for a recorded 1 nanometer thickness loss. This calculation assumes that material is lost from the second ring face uniformly across the measured face length and in each cylinder. The second ring profile is a ramped napier face, so wear from the ring is likely more concentrated to the wedged point of the napier profile than uniform across the entire width of the ring face. Only detailed 3D wear rate modelling using CAD driven software could refine this basic model further, and for the comparative study in this program, the simple approach is sufficient.

The data processing provides rate fits of the accumulation of isotope material within the circulating oil volume (engine to sample circuit). In order to perform the data fits, the curve areas are calculated for the Gaussian fits of each isotope peak for each individual acquisition. As each isotope has a characteristic energy emission or set of emissions as they decay, the isotope is identifiable by the peak created about that characteristic energy level. The resultant bell-curve

distribution around the characteristic energy for each isotope is a byproduct of the geometric efficiency of the detector well and the various incident angles of decay photons impacting the detector. The peak areas are corrected for the mass and thickness loss calibrating factors and background radiation before being plotted in Origin® software. Figure E3 shows the cumulative plot for the chromium-51 isotope for the transient speed, high load, and 115°C test on oil A. Each individual point represents a single acquisition over the two hour test period. One of two fit criteria is chosen to approximate the accumulation profile for the given isotope.

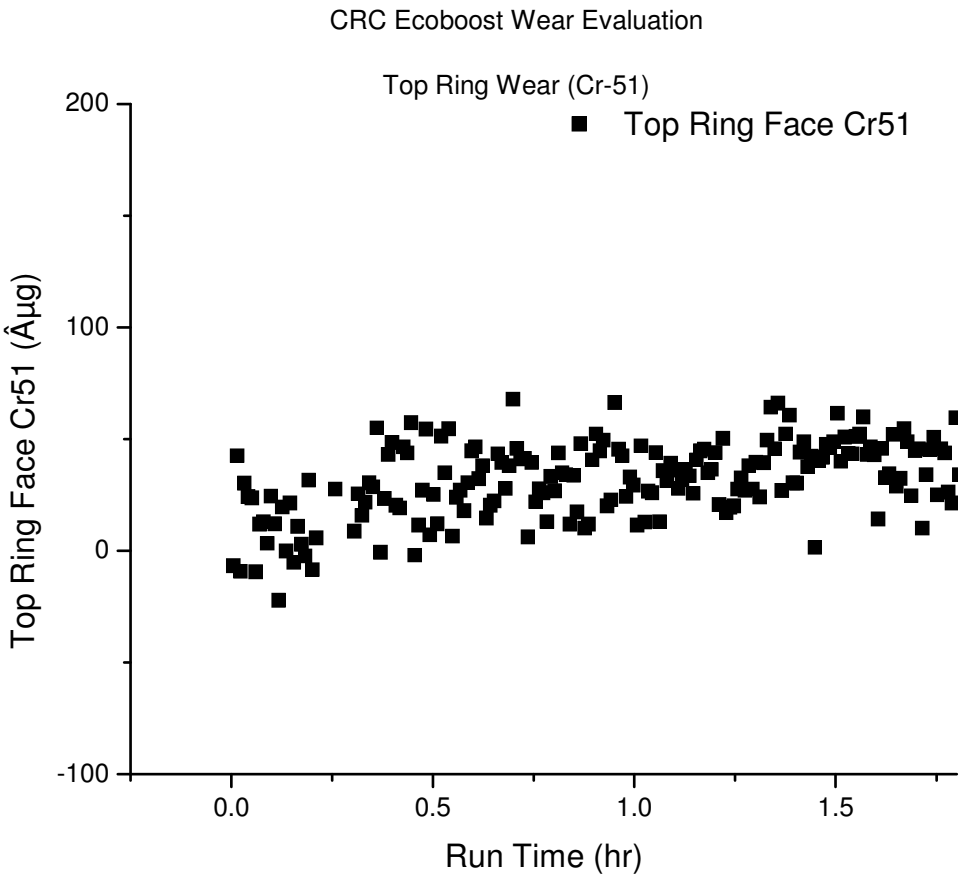


**Figure E3. Chromium-51 Wear for Transient speed, high load test cycle at 115°C**

In the case of the transient speed, high load test at 115°C, the chromium-51 cumulative trend was fit using a non-linear exponential decay fit. The alternative would be a linear fit method. Figure E4 illustrates the non-linear exponential decay fit of the cumulative data. The red line represents the cumulative trend, while the green line represents the rate of accumulation. The green line depicts the derivative of the cumulative red trendline.

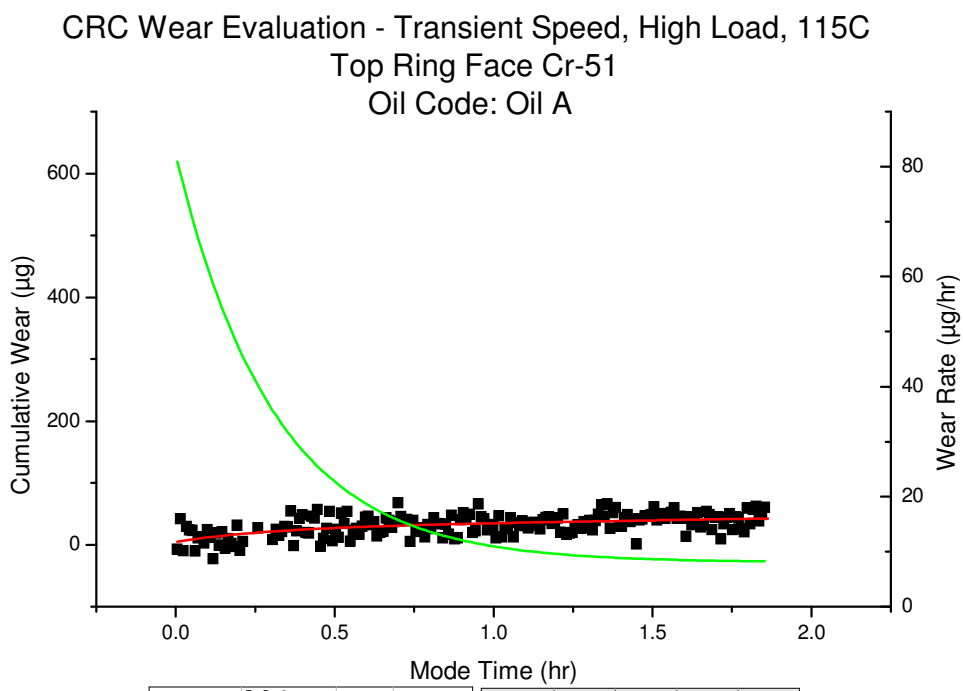


| | | | |
|---|---|---|---|
| Model | ExpDec2 | | |
| Equation | y = y0+A1*exp(-x/t1) + A2*x | | |
| Reduced Chi-Sqr | 213.42583 | | |
| Adj. R-Square | 0.27406 | | |
| | | Value | Standard Error |
| Top Ring Face Cr5 | y0 | 27.68286 | 11.28892 |
| Top Ring Face Cr5 | A1 | -22.83874 | 10.04517 |
| Top Ring Face Cr5 | t1 | 0.30888 | 0.29343 |
| Top Ring Face Cr5 | A2 | 8.07578 | 7.13745 |

| Cr51 Mode 1 | Cr51 Mode 1 | Cr51 Mode 1 | Cr51 Mode 1 | Cr51 Mode 1 |
|---|---|---|---|---|
| | Wear Rate | SE | Units | RSE% |
| Initial | 82.02 | 77.73 | µg/hr | 94.8 |
| Steady State | 8.08 | 7.14 | µg/hr | 88.4 |
| Time Constant | 0.31 | 0.29 | hr | 95.0 |

**Figure E4. Non-Linear Exponential Decay Fit for Top Ring Face Wear**

With a non-linear exponential decay fit, the steady-state wear rate is the comparative metric when looking at the results of the various test conditions and oil-to-oil response. The linear fits only report steady state gain and offset variables. These steady state rates result in the linear and the exponential decays producing comparable data that lends well to comparison regardless of the fit method. Figures E5 through E8 show the results for both oils at all conditions for each component being measured for wear.

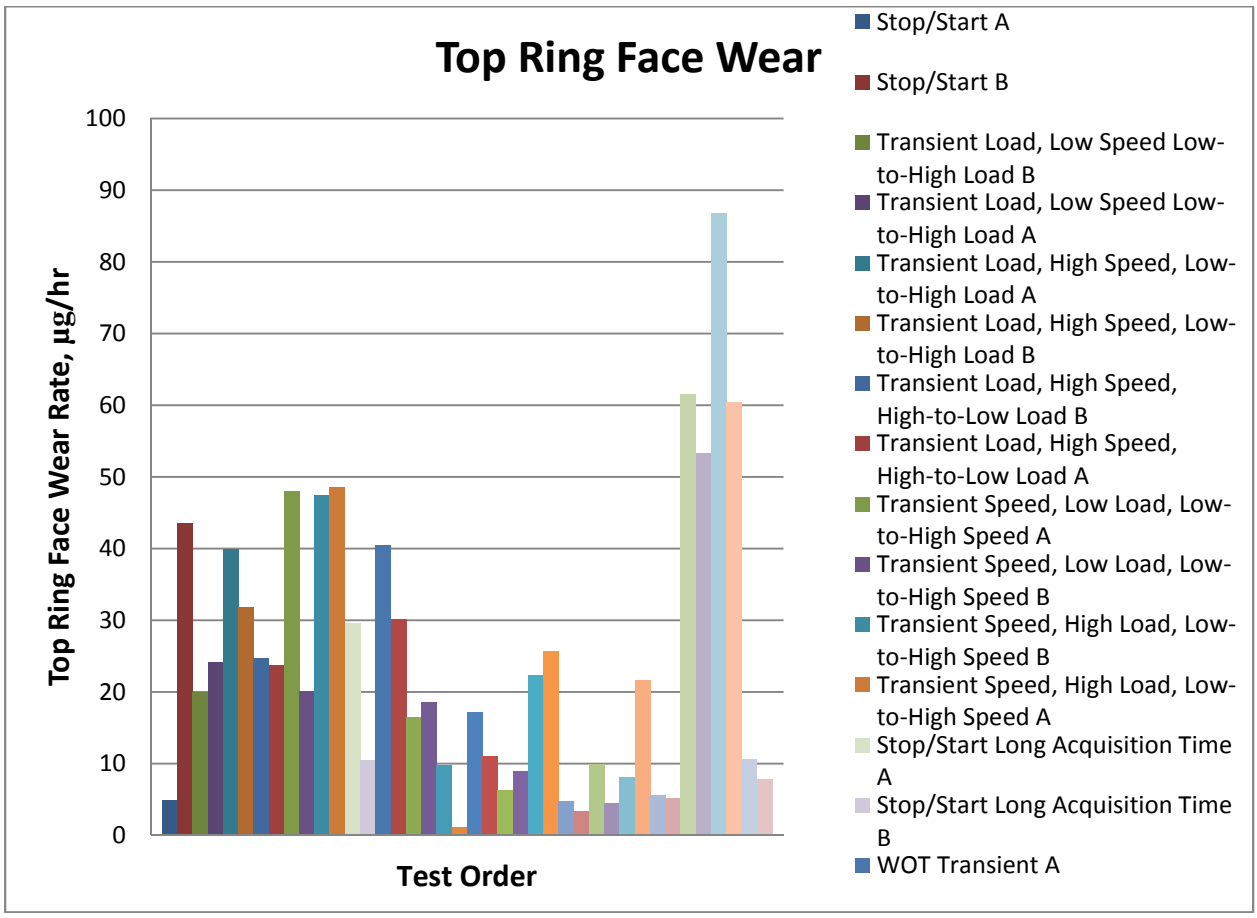


**Figure E5. Top Ring Face Wear for Complete Test Matrix in Chronological Testing Order**

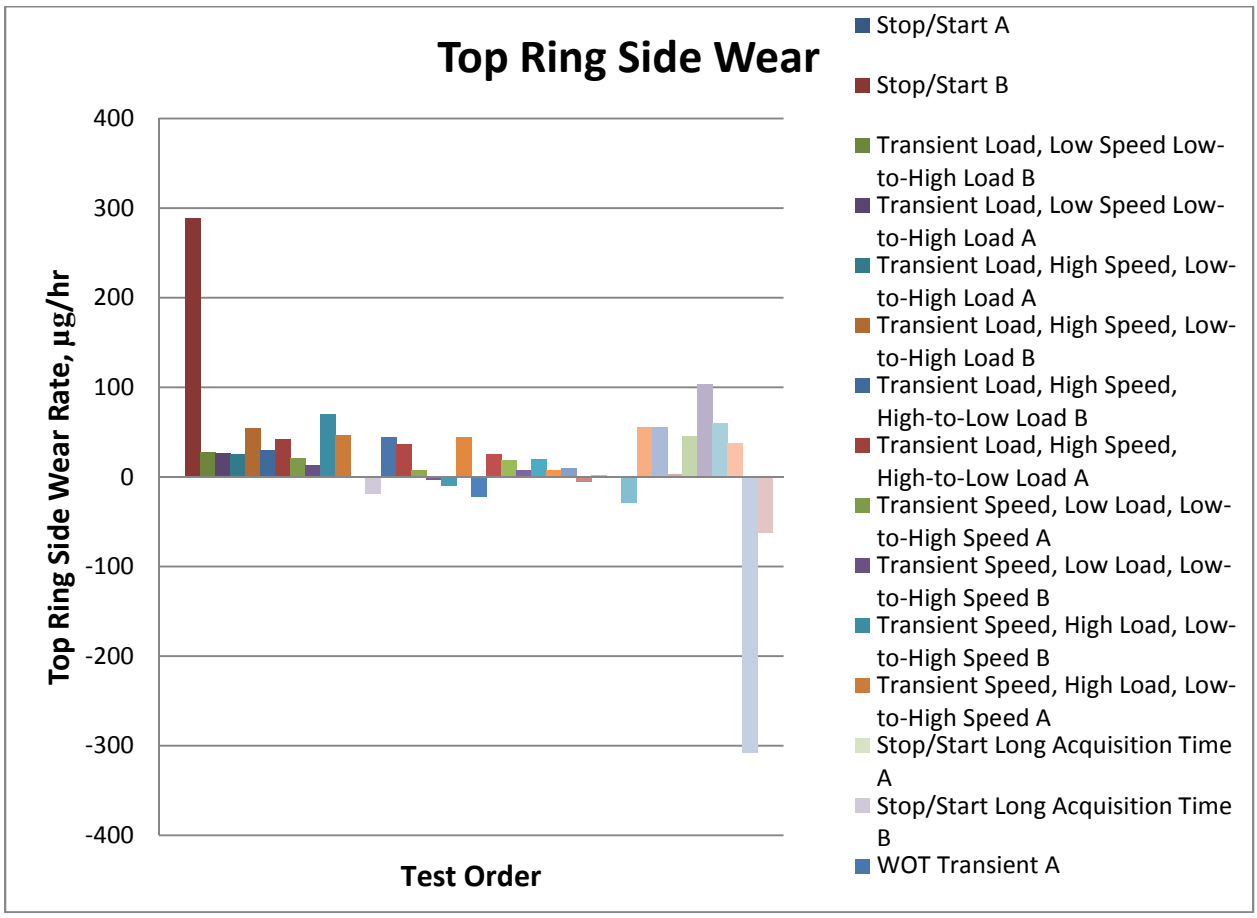


**Figure E6. Top Ring Side Wear Summary for Complete Test Matrix in Chronological Testing Order**

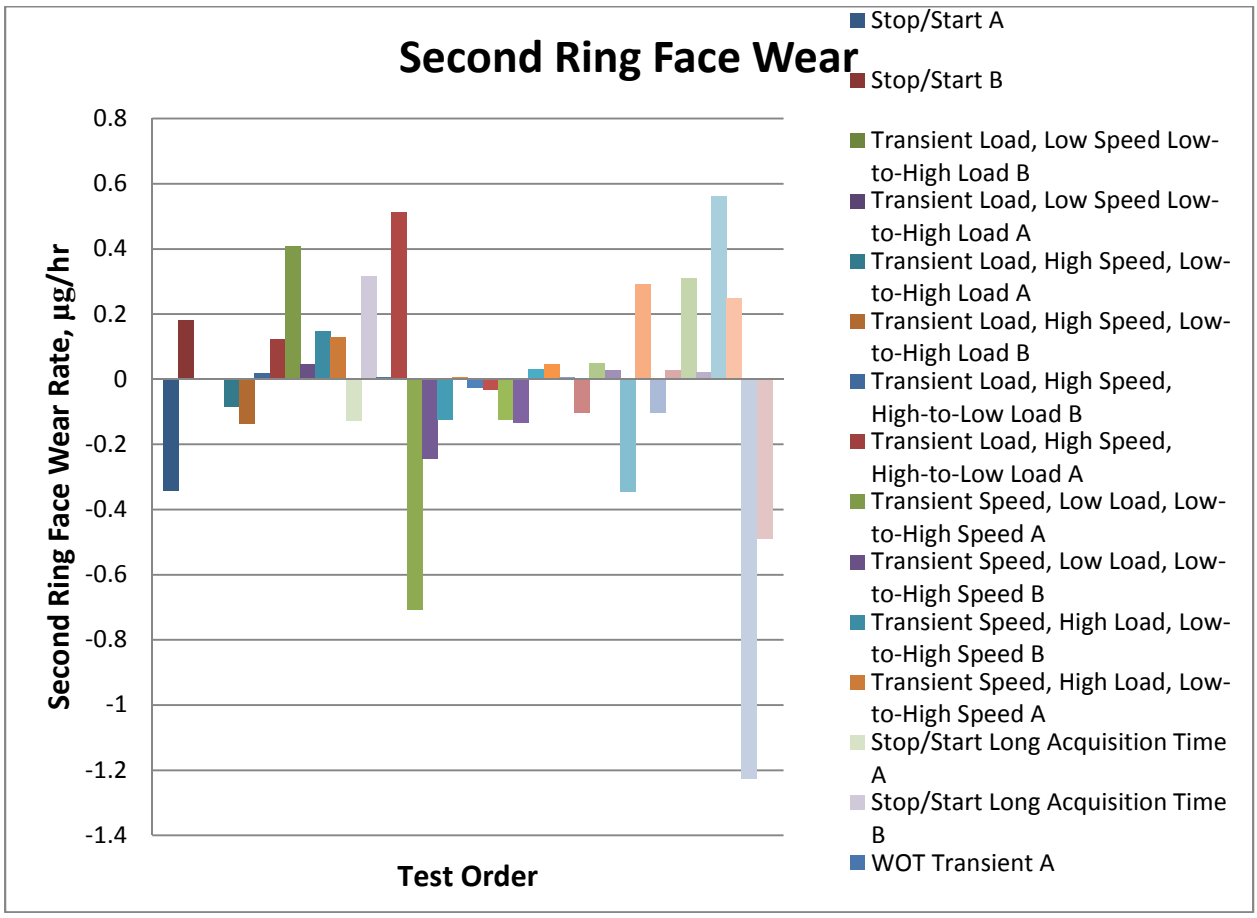


**Figure E7. Second Ring Face Wear Summary for Complete Test Matrix in Chronological Testing Order**

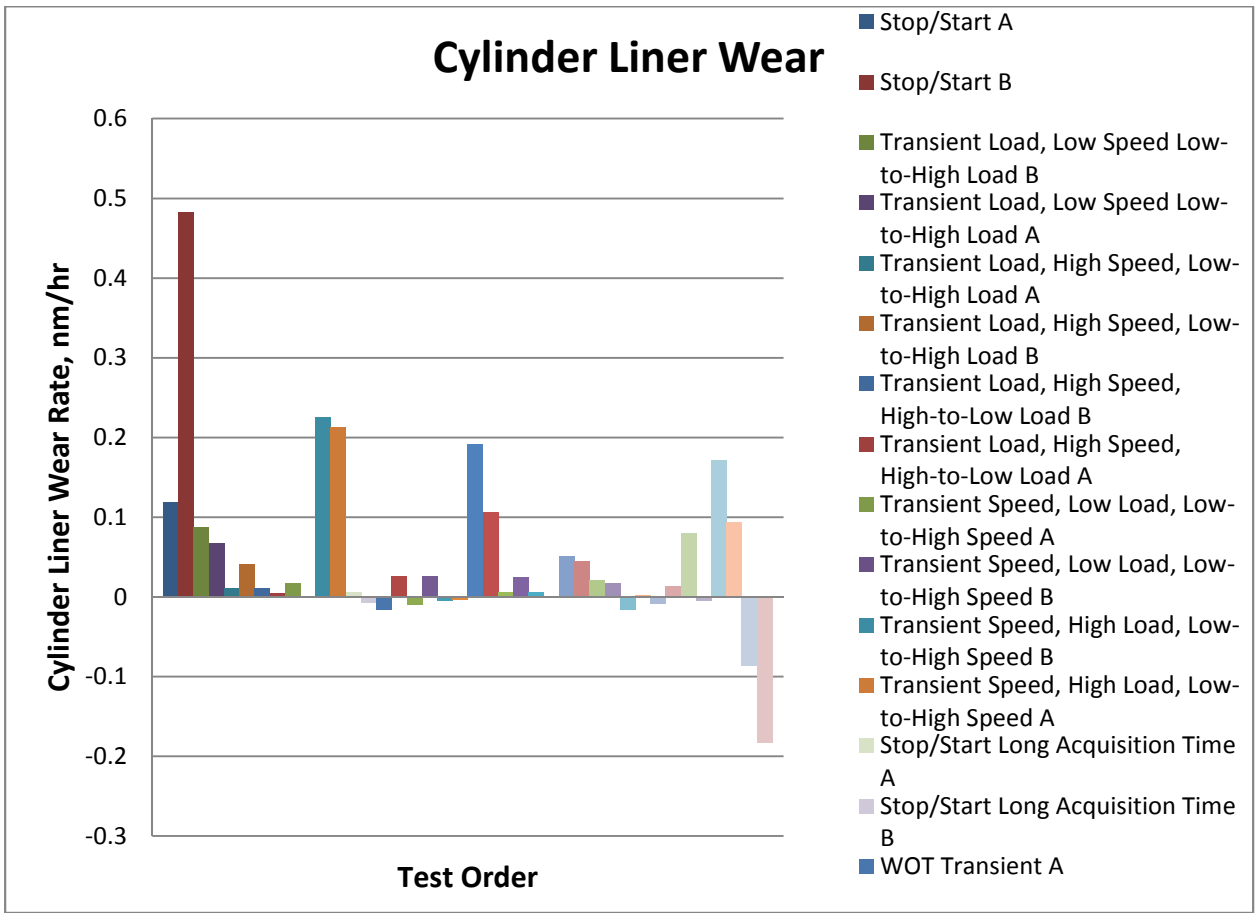


**Figure E8. Cylinder Liner Wear Summary for Complete Test Matrix in Chronological Testing Order**

In a number of the tests, negative wear rates were recorded. This is not an unusual occurrence when using RATT® to measure real time wear of components. It is usual for this to occur in test conditions where the radioactive wear particles are lost due to oil consumption at a faster rate than they are created. In almost all these circumstances it is reasonable to assume that the wear rates must be low, because if they are not, an increase in wear particles would be detected. One possible exception to this is the wide open throttle, 5000rpm Cold test condition where significant losses were measured in all the engine components except the top ring face. For this to accumulate a measurable mass loss while sufficient oil was being lost to the exhaust stream, suggests that wear of the top ring face may have been exceptionally high, especially considering its location in relation to the lubricant loss route. Oil consumption during testing was monitored using a weigh bucket. However, oil loss was never sufficient during any given day to register on the scales, and the engine was charged with fresh oil each day.

# APPENDIX F

# Elemental Mass Concentrations for Engine Parts

| | Percent Mass Concentration by Element, % | | | | | | | | | | | | | | | | | | | | | |
|---|---|---|---|---|---|---|---|---|---|---|---|---|---|---|---|---|---|---|---|---|---|---|
| | Na | Mg | Al | Si | V | P | K | S | Ca | Ti | Cr | Mn | Fe | Co | Ni | Nb | Mo | W | Cu | Sn | Zn | Pb |
| Wrist Pin Base metal | | | 0.3 | 0.46 | | | | | | | 0.54 | 0.55 | 98.14 | | | | | | | | | |
| Wrist Pin Surface Coating | | 1.47 | 1.13 | 3.2 | | 1.5 | | 2.86 | 1.92 | | 4.68 | 3.04 | 78.81 | | | | | | 0.27 | | | |
| Piston Skirt Base metal | | 1.26 | 68.96 | 24.22 | | | | | | | | 0.22 | 0.62 | | 1.86 | | | | 2.87 | | | |
| Cylinder Liner Base metal | | | 0.19 | 3.43 | | 0.23 | | | | | 0.12 | 0.72 | 94.22 | | 0.33 | | 0.76 | | | | | |
| Main Bearing Base metal | | | 0.37 | 0.25 | | | | | | | | 0.27 | 99.1 | | | | | | | | | |
| Main Bearing Coating Layer | | | 89.35 | 5 | 0.22 | | | | | | | 0.21 | 0.26 | | | | | | 0.73 | 4.23 | | |
| Main Bearing Thrust Surface | | | 0.29 | 0.23 | | | | | | | | 0.29 | 99.18 | | | | | | | | | |
| Wrist Pin Bushing Base metal | | | 0.35 | 0.22 | | | | | | | | 0.67 | 98.75 | | | | | | | | | |
| Wrist Pin Bushing ID Layer | | | 0.28 | 0.22 | | | | | | | | | | | | | | | 94.58 | 4.92 | | |
| Rod Bearing ID Layer | | | 89.11 | 5.2 | 0.21 | | | | | | | | | | | | | | 1.1 | 4.38 | | |
| Rod Bearing Base Material | | | 0.62 | 0.66 | | | | | | | | 0.34 | 98.37 | | | | | | | | | |
| Top Ring Base metal | | | | 2.17 | | | | | | | 0.61 | 0.65 | 96.57 | | | | | | | | | |
| Top Ring Contact Surface | | | 0.57 | 0.42 | | | | | | | 98.35 | | 0.66 | | | | | | | | | |
| 2nd Ring Base Metal | | | | 0.55 | | | | | | | 0.07 | 0.74 | 98.64 | | | | | | | | | |
| Oil Ring Spacer | | | 0.23 | 0.94 | 0.1 | | | | | | 17.86 | 1.02 | 69.52 | | 9.59 | | 0.36 | | 0.38 | | | |
| Oil Ring Side Rails | | | 0.26 | 0.63 | 0.05 | | | | | | 18.06 | 0.24 | 78.99 | | 0.2 | | 1.57 | | | | | |
| | | | | | | | | | | | | | | | | | | | | | | |
| Turbine Wheel | | | 9.43 | 0.19 | | | | | | 1.04 | 12.51 | | 0.61 | | 67.47 | 3.18 | 4.69 | 0.88 | | | | |
| Turbocharger Compressor Wheel | | 0.62 | .81.03 | 16.72 | | | | | | 0.12 | | | 0.21 | | | | | | 1.3 | | | |
| Turbine Shaft | | | 0.36 | 0.82 | | | | | | | 1.01 | 0.71 | 96.45 | | 0.18 | | 0.47 | | | | | |
| Turbo Journal Bearing | | | 1.93 | 1.19 | | | | | | | | 2.05 | 0.48 | | | | | | 56.52 | | 36.69 | 1.14 |
| Turbo Thrust Bearing | | | | 0.3 | | | | | | | | | | | | | | | 64.46 | | 35.24 | |
| | | | | | | | | | | | | | | | | | | | | | | |
| Valve Bucket | | | 0.32 | 0.3 | | | | | | | 0.77 | 0.95 | 97.66 | | | | | | | | | |
| Valve Guide | | 0.48 | | 1.02 | | 0.69 | | | | | | 0.17 | 93.59 | | | | | | 4.05 | | | |
| Valve Spring | | | | 2.43 | | | | | | | 0.59 | 0.63 | 96.34 | | | | | | | | | |
| Valve Keeper | | | | 0.26 | | | | | | | 0.09 | 0.31 | 99.33 | | | | | | | | | |
| Intake Valve Seat | | 0.44 | 0.49 | 0.78 | 0.07 | | | | | | 2.1 | 0.55 | 83.79 | 8.29 | 1.31 | | 2.08 | | 0.09 | | | |
| Intake Valve Stem | | | 0.31 | 2.4 | 0.04 | | | | | | 8.09 | 0.34 | 88.52 | | 0.31 | | | | | | | |
| Intake Valve Face | | | | 1.33 | | | | | | | 7.63 | 0.31 | 90.5 | | 0.23 | | | | | | | |
| Exhaust Valve Face | | | | | 0.11 | | | | | | 22.27 | 8.7 | 58.46 | | 3.69 | 3.58 | | 3.18 | | | | |
| Exhaust Valve Stem | | | | 3.99 | | | | | | | 8.72 | 0.43 | 86.63 | | 0.23 | | | | | | | |
| Exhaust Valve Seat | | | 0.4 | 0.32 | | | | | | | | 0.47 | 91.4 | | | | 0.78 | | 6.63 | | | |
| | | | | | | | | | | | | | | | | | | | | | | |
| Timing Chain Link | | | 0.18 | 0.62 | | | | | | | 0.1 | 0.71 | 98.39 | | | | | | | | | |
| Timing Chain Gear | | | | 0.54 | | | | | | | 1.09 | 0.82 | 97.55 | | | | | | | | | |
| Timing Chain Pin | | | 1.85 | 0.58 | | | | | | | 1.34 | 0.51 | 94.95 | | 0.18 | | 0.59 | | | | | |
| | | | | | | | | | | | | | | | | | | | | | | |
| Camshaft Bearing Base Metal | | | 0.33 | 0.25 | | | | | | | | 0.21 | 99.21 | | | | | | | | | |
| Camshaft Bearing Babbitt | | | 88.23 | 5.53 | 0.21 | | | | | | | | 0.3 | | | | | | 0.73 | 4.93 | | |
| Camshaft Lobe | | | | 1.92 | | | | | | | 0.12 | 0.69 | 96.92 | | | | 0.34 | | | | | |
| | | | | | | | | | | | | | | | | | | | | | | |
| Oil Pump Gear | | | 0.17 | 0.3 | | | | | | | 0.05 | 0.51 | 96.36 | | | | 0.63 | | 1.97 | | | |
| Oil Pump Shaft | | | 0.28 | 0.32 | | | | | | | | 0.85 | 97.59 | | | | 0.96 | | | | | |
| Oil Pump Bearing | | 0.68 | 82.77 | 13.38 | | | | | | | | 0.16 | 0.8 | | | | | | 1.29 | | 0.91 | |
| | | | | | | | | | | | | | | | | | | | | | | |
| Balance Shaft Bearing Base Metal | | | 0.42 | 0.3 | | | | | | | | 0.22 | 99.07 | | | | | | | | | |
| Balance Shaft Bearing Babbit | | | 81.62 | 9.92 | 0.2 | | | | | | | 0.12 | 1.23 | | | | 0.16 | | 0.72 | 6.04 | | |
| Balance Shaft Gear | | | 0.29 | 0.66 | | | | | | | 0.83 | 0.72 | 96.53 | | 0.26 | | 0.69 | | | | | |
| | | | | | | | | | | | | | | | | | | | | | | |
| Block | | 0.51 | 81.45 | 14.45 | | | | | | 0.15 | | 0.31 | 0.46 | | | | | | 2.2 | | 0.46 | |
| Crankshaft (from Counterweight) | | | 0.26 | 2.75 | | | | | | | | 0.66 | 95.26 | | | | | | 1.06 | | | |
| Cylinder Head | | 0.72 | 82.3 | 12.97 | | | | | | 0.18 | | 0.36 | 0.58 | | | | | | 2.49 | | 0.41 | |
| | | | | | | | | | | | | | | | | | | | | | | |
| Mahle Piston Surface | 2.78 | 0.53 | 54.87 | 28.5 | | 9.36 | 0.16 | | 1.63 | | | | 0.31 | | 0.95 | | | | 1.18 | | | |
| Mahle Piston Base Metal | | 1.56 | 75.55 | 21.39 | | | | | | | | | 0.2 | | 0.63 | | | | 0.68 | | | |

# APPENDIX G

# Fuel Specifications

P-4-5
GA-9639
1/4/16

**haltermannsolutions**

# Product Information

Telephone: (800) 988-2542

FAX: (281) 457-1469

**PRODUCT:** EEE-Lube Cert Gasoline

**Batch No.:** EL1621NX10

**PRODUCT CODE:** HF0003

**Tank No.:** 63

**Date:** 12/30/2016

| TEST | METHOD | UNITS | HALTERMANN Specs MIN | TARGET | MAX | RESULTS |
|---|---|---|---|---|---|---|
| Distillation - IBP | ASTM D86[2] | °C | 23.9 | | 35.0 | 32.3 |
| 5% | | °C | | | | 45.6 |
| 10% | | °C | 48.9 | | 57.2 | 52.4 |
| 20% | | °C | | | | 62.1 |
| 30% | | °C | | | | 73.6 |
| 40% | | °C | | | | 89.3 |
| 50% | | °C | 93.3 | | 110.0 | 103.3 |
| 60% | | °C | | | | 110.7 |
| 70% | | °C | | | | 116.6 |
| 80% | | °C | | | | 126.8 |
| 90% | | °C | 151.7 | | 162.8 | 159.5 |
| 95% | | °C | | | | 172.7 |
| Distillation - EP | | °C | | | 212.8 | 202.9 |
| Recovery | | vol % | | Report | | 97.4 |
| Residue | | vol % | | Report | | 1.3 |
| Loss | | vol % | | Report | | 1.3 |
| Gravity @ 60°F/60°F | ASTM D4052[2] | °API | 58.7 | | 61.2 | 58.9 |
| Density @ 15° C | ASTM D4052[2] | kg/l | 0.734 | | 0.744 | 0.743 |
| Reid Vapor Pressure | ASTM D5191[2] | kPa | 60.1 | | 63.4 | 60.6 |
| Carbon | ASTM D3343[1] | wt fraction | | Report | | 0.8657 |
| Carbon | ASTM D5291 | wt fraction | | Report | | 0.8680 |
| Hydrogen | ASTM D5291 | wt fraction | | Report | | 0.1320 |
| Hydrogen/Carbon ratio | ASTM D5291 | mole/mole | | Report | | 1.812 |
| Oxygen | ASTM D4815 | wt % | | | 0.05 | None Detected |
| Sulfur | ASTM D5453 | mg/kg | 3 | | 15 | 3 |
| Lead | ASTM D3237[2] | mg/l | | | 2.6 | None Detected |
| Phosphorous | ASTM D3231[2] | mg/l | | | 1.3 | None Detected |
| Composition, aromatics | ASTM D1319 | vol % | 26.0 | | 32.5 | 29.3 |
| Composition, olefins | ASTM D1319 | vol % | | | 10.0 | 3.0 |
| Composition, saturates | ASTM D1319 | vol % | | Report | | 67.7 |
| Particulate matter | ASTM D5452[2] | mg/l | | | 1 | 1 |
| Oxidation Stability | ASTM D525[2] | minutes | 1000 | | | 1000+ |
| Copper Corrosion | ASTM D130[2] | | | | 1 | 1a |
| Gum content, washed | ASTM D381[2] | mg/100mls | | | 5.0 | <0.5 |
| Fuel Economy Numerator/C Density | ASTM D5291 | | 2401 | | 2441 | 2437 |
| C Factor | ASTM D5291 | | | Report | | 1.0038 |
| Research Octane Number | ASTM D2699[2] | | 96.0 | | | 97.9 |
| Motor Octane Number | ASTM D2700[2] | | | Report | | 89.3 |
| Sensitivity | D2699/2700[2] | | 7.5 | | | 8.6 |
| Net Heating Value, btu/lb | ASTM D3338[1] | btu/lb | | Report | | 18464 |
| Net Heating Value, btu/lb | ASTM D240 | btu/lb | | Report | | 18532 |
| Color | VISUAL | 1.75 ptb | | Red | | Red |

APPROVED BY:

[1] Haltermann Solutions is accredited to ISO/IEC 17025 by A2LA for the tests referred to with this footnote.
[2] Tested by ISO/IEC 17025 accredited subcontractor.

Gasoline and diesel specialty fuels from Haltermann Solutions shall remain within specifications for a minimum of 3 years from the date on the COA so long as the drums are sealed and unopened in their original container and stored in a warehouse at ambient conditions. Specialty fuels that have been intentionally modified for aggressive or corrosive properties are excluded.

# APPENDIX H

# Ford 8hr Run-in

**Eight Hour Break-In.** Run as follows:

| **Stage No.** | **Time per Stage** Hr:Min | **Total Time** Hr:Min | **Engine Speed Setpoint** rpm | **BMEP Setpoint** bar (psi)-lb/ft |
|---|---|---|---|---|
| 1 | 0:12 | 0:12 | Idle | Min. Load ^ |
| 2 | 0:18 | 0:30 | Idle | Min. Load ^ |
| 3 | 0:30 | 1:00 | 1500 | 2.5-28.2 lb/ft |
| 4 | 0:30 | 1:30 | 2000 | 4.5-52.8 |
| 5 | 0:30 | 2:00 | 2500 | 7.0-82.1 |
| 6 | 0:30 | 2:30 | 3000 | 8.5-99.7 |
| Optional: Shut down engine to drain oil and remove oil filter. Replace drain plug with drain valve. Install new oil and new oil filter. If specified, install bottles in the pushover and pullover sides of the crankcase ventilation system. | | | | |
| 7 | 0:15 | 2:45 | 3000 | Full Load * |
| 8 | 3:00 | 5:45 | 3000 | Full Load * |
| 9 | 0:15 | 6:00 | 2000 | 4.5-52.8 |
| 10 | 0:15 | 6:15 | 3250 | Full Load * |
| 11 | 0:15 | 6:30 | 3500 | Full Load * |
| 12 | 0:15 | 6:45 | 3750 | Full Load * |
| 13 | 0:15 | 7:00 | 4000 | Full Load * |
| 14 | 0:15 | 7:15 | 4250 ** | Full Load * |
| 15 | 0:15 | 7:30 | 4500 ** | Full Load * |
| 16 | 0:15 | 7:45 | 4750 ** | Full Load * |
| 17 | 0:15 | 8:00 | 5000 ** | Full Load * |

^ "Min. Load" is defined as the greater value of either: 47 ± 7 N-m (35 ± 5 ft-lbs) engine load or the load required to maintain zero crankcase pressure.

* For boosted applications, "full load" points are set to zero boost, meaning intake manifold pressure equal to barometric pressure.

** DO NOT EXCEED MAXIMUM RATED ENGINE SPEED DURING BREAK-IN. If this setpoint speed exceeds the maximum rated engine speed, run at maximum rated speed instead.

For this project, this 8hr run-in was repeated until 67hrs of run-in was achieved.

# APPENDIX I

# End of Test Parts – Photographs and Discussions

Figures I1-4 show the EOT rod bearings. Since this testing program ran without an oil filter, higher than expected levels of embedded particles and wiping marks were present. Overall levels of normal bearing wear were near zero as corroborated by the radiation data.

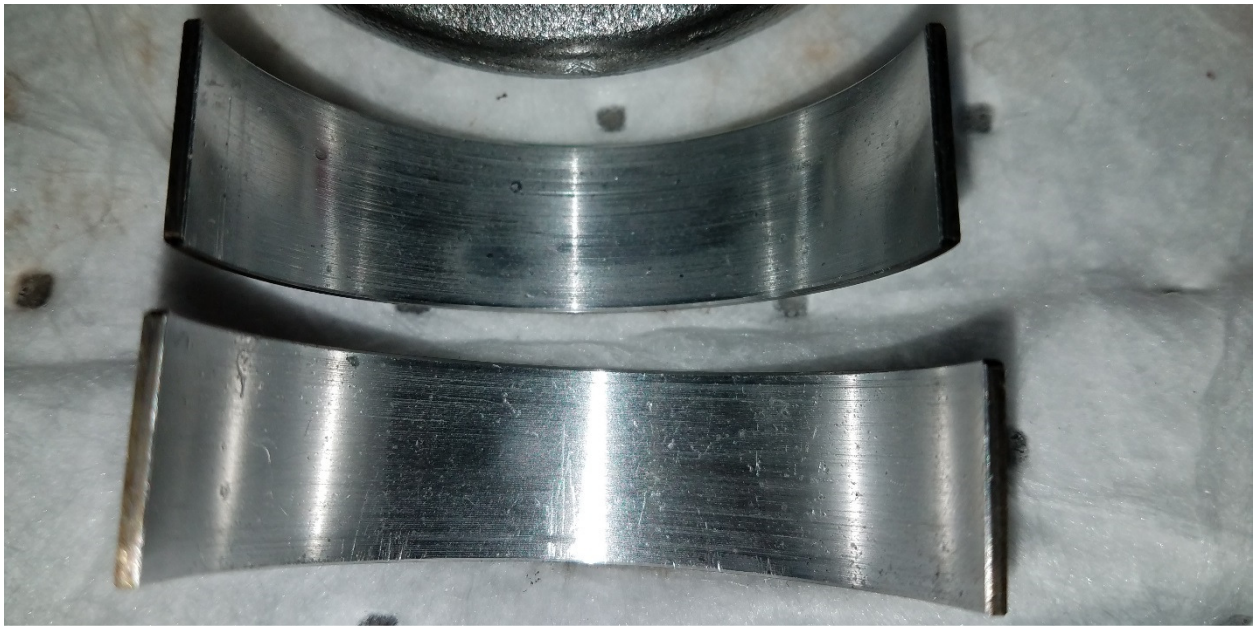

**Figure I1. Rod Bearings Cylinder 1**

**Figure I2. Rod Bearings Cylinder 2**

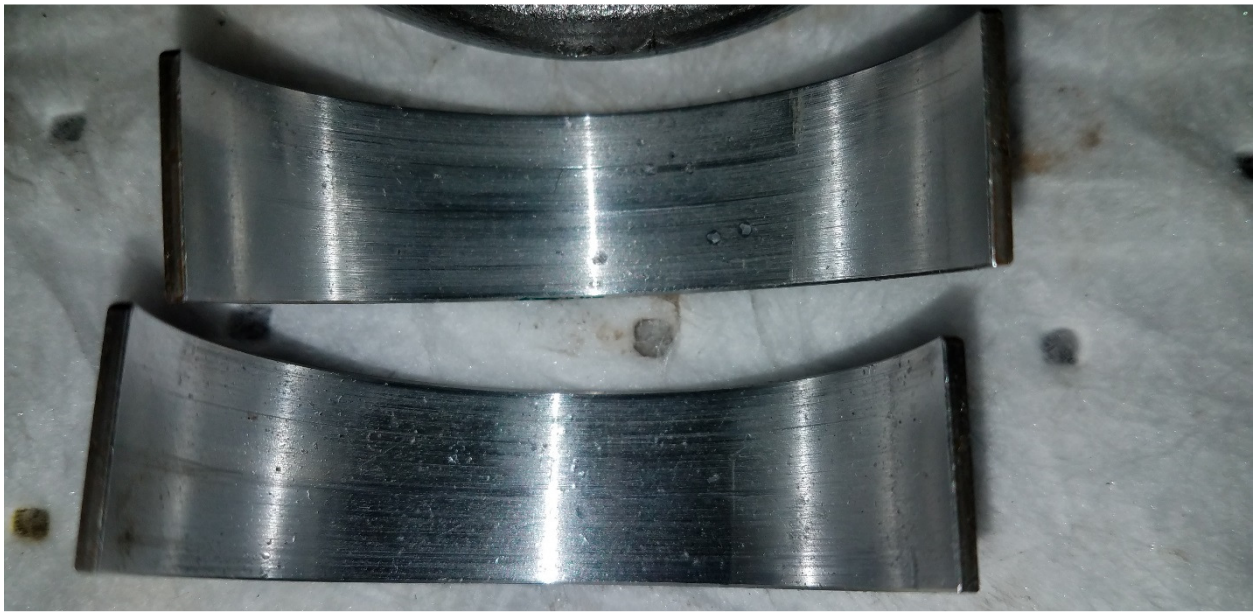

**Figure I3. Rod Bearings Cylinder 3**

**Figure I4. Rod Bearings Cylinder 4**

Between the end of the test program and disassembly of the engine, the intercooler leaked fluid from the chiller (alcohol-water mix) into the engine. So some rust was present on the liners during posttest inspection. Figures I5-8 show the extent of liner wear around the mid stroke on thrust and anti-thrust sides. Some streaking, bore polishing, and light scuffing, is observed.

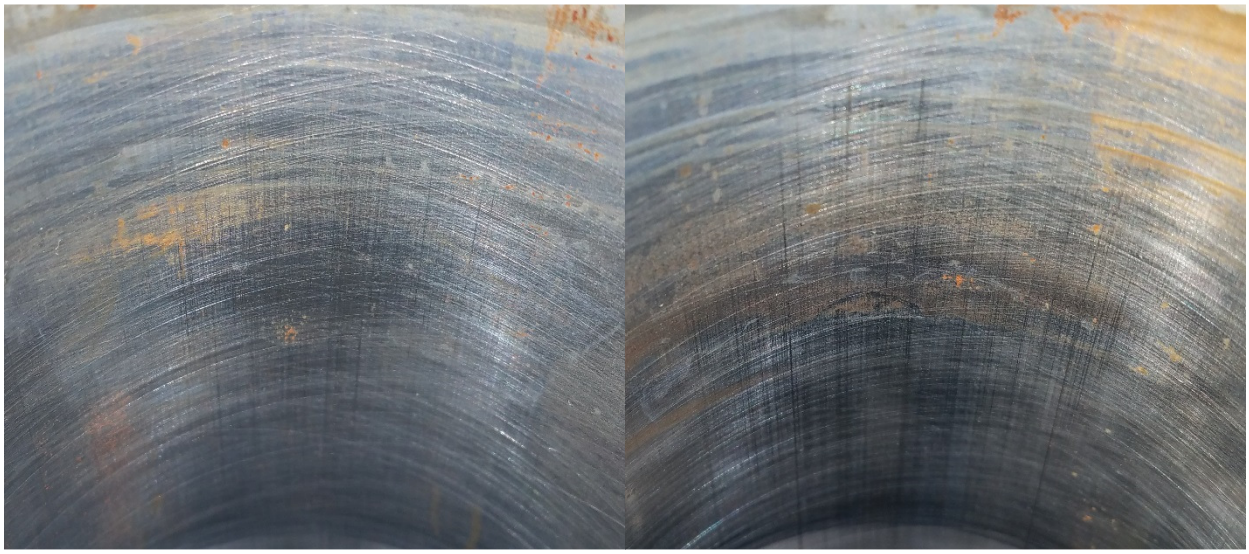

**Figure I5. Cylinder 1 Thrust (left), Anti-Thrust (right). Some light streaking is observed, along with bore polishing at mid-stroke.**

**Figure I6. Cylinder 2 Thrust (left), Anti-Thrust (right). Some light streaking is observed, along with a small scuff outlined in red on the thrust side.**

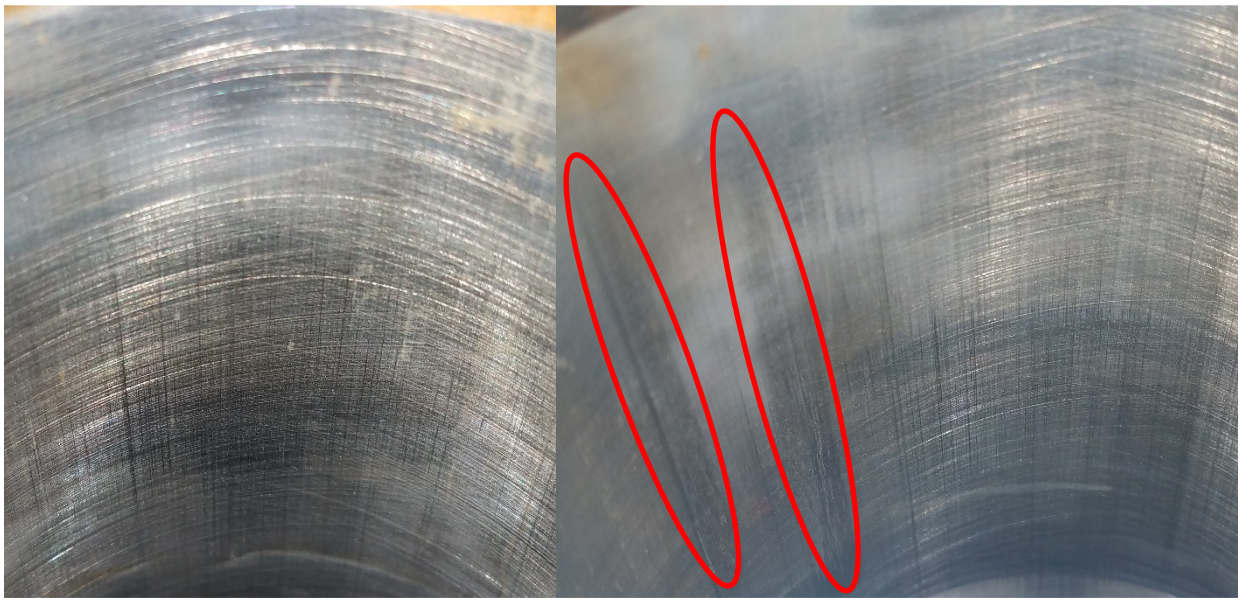

**Figure I7. Cylinder 3 Thrust (left), Anti-Thrust (right). Some light streaking is observed, along with bore polishing at mid-stroke.**

On the Anti-Thrust side, scuffing is observed (outlined in red). A scuffing source can be found in the damaged #3 piston ring as shown in Figure I9.

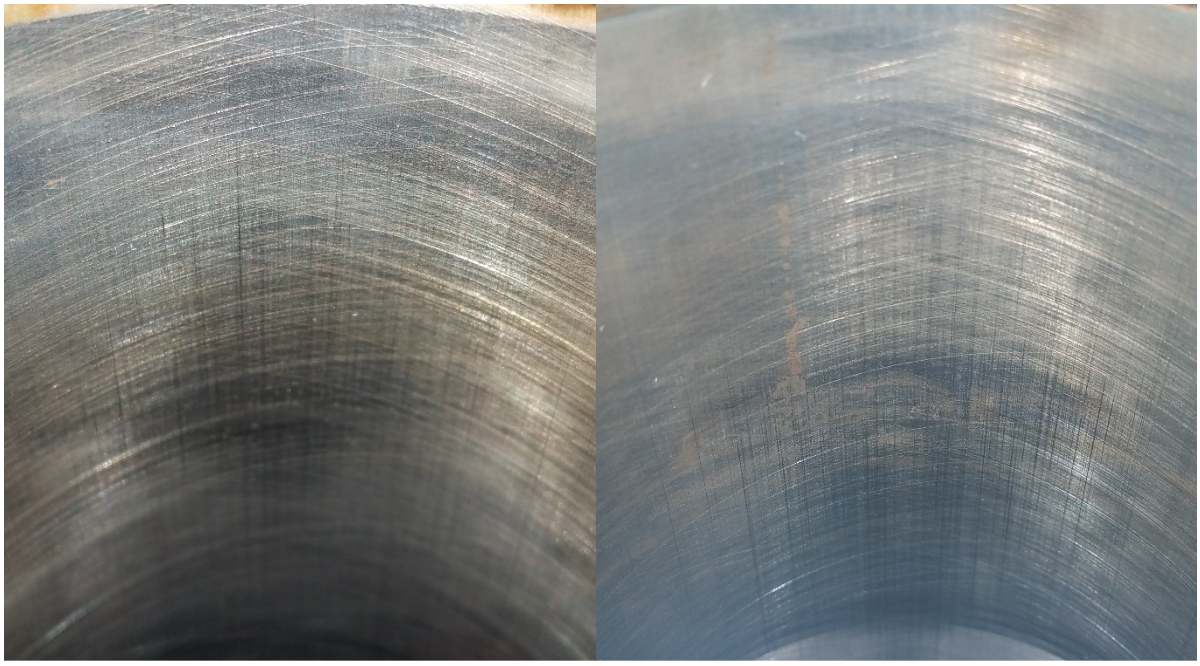

**Figure I8. Cylinder 4 Thrust (left), Anti-Thrust (right). Some light streaking is observed, along with bore polishing at mid-stroke.**

**Figure I9. Top Piston Ring #3.**

A 5-6mm section of the chrome insert was broken off during testing. It is unknown when this event occurred, but it is likely that it occurred toward the end of the testing. Due to the location of the cylinder scuff on the anti-thrust side, no radiation wear data was accumulated related to this event. Figure I10 shows a radioactive sliver found in the sump, posttest, believed to be the missing chrome segment.

**Figure I10. Potential Missing Chrome Segment from Top Ring #3.**

Further evidence of the escapement of this chrome piece can be seen in the top ring groove of piston #3 (figure I11). There was a ~5mm area on the bottom side of the top ring groove that showed evidence of being pushed down, bent, or otherwise distressed. It is believed that the chrome piece was trapped between the ring and the groove and damaged the softer aluminum before escaping down into the sump.

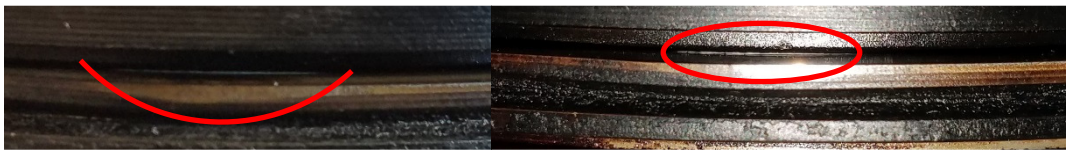

**Figure I11. Piston #3 Top Ring Groove Damage (lit and unlit). Red arc on left shows direction of groove damage. Red oval on right shows location of damage.**

Another interesting finding during posttest inspection was the presence of damage marks on the outer edge of the piston crown on the thrust side. Some corresponding witness marks were also found on the cylinders at TDC. It is believed that these marks were due to the pistons overheating and light end-gas knock during severe engine operation. Figures I12-15 show these observations. The strongest witness marks were observed on the #4 cylinder liner.

**Figure I12. Piston #1 Crown Damage and Cylinder Liner Thrust Side TDC.**

**Figure I13. Piston #2 Crown Damage and Cylinder Liner Thrust Side TDC.**

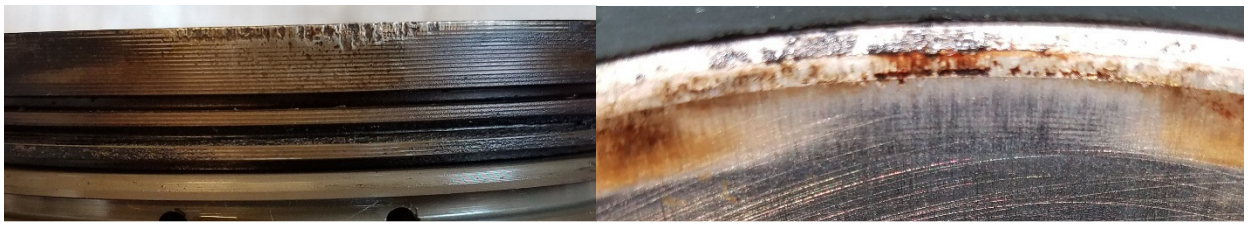

**Figure I14. Piston #3 Crown Damage and Cylinder Liner Thrust Side TDC.**

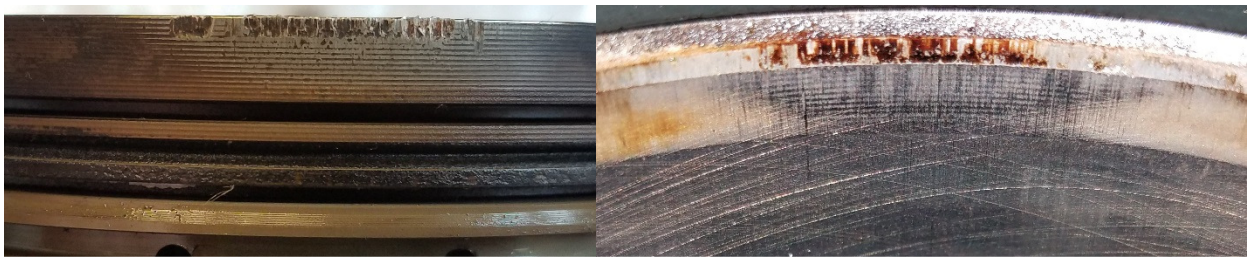

**Figure I15. Piston #4 Crown Damage and Cylinder Liner Thrust Side TDC.**

During posttest inspections, it was observed that there was some wear on the camshaft journals and the tri-lobe for the fuel pump. 3-D white light images were taken using a Bruker NPFLEX to characterize the amount of wear. The results can be seen in figures I16-24. Some cam journals showed near zero wear, but others, along with the fuel pump lobe, showed up to 4 microns of wear depth.

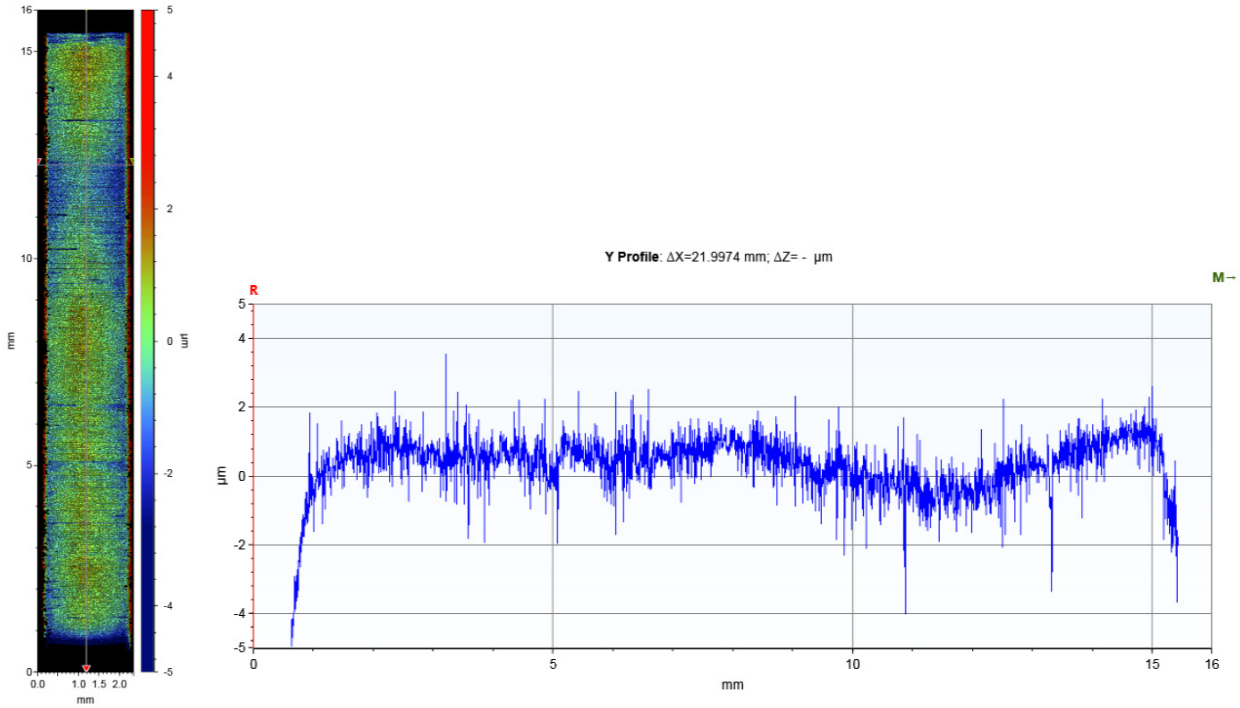


**Figure I16. Camshaft Journal #1.**

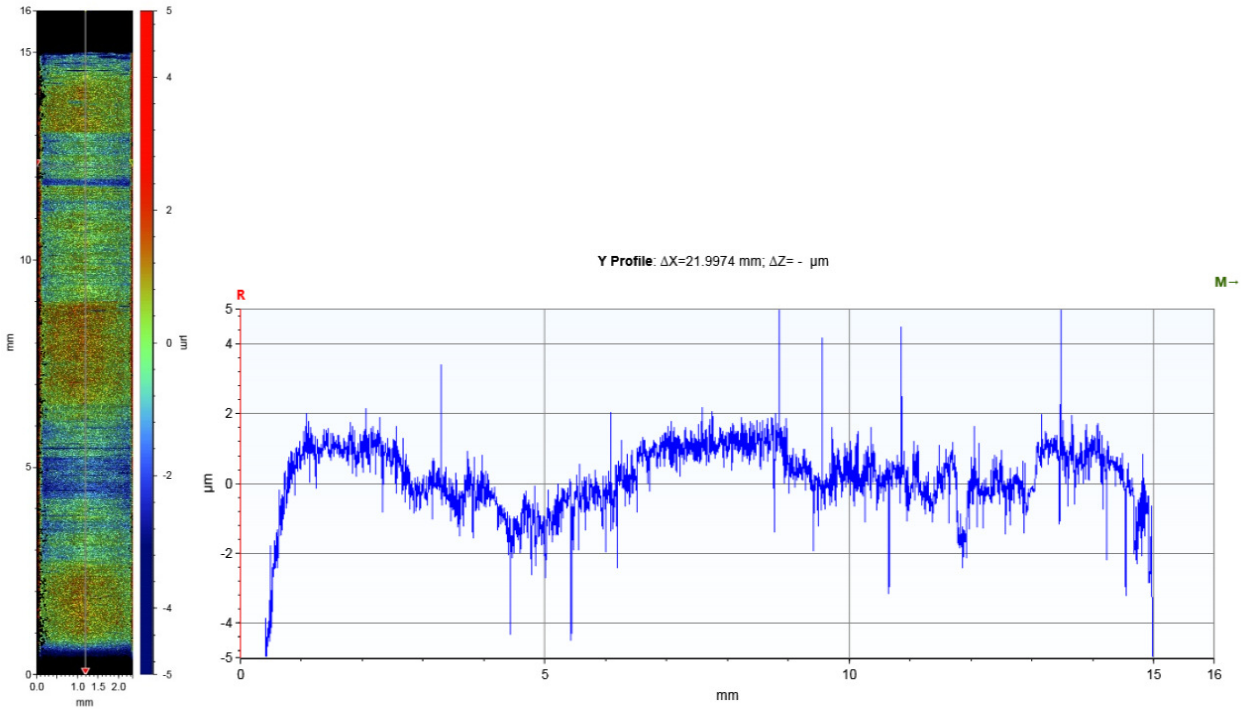


**Figure I17. Camshaft Journal #2.**

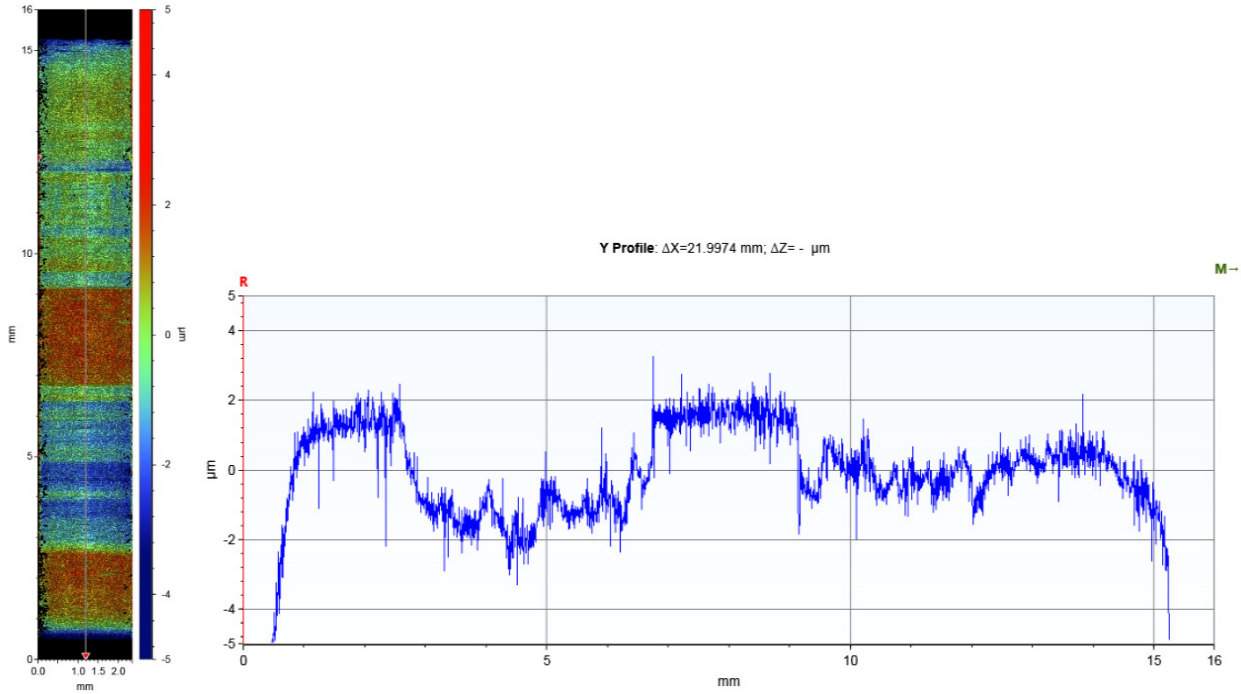


**Figure I18. Camshaft Journal #3.**

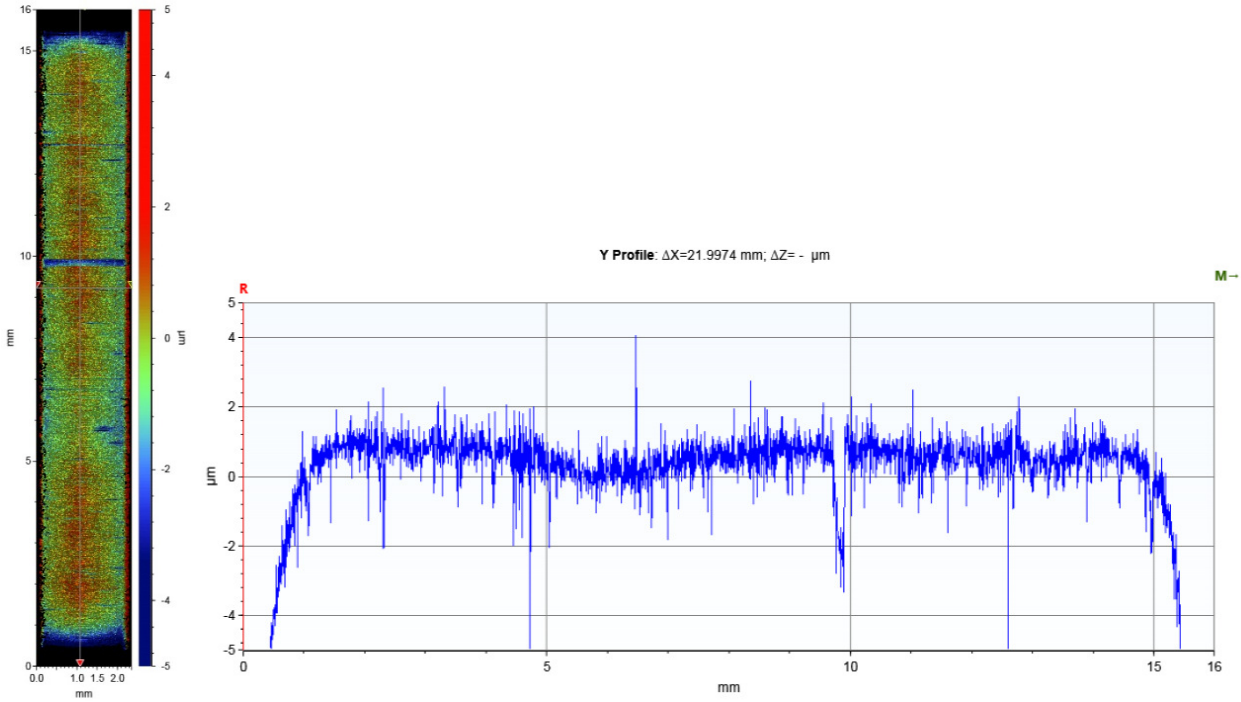


**Figure I19. Camshaft Journal #4.**

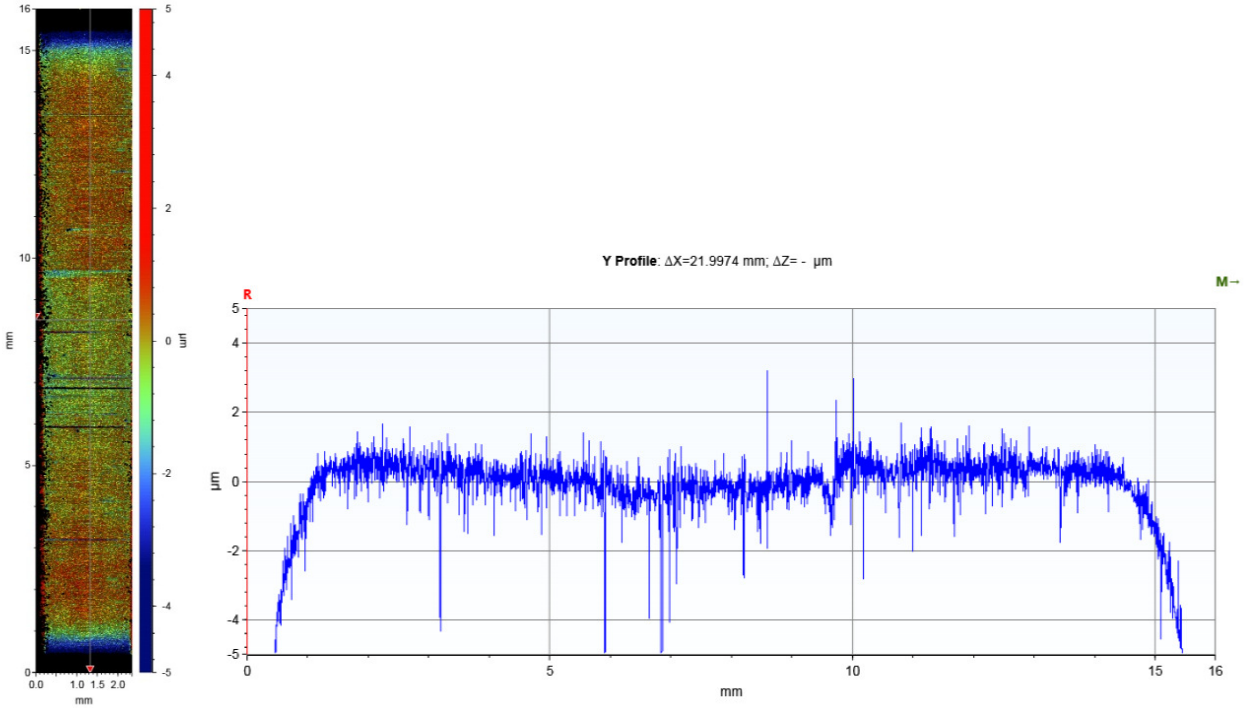


**Figure I20. Camshaft Journal #5.**

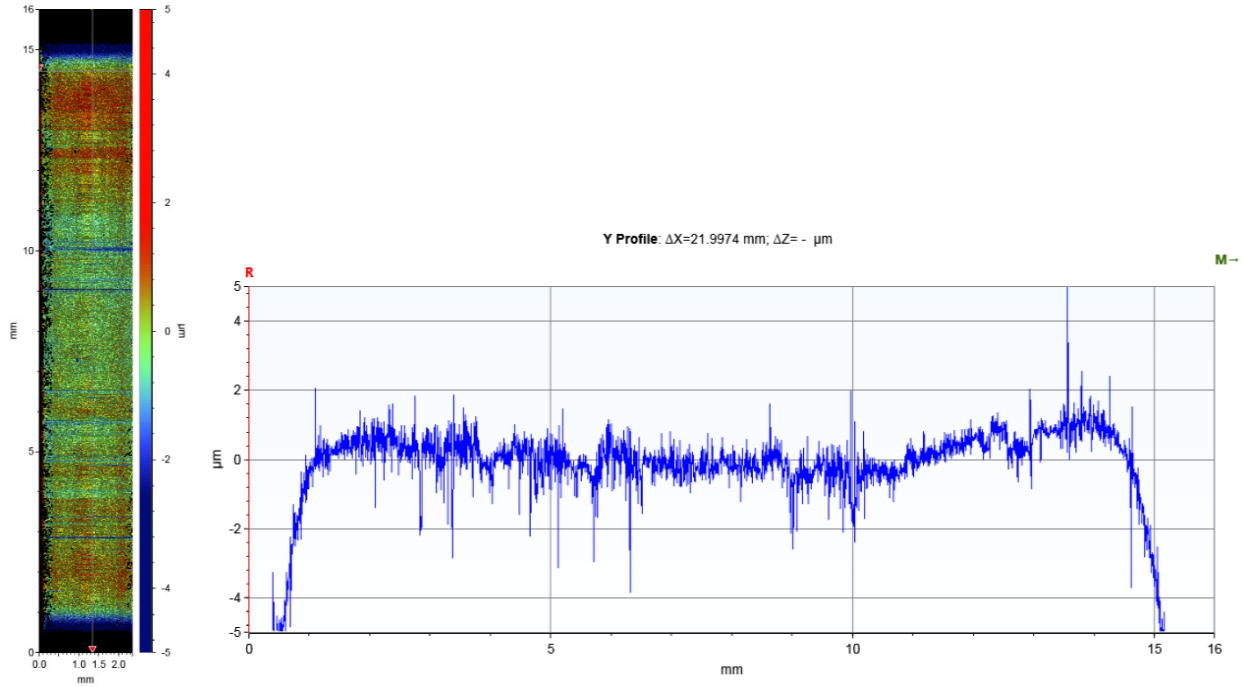


**Figure I21. Camshaft Journal #6.**

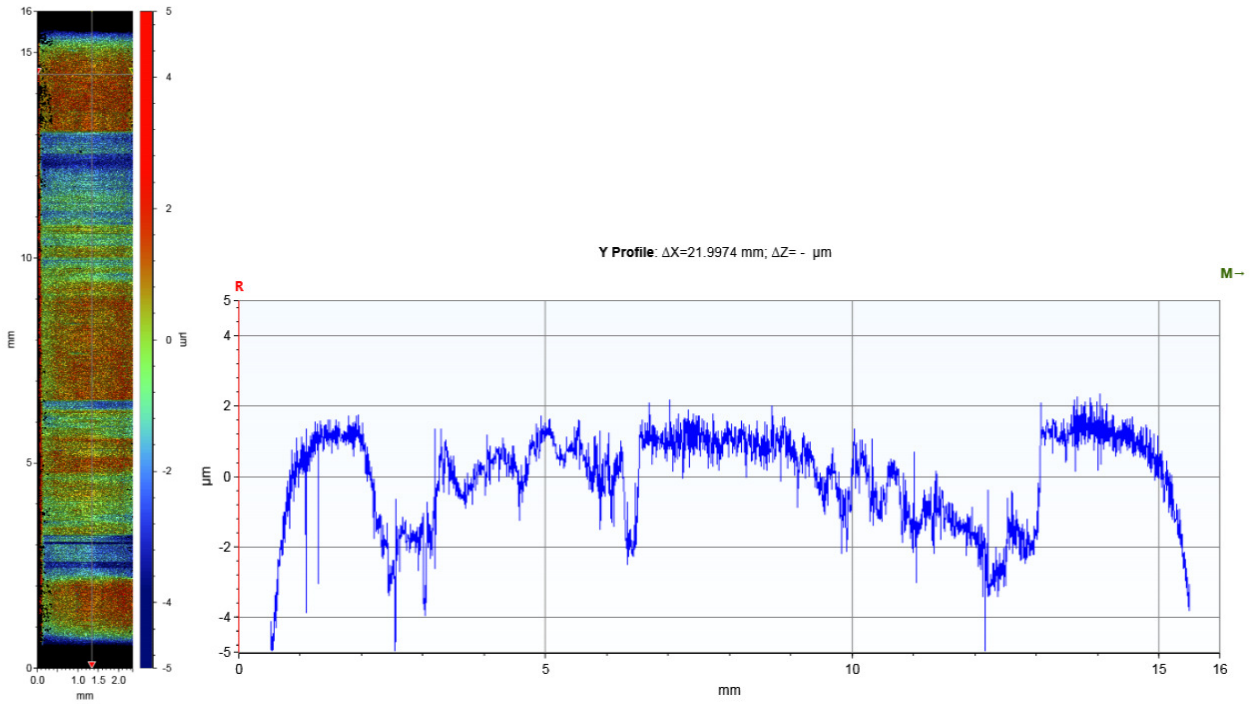


**Figure I22. Camshaft Journal #7.**

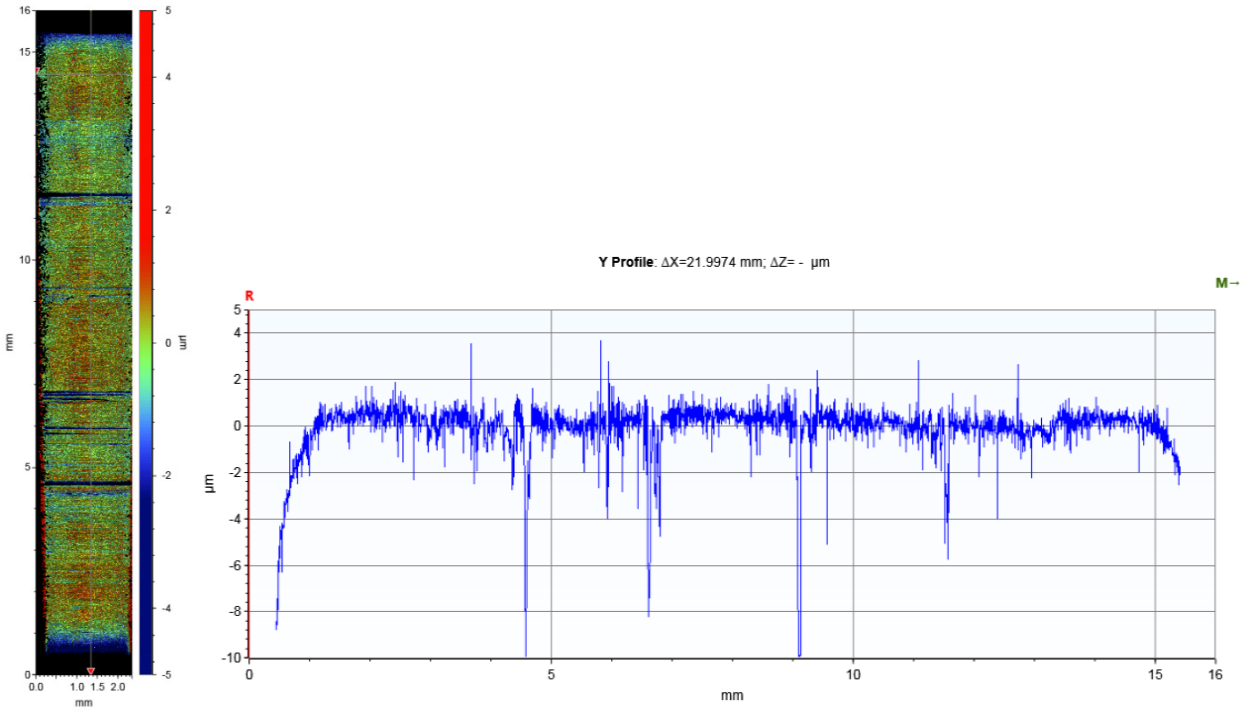


**Figure I23. Camshaft Journal #8.**

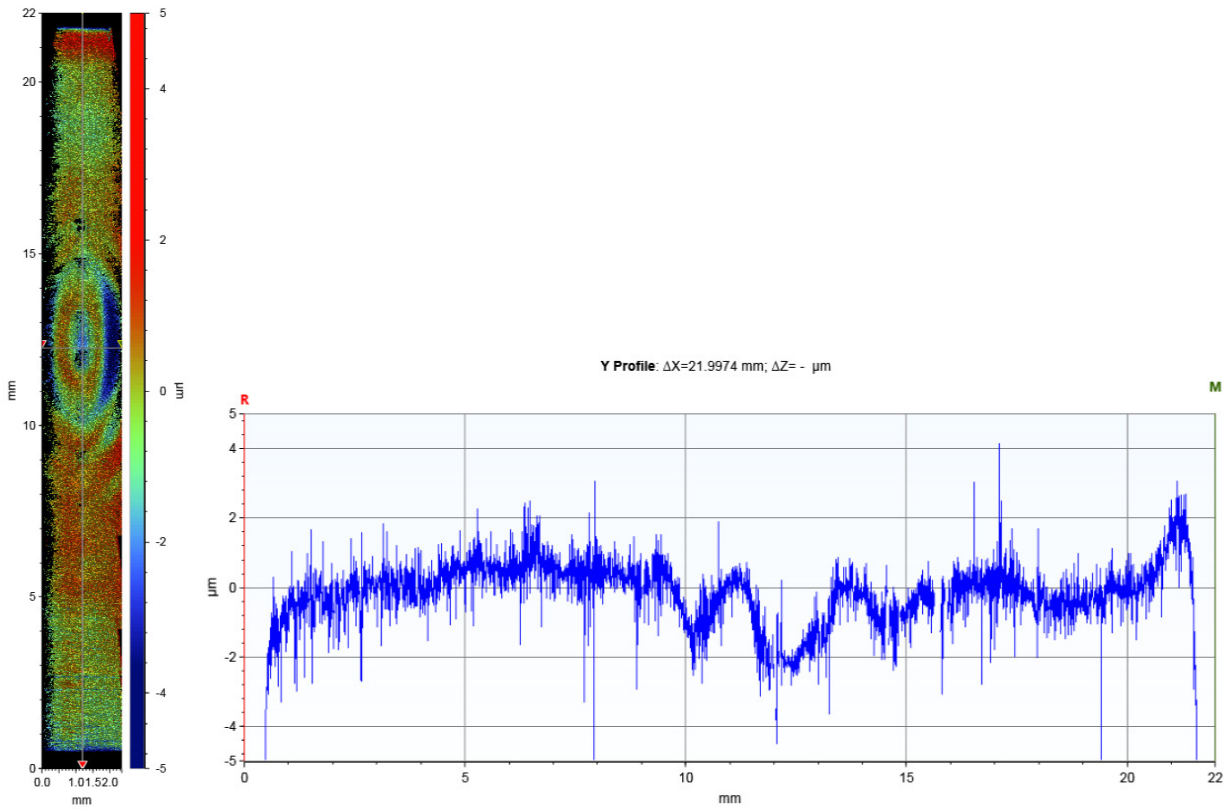


**Figure I24. Camshaft Fuel Pump Tri-Lobe (Nose).**

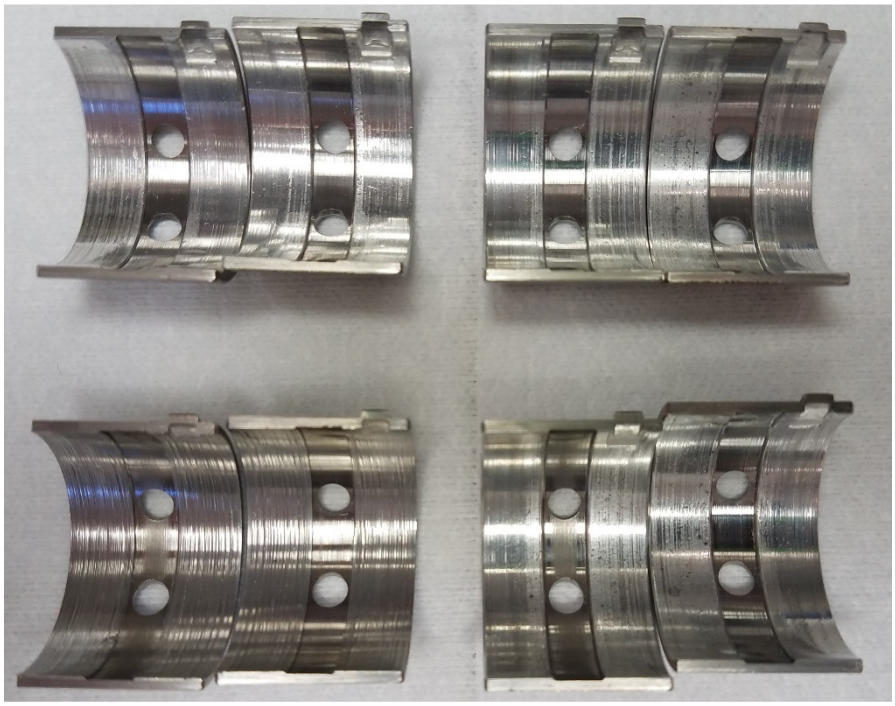

**Figure I25. Balance Shaft Bearings**

The balance shaft bearings which reside in a dual-mass balance unit below the crankshaft exhibited an unexpected amount of unidirectional wear. Similar wear was not observed on the balance shaft journals.